NBS MEASUREMENT SERVICES: RADIOMETRIC STANDARDS IN THE VACUUM ULTRAVIOLET

Jules Z. Klose

J. Mervin Bridges

William R. Ott

Center for Radiation Research
National Measurement Laboratory
National Bureau of Standards
Gaithersburg, MD 20899

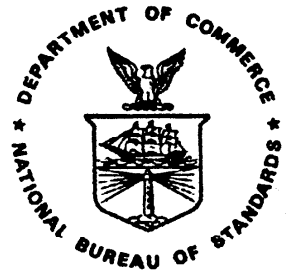

U.S. DEPARTMENT OF COMMERCE, Malcolm Baldrige, Secretary
NATIONAL BUREAU OF STANDARDS, Ernest Ambler, Director
Issued June 1987

Library of Congress Catalog Card Number: 87–619833

National Bureau of Standards Special Publication 250-3
Natl. Bur. Stand. (U.S.), Spec. Publ. 250-3, 137 pages (June 1987)
CODEN: XNBSAV

U.S. GOVERNMENT PRINTING OFFICE
WASHINGTON: 1987

For sale by the Superintendent of Documents, U.S. Government Printing Office, Washington, DC 20402–9325

PREFACE

The calibration and related measurement services of the National Bureau of Standards are intended to assist the makers and users of precision measuring instruments in achieving the highest possible levels of accuracy, quality, and productivity. NBS offers over 300 different calibration, special test, and measurement assurance services. These services allow customers to directly link their measurement systems to measurement systems and standards maintained by NBS. These services are offered to the public and private organizations alike. They are described in NBS Special Publication (SP) 250, NBS Calibration Services Users Guide.

The Users Guide is being supplemented by a number of special publications (designated as the "SP 250 Series") that provide a detailed description of the important features of specific NBS calibration services. These documents provide a description of the: (1) specifications for the service; (2) design philosophy and theory; (3) NBS measurement system; (4) NBS operational procedures; (5) assessment of measurement uncertainty including random and systematic errors and an error budget; and (6) internal quality control procedures used by NBS. These documents will present more detail than can be given in an NBS calibration report, or than is generally allowed in articles in scientific journals. In the past NBS has published such information in a variety of ways. This series will help make this type of information more readily available to the user.

This document (SP 250-3), NBS Measurement Services: Radiometric Standards in the Vacuum Ultraviolet, by J. Z. Klose, J. M. Bridges, and W. R. Ott is the third to be published in this new series of special publications. It covers the calibration of the spectral radiance and spectral irradiance of ultraviolet-emitting lamps over the wavelength range of 115 to 330 nm (see test numbers 40010s-40040s in the SP 250 Users Guide). Inquiries concerning the technical content of this document or the specifications for these services should be directed to the authors or one of the technical contacts cited in SP 250.

The Center for Radiation Research (CRR) is in the process of publishing 21 documents in this SP 250 series, covering all of the calibration services offered by CRR. A complete listing of these documents can be found inside the back cover.

NBS would welcome suggestions on how publications such as these might be made more useful. Suggestions are also welcome concerning the need for new calibration services, special tests, and measurement assurance programs.

George A. Uriano
Director
Measurement Services

Chris E. Kuyatt
Director
Center for Radiation Research

ABSTRACT

The radiometric calibration program carried out by the vacuum ultraviolet radiometry group in the Atomic and Plasma Radiation Division of the National Bureau of Standards is presented in detail. The calibration services are first listed, followed by descriptions of the primary standards, which are the hydrogen arc and the blackbody line arc, and the secondary standards, which are the argon mini- and maxi-arcs and the deuterium arc lamp. Next, the calibration methods involving both spectral radiance and irradiance are discussed along with their uncertainties. Finally, the intercomparison of standards as a method of quality control is described.

Key words: arc (argon); arc (blackbody); arc (hydrogen); irradiance; lamp (deuterium); radiance; radiometry; standards (radiometric); ultraviolet; vacuum ultraviolet.

TABLE OF CONTENTS

LIST OF TABLES

LIST OF FIGURES

I. Introduction

The vacuum ultraviolet (VUV) region of the spectrum has become important in several areas of research and development. These include space-based astronomy and astrophysics, thermonuclear fusion research, ultraviolet laser development, and general atomic physics research. Applications of VUV radiation in chemical, biophysical, and medical fields are widespread. Many applications require a knowledge of not only the wavelength of the radiation involved but also the intensity or flux of radiation. This implies a calibration of some type. The calibration may be based upon a standard source, i.e., one whose output is known, or a standard detector, i.e., one whose response to a given radiation level is known. Two general cases can be distinguished. In the first case one wishes to determine how much radiation a source such as the sun or a plasma device is emitting at a given wavelength. Usually, the source is not monochromatic, so a monochromator must be used to select the desired wavelength. In this case the most direct procedure is to employ a standard source. The source to be investigated as well as the standard source are set up in turn so that radiation from each source passes through the same monochromator and optical elements. The calibration is performed essentially by a direct substitution of the standard source for the one to be calibrated.

The second case occurs when one wishes to know the flux in a monochromatic beam of radiation, such as the flux emerging from the exit slit of a monochromator. For this determination a standard detector is more appropriate; the flux is determined by simply measuring the signal when the detector is irradiated with the beam to be calibrated. If one were to attempt to perform the calibration in the first case above using a standard detector or in the second case using a standard source, one would in both cases need to know the spectral efficiency of the monochromator used in the measurement. This would require an additional measurement using a second monochromator and would introduce additional uncertainties and complexities. Therefore a need exists for both standard sources and standard detectors.

Standard sources may be divided into primary standards and secondary or transfer standards. Primary standards are ones whose output is known from basic principles. The primary standards of VUV radiation include plasma sources, especially the wall-stabilized hydrogen and blackbody line arcs, and electron storage rings emitting synchrotron radiation.

There are storage rings at several laboratories, including NBS, which are used as primary VUV radiation standard sources. They produce continuum radiation for wavelengths $\gtrsim$ 0.03 nm. Limited access to storage rings, however, makes it desirable for most workers to have available other standard VUV sources. The wall-stabilized hydrogen and blackbody line arcs were developed to provide alternative primary standard sources. These sources, however, are also not able to be easily used for calibrations. Hence, secondary or transfer standards which are relatively easy to apply have been developed. These include the deuterium lamp and the argon mini-arc. These sources are more readily available and make possible relatively inexpensive and convenient calibrations. Even for researchers having access to a storage

ring the secondary standards can be useful in making possible more frequent calibrations. Also, the secondary standards possess some useful properties not characteristic of the available primary standards such as, for example, emission over a relatively large solid angle.

The two principal radiometric quantities which are measured and calibrated are radiance and irradiance. For an object or source which emits radiation, the radiance is the radiant power emitted per area per solid angle: $L = [\text{watts cm}^{-2} \text{ sr}^{-1}]$. If the source emits a continuum, i.e., emits radiation at all wavelengths near a particular wavelength, the spectral radiance is the radiance per wavelength interval or bandpass: $L_\lambda = [\text{watts cm}^{-2} \text{ sr}^{-1} \text{ nm}^{-1}]$. The radiance will in general vary over the source area, the direction, and the wavelength. The definition assumes that the area, solid angle, and wavelength band are small enough that the radiance does not vary greatly within these quantities. Spectral irradiance is the radiant power incident upon a target per area per wavelength band: $E_\lambda = [\text{watts cm}^{-2} \text{ nm}^{-1}]$. A source of radiation may serve as a standard source of irradiance by operating it at a given distance from the target area. Some sources may be used as either standard radiance or standard irradiance sources. A separate calibration must be performed, however, for each quantity.

The services performed by the Atomic and Plasma Radiation Division of the National Bureau of Standards include tests and calibrations of portable secondary VUV standard radiance and irradiance sources. These are usually deuterium lamps and argon arcs. Also included, however, are special sources such as rare-gas dimer lamps, which emit continuum radiation over limited wavelength ranges, and hollow cathode lamps, which emit spectral lines in the wavelength range from the VUV through the visible. All sources are generally supplied by customers. The main groups of customers have included those in the fields of space-based astronomy and solar physics who have used standard sources to calibrate satellite, rocket, or balloon-borne spectrometers. Other customers have needed calibrations in the 100-300 nm range for plasma radiation studies.

II. NBS Radiometric Standards in the Near and Vacuum Ultraviolet

A. Spectral Irradiance Standard, Argon Mini-Arc (140-330 nm), SP250 No. 40010S (7.6B)

An argon mini-arc supplied by the customer is calibrated for spectral irradiance at 10 nm intervals in the wavelength region 140-330 nm. Absolute values are obtained by comparing the radiative output with laboratory standards of both spectral irradiance and spectral radiance. The spectral irradiance measurement is made at a distance of 50 cm from the field stop. Uncertainties (2σ) are estimated to be less than ±10% in the wavelength region 140-200 nm and within ±6% in the wavelength region 200-330 nm. A measurement of the spectral transmission of the arc window is included in order that the calibration be independent of possible window deterioration or damage.

B. Spectral Radiance Standard, Argon Mini-Arc (115-330 nm), SP250 No. 40020S (7.6C)

The spectral radiance of argon mini-arc radiation sources is determined to within a 2σ uncertainty of less than 6% over the wavelength range 140-330 nm and 11% over the wavelength range 115-140 nm. The calibrated area of the 4 mm diameter radiation source is the central 0.3 mm diameter region. Typical values of the spectral radiance are: at 250 nm, L_λ = 30 mW cm^{-2} nm^{-1} sr^{-1}; and at 150 nm, L_λ = 3 mW cm^{-2} nm^{-1} sr^{-1}. The transmission of the demountable lamp window and that of an additional MgF_2 window are determined individually so that the user may check periodically for possible long term variations.

C. Spectral Irradiance Standard, Deuterium Arc Lamp (165-200 nm), SP250 No. 40030S (7.6D)

The lamp is calibrated at ten wavelengths from 165 to 200 nm at a distance of 50 cm. Its spectral irradiances are about 0.05 μW cm^{-2} nm^{-1} at 165 nm, 0.03 μW cm^{-2} nm^{-1} at 170 nm, and 0.05 μW cm^{-2} nm^{-1} at 200 nm. The approximate 2σ uncertainty relative to SI units is estimated to be less than 10%. The lamp is normally supplied by NBS and requires 300 mA at about 100 V.

D. Special Tests of Radiometric Devices in the Near and Vacuum Ultraviolet, SP250 No. 40040S (7.6A)

Tests of customer supplied radiometric devices not included above are performed at the direction of the customer.

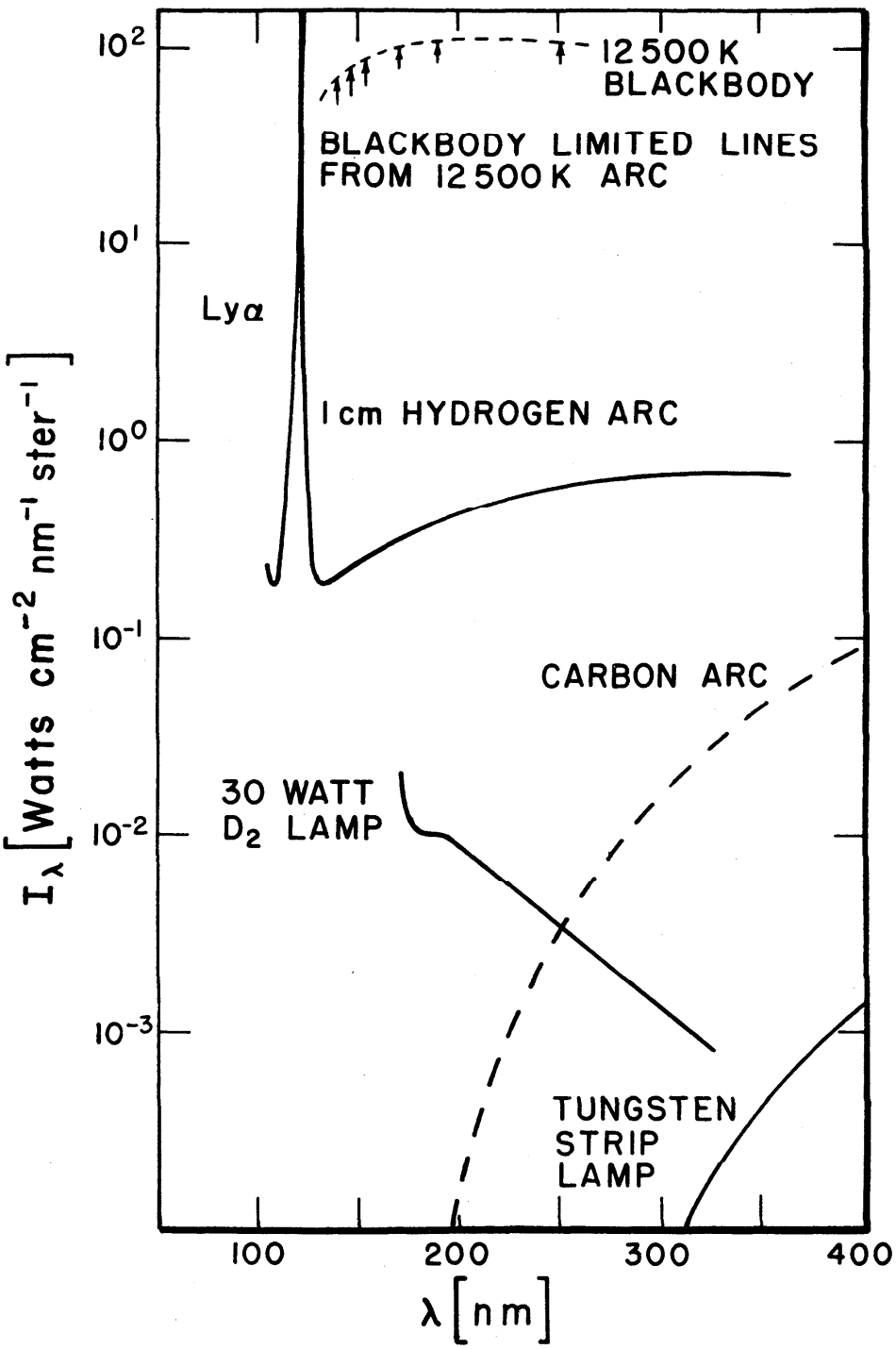

Figure 1. Comparisons of spectral radiances for far UV sources. The output of the hydrogen arc is given for the temperature of maximum continuum emission; the outputs of the other sources are at typical operating conditions.

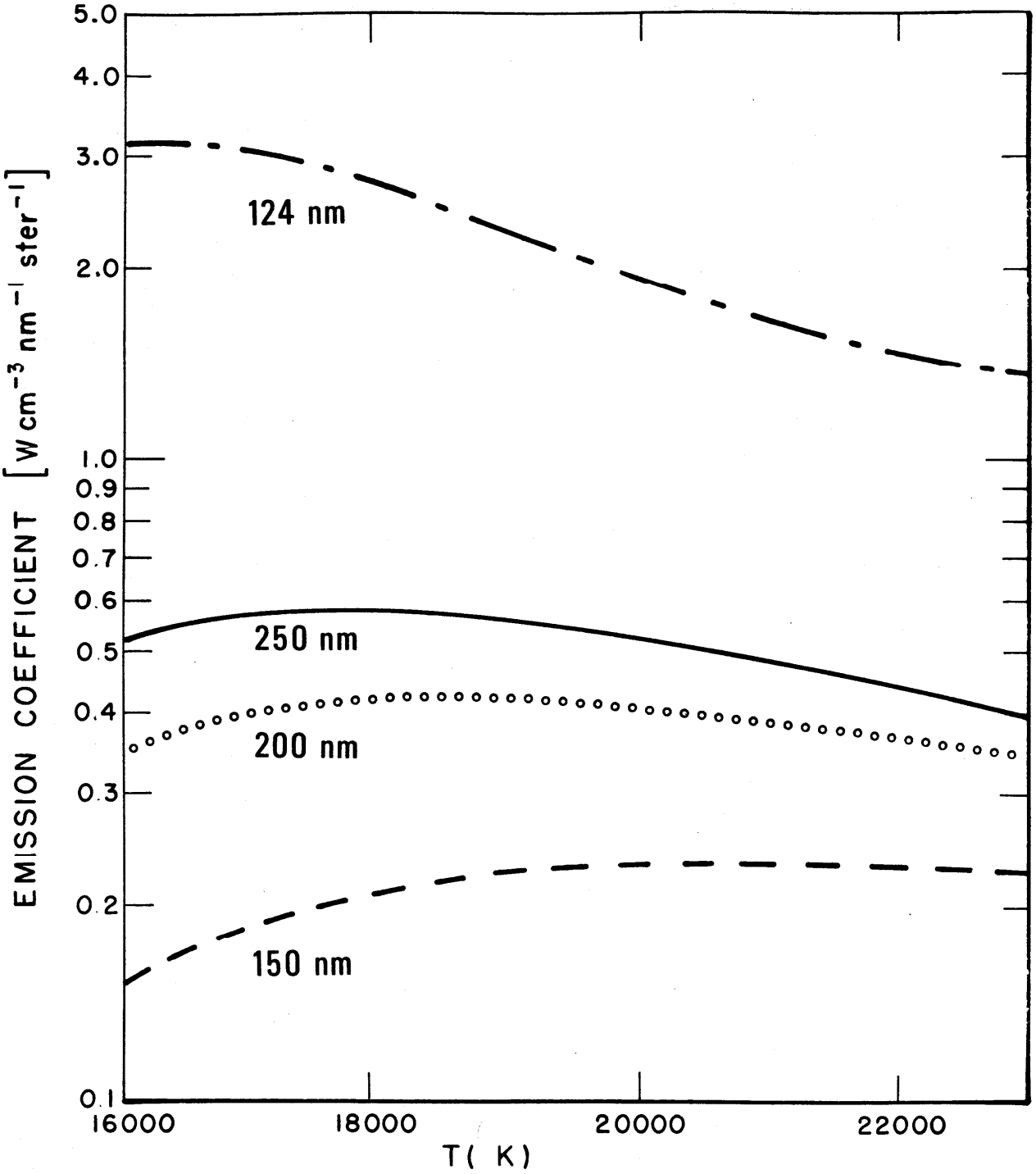

Figure 2. The emission coefficient for a 1-atm hydrogen plasma in LTE as a function of temperature for several wavelengths: 250 nm (___); 200 nm (ooo); 150 nm (---); and 124 nm (—·—).

III. Apparatus

A. Primary Standards

1. The Hydrogen Arc

a. Physical Principles

A high temperature wall-stabilized steady-state hydrogen arc has been developed as our primary standard of spectral radiance.[1] This type of arc lends itself to such a use because at sufficiently high temperatures it yields absolute intensities independent of other radiometric standards or of the accuracy of any plasma diagnostics. Previous efforts at lower powers were hindered by large uncertainties in plasma diagnostics, a difficulty that has been overcome in the high temperature arc. Figure 1 illustrates the UV spectrum of several of the more common standard sources, including that part of the hydrogen arc spectrum that is the subject of this paper.

The method depends upon the phenomenon that the continuum emission coefficient for a strongly ionized hydrogen plasma which is in or close to the condition of local thermodynamic equilibrium (LTE) is calculable to within one percent.[2] This follows from the fact that the essential spectroscopic constants, i.e., the continuum absorption coefficients and transition probabilities, are exactly known for atomic hydrogen. The continuum intensities emitted from a typical pure hydrogen wall-stabilized arc discharge in the spectral region above 91.5 nm are optically thin and a function of the electron density and temperature.[3,4] In the low power hydrogen arc the electron density and temperature are determined from plasma diagnostics in the visible using available radiometric standards.[3] These quantities are then used to calculate the continuum intensities in the VUV. There are known to be significant uncertainties in the plasma diagnostics, and as a result we have adopted as our primary standard a higher power hydrogen arc which operates such that a 2 mm diameter wall-stabilized discharge reaches a temperature of about 20,000 K. For these conditions the continuum emission coefficient as a function of temperature shows a broad maximum which shifts with wavelength as is shown in Fig. 2. This optimum condition is brought about essentially by the compensating effects of an increase in the ionization fraction and a decrease in the total number density as the temperature is increased in a constant 1-atm pressure operating environment. Beyond this maximum[5,6] the ionization is practically complete, and any further increase in arc temperature results only in a gradual decrease in intensity because of the decrease in the number density. The weak wavelength dependence of this maximum seen in Fig. 2 occurs because of the change in the energy distribution of the equilibrated electrons as the electron temperature is varied.

Figure 3 shows the measured radial dependence of the hydrogen continuum emission coefficient at 190 nm and the corresponding calculated LTE temperature[2] for an arc current of 80 A. Because the maximum in the coefficient is broad and the absolute magnitude of the peak intensity is not very sensitive to the electron temperature, the emission characteristics of the plasma are nearly homogeneous over its central region which extends to about 0.6 mm from the arc axis. This is especially significant if only a

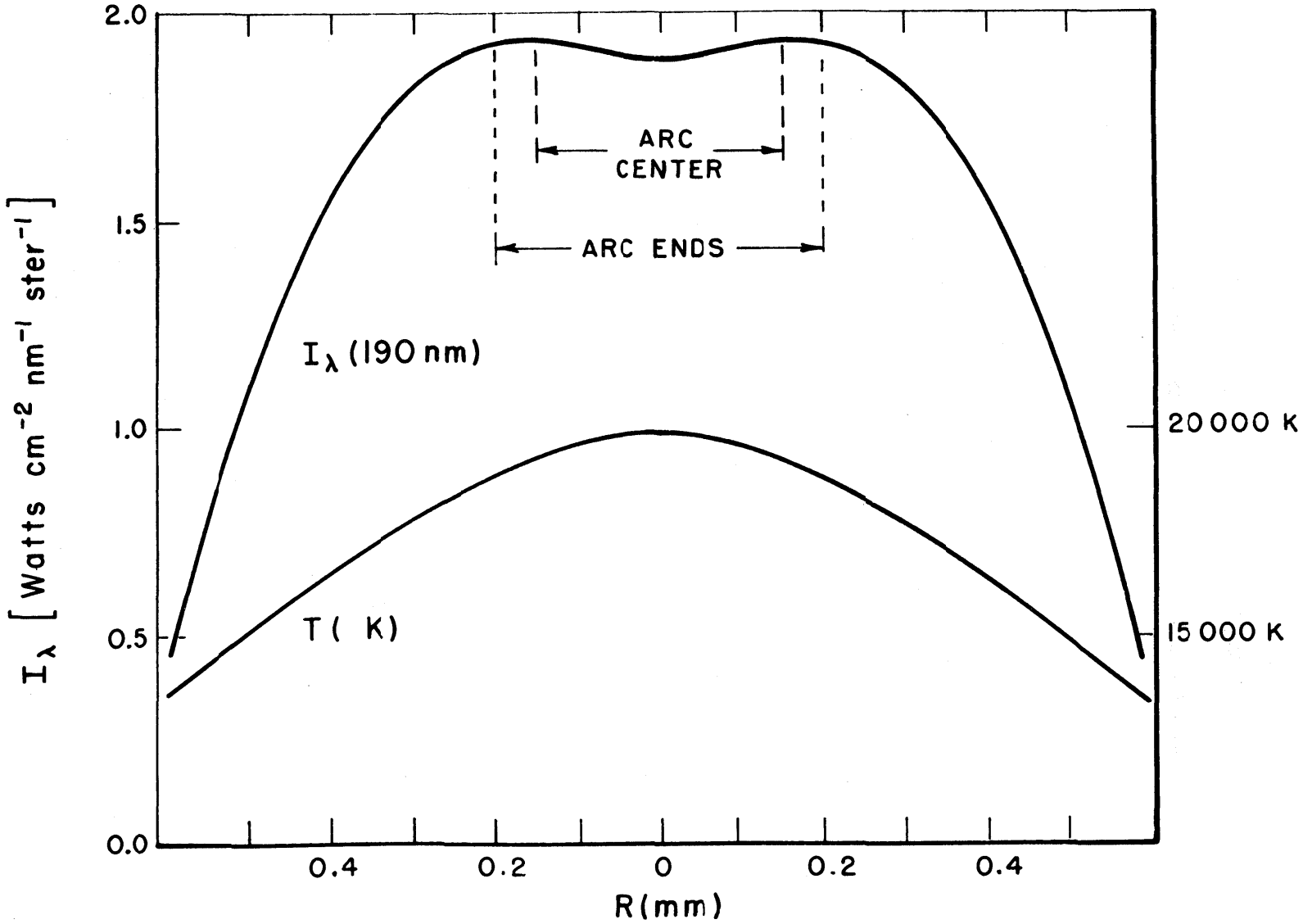

Figure 3. Radial dependence of the continuum intensity and arc temperature for a 2-mm wall-stabilized hydrogen arc operating at 80 A. The dashed lines define the dimensions of the plasma that is observed by spectrometers.

Table I. Maximum Emission Coefficient from a 1-atm Hydrogen Plasma in LTE Calculated as a Function of Wavelength[a]

λ (nm)	ϵ (W cm^{-3} nm^{-1} sr^{-1})	T(K)	$\frac{\text{Ly}\alpha}{\epsilon}$ (%)
350	0.73	17,000	0
300	0.68	17,000	0
250	0.59	17,500	0.01
200	0.424	18,500	0.07
190	0.386	18,800	0.11
180	0.347	19,200	0.20
170	0.308	19,500	0.34
160	0.269	20,000	0.65
150	0.232	21,000	1.3
140	0.200	21,700	4
130	0.245	17,500	54
128	0.372	16,500	77
126	0.79	16,500	90
124	3.22	16,000	98

[a]The percentage of this emission due to Lyα and the arc temperature required for maximum emission are also listed.

small sample of the region is observed as indicated in the figure. First, it means that the alignment precision, which was responsible for much of the uncertainty in the low power arc method, is not critical here. Second, it means that the arc current necessary to obtain the maximum emission coefficient is also not critical.

Additional advantages of operating the hydrogen arc under such conditions are: (1) the H_2 Lyman band molecular emission, which limited the low power hydrogen arc to wavelengths above 165 nm, is negligible; (2) the assumption of LTE appears to be very closely fulfilled as shown by experimental consistency checks, theoretical validity criteria,[7] and variations in arc current which produce only very small deviations from LTE;[3,8] and (3) the hydrogen arc as it is described here constitutes a true primary standard of spectral radiance in that except for the minor uncertainties associated with the theoretical model for the plasma, knowledge of the absolute continuum intensities does not depend on any other standards of calibration or sophisticated plasma diagnostics and requires only a measurement of the ambient pressure ($\approx$1 atm) and the arc length. The procedure for applying the arc as a radiometric standard involves only adjusting the arc current for maximum signal at the wavelength of interest. The overall system efficiency is given then by the ratio of the detector response to the hydrogen arc spectral radiance calculated using the maximum LTE emission coefficient at 1-atm pressure and the actual physical length of the discharge.

Figure 1 shows the wavelength dependence of the maximum emission coefficient of the hydrogen arc plasma, and Table I lists the values of the same quantity obtained through a calculation of the hydrogen continuum.[2] The Stark broadened wing of the Lyman α line at 122 nm has been included in these calculations and, as can be seen from the table, becomes significant at wavelengths below 140 nm.[9] The uncertainty in the calculated continuum emission coefficient is estimated to be about 2%, due mostly to uncertainties in the high density plasma corrections.[2] Combining this uncertainty in quadrature with the uncertainties in the Stark broadening calculations, the uncertainty in the total emission coefficient comes out to be 2% above 140 nm, 8% at 130 nm, and 13% at 124 nm. These uncertainties and all those succeeding unless stated otherwise are taken to be 2 standard deviations (2σ), i.e., as having a confidence limit of about 95%.

Three factors are of special concern in applying the high power hydrogen arc standard: the arc length, spatial resolution, and off-axis H_2 emission. Figure 4 is a schematic of the hydrogen arc.[1,4,10] The arc is struck between a set of four tungsten anodes and four tungsten cathodes that are symmetrically located and share the current load equally. At each end of the 2-mm diameter channel formed by the twenty water-cooled stacked copper plates, the discharge expands and separates into four smaller arcs terminating at each of the electrode tips. The length of this inhomogeneous region is made small compared to the total length of the arc, and the emission coefficient and temperatures are lower than in the channel. Therefore, its contribution to the total arc signal obtained in an end-on measurement along the axis of the discharge is small but not precisely known. The minimum possible length of the arc is 5.05 cm, the total length of the channel formed by the twenty arc plates, and the maximum length is 5.5 cm, the total distance

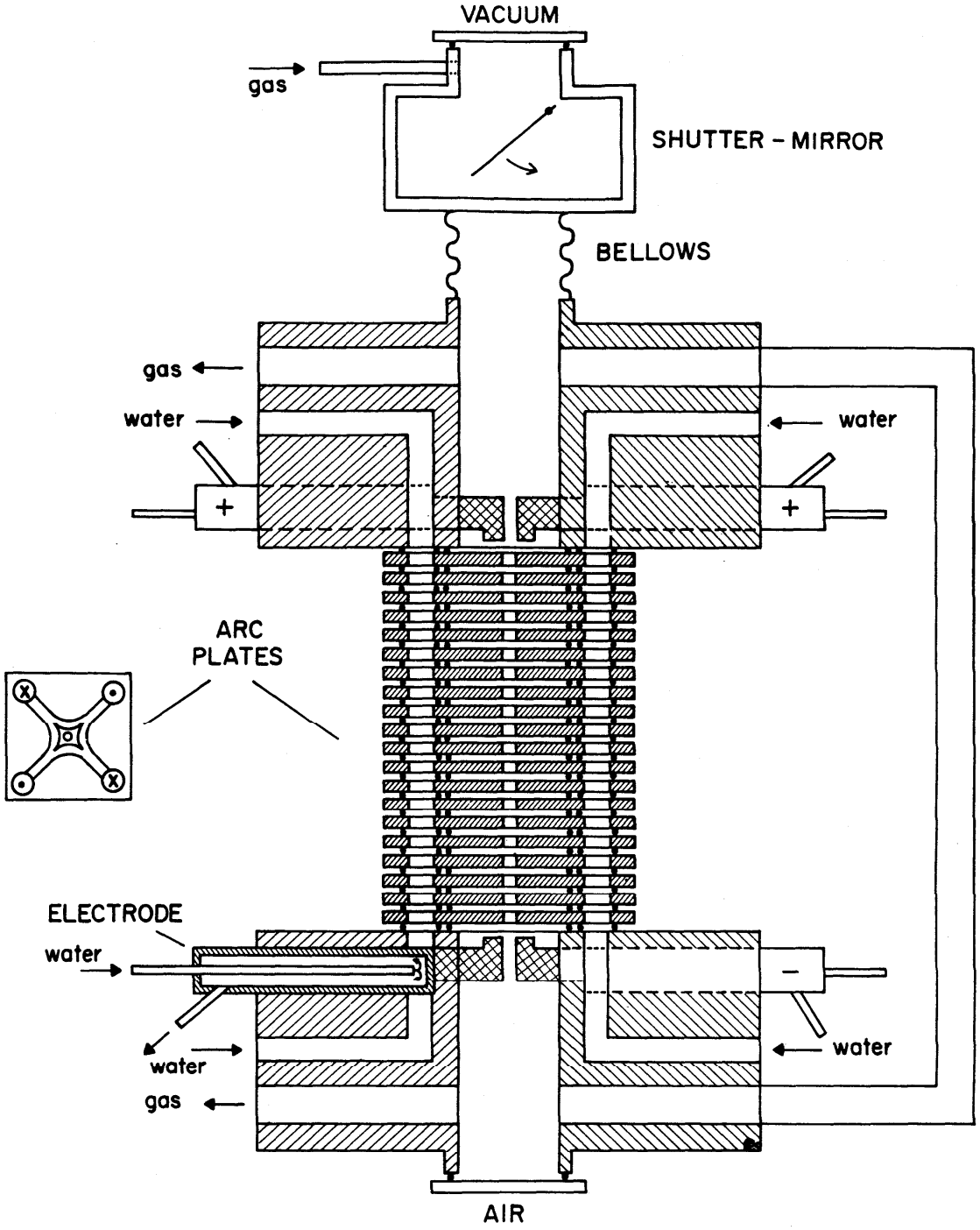

Figure 4. Schematic of the hydrogen wall-stabilized arc. A cutaway top view drawing of one of the arc plates illustrates the flow of cooling water through specially machined channels within each plate. The symbols in the four corners show the direction of water flow.

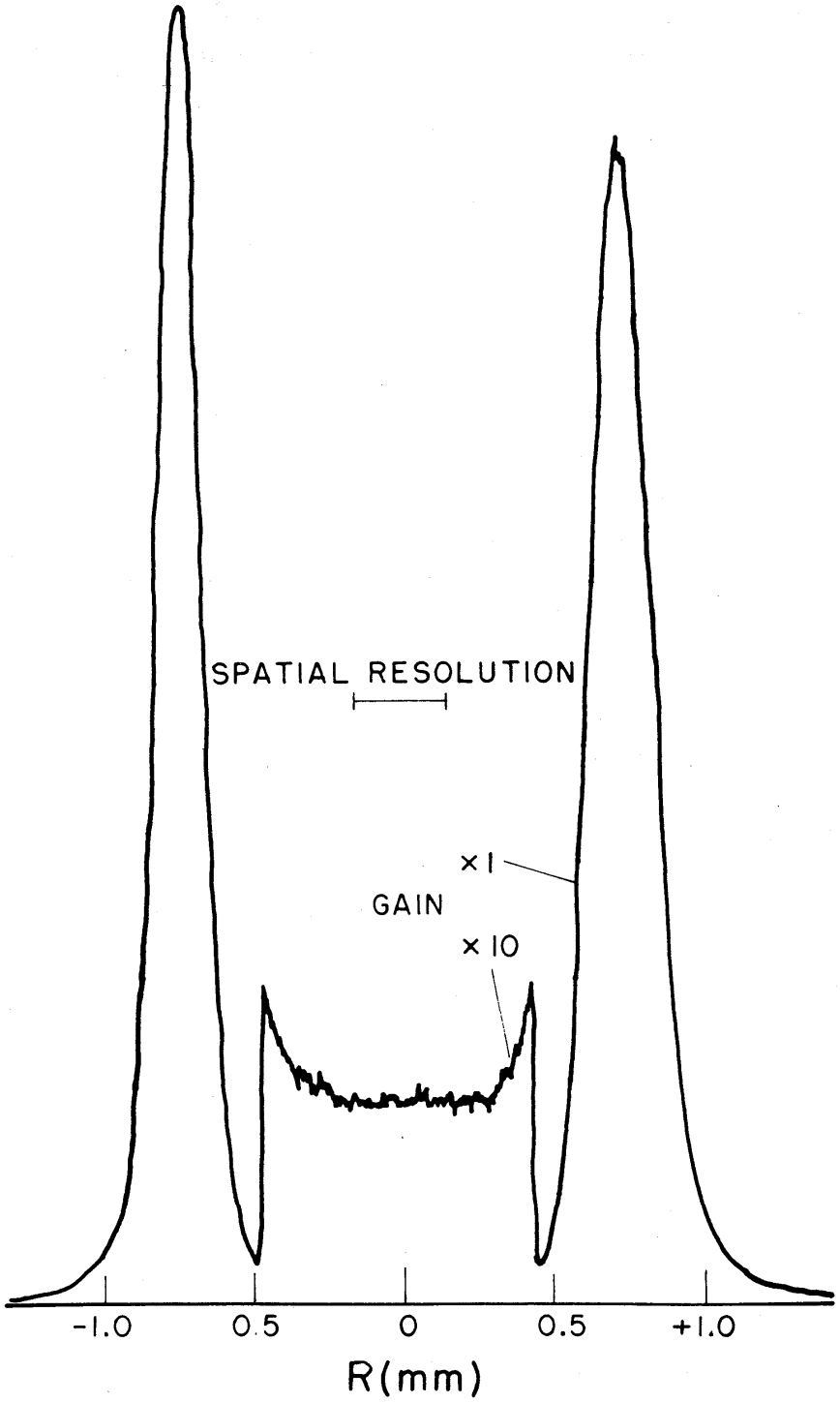

Figure 5. The radial dependence of the hydrogen arc spectral radiance at 160.6 nm for an arc axis temperature of about 19,500 K. The intense off-axis radiation is due to Lyman band molecular emission. The nearly uniform radiation in the vicinity of the axis contains no molecular contributions, but is due to the hydrogen continuum that is being used as a spectral radiance standard.

between the electrodes. The estimated length of the homogeneous hydrogen arc plasma was thus taken to be 5.3 cm with an uncertainty of 5% (2σ).

Spatial resolution is not much of a problem for the high power arc since the emission characteristics are nearly uniform in the vicinity of the arc axis. The regions of the arc that fall into the cone of observation determined by the f/200 aperture and the 0.30 mm field stop are illustrated in Fig. 3. Thus, knowledge of the emission coefficient as a function of radial position allows the calculation of the effect of spatial averaging. The main result is that the integrated emission coefficient $\bar{\varepsilon}$ has a maximum about 1% lower than ε_{max} from a truly homogeneous plasma with an axis temperature $T(\bar{\varepsilon})$ slightly higher than $T(\varepsilon_{max})$. The arc plasma is cylindrically symmetric, and because the area of the differential shells increases as $2\pi r\Delta r$, the off axis regions are weighted more than the axis region. Therefore, when one obtains maximum signal, the current has been adjusted so that the temperature maximum occurs slightly off-axis as seen in Fig. 3.

Below 165 nm the Lyman bands of H_2 are emitted from low temperature off-axis regions. Figure 5 shows a semilog plot of a radial scan of the arc at a wavelength where one of the stronger H_2 features can be observed. The off-axis line peak is about 100 times larger than the on-axis hydrogen continuum, but clearly if the observation column is restricted to no more than the central 0.5 mm diameter plasma, H_2 lines should not be observed. Molecular emission from the the inhomogeneous end regions also is a possibility. However, none is observed since the arc terminates at points that are out of the line of observation (the cooler plasma regions are off-axis) and because the end-layer on-axis temperature gradient is quite sharp (the length of the cool plasma is then very short).

In Fig. 6 the calculated spectral radiance of the high power hydrogen arc is compared with calibrations of that arc made with several other standard sources.[1] The theoretical spectral radiance is the product of the theoretical maximum hydrogen plasma emission coefficient and the arc length. This quantity is graphed as a shaded area which represents the rms uncertainty due to the previously described uncertainties in both the calculated emission coefficient and the arc length. The solid and open circles represent the measured continuum intensities using, respectively, a calibrated tungsten strip lamp[11] and blackbody limited lines from another arc for spectral radiance normalization. The crosses represent the measured intensities using the low power hydrogen-arc standard. The error bars attached to the data points represent uncertainties associated not with the hydrogen arc but with the various standards used to calibrate the spectral radiance. The discontinuity in the wavelength scale is due to the interruption of the hydrogen spectrum by the Balmer line series of atomic hydrogen, which dominates the high temperature arc spectrum above 360 nm except for a small region around 560 nm between H_α and H_β. Inspection of Fig. 6 leads us to conclude that the various standards are consistent with one another over the entire range of comparison.

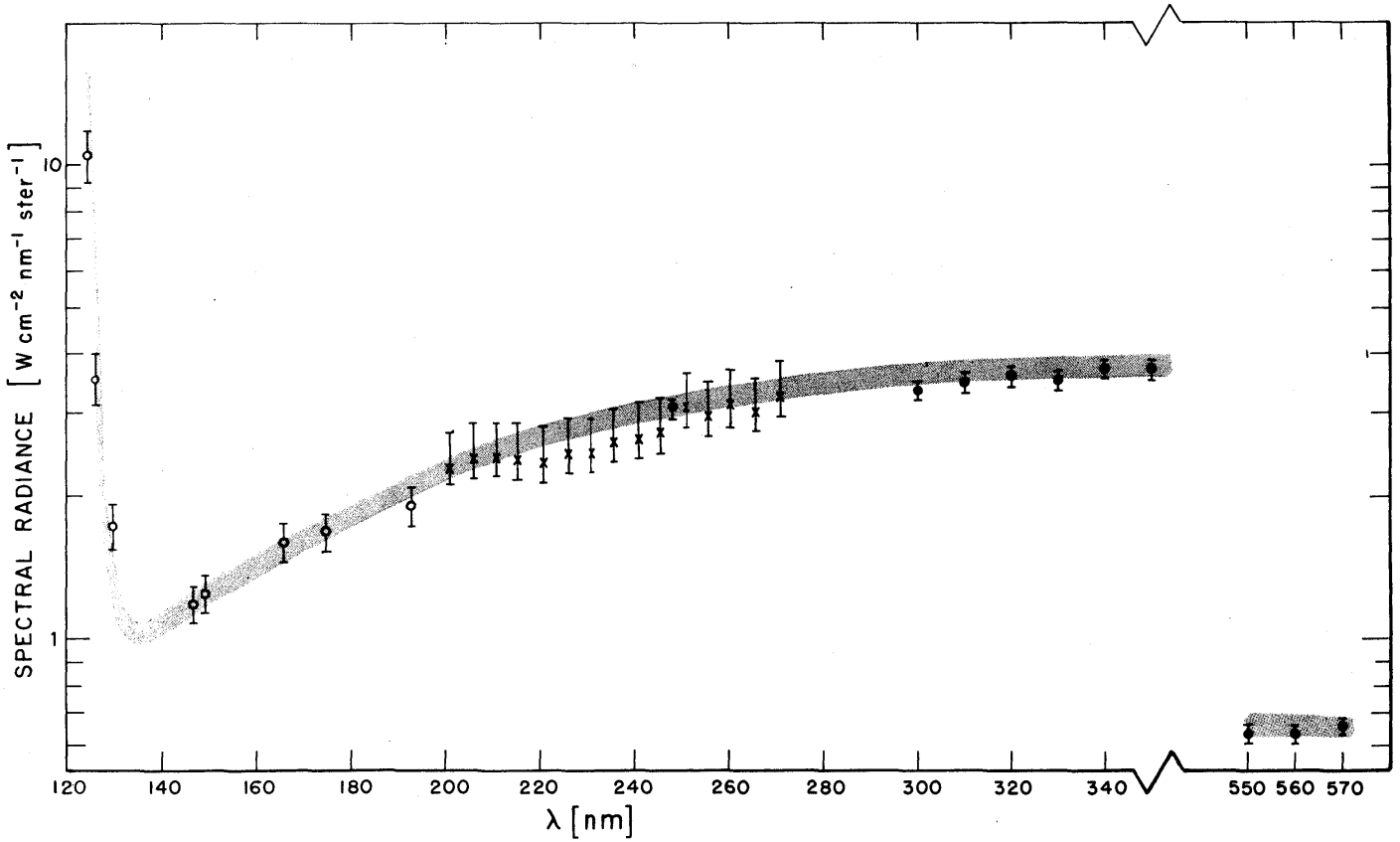

Figure 6. Maximum spectral radiance vs wavelength calculated for a 5.3-cm length hydrogen arc plasma in LTE at 1 atm pressure. The calculation is shown as a grid and represents the rms uncertainty due to uncertainties in the arc length (±5%) and the calculated emission coefficient (between 2% and 13%). The points are actual measurements of the spectral radiance calibrated either with a tungsten strip lamp (•), blackbody limited lines (o), or a low power hydrogen arc (x).

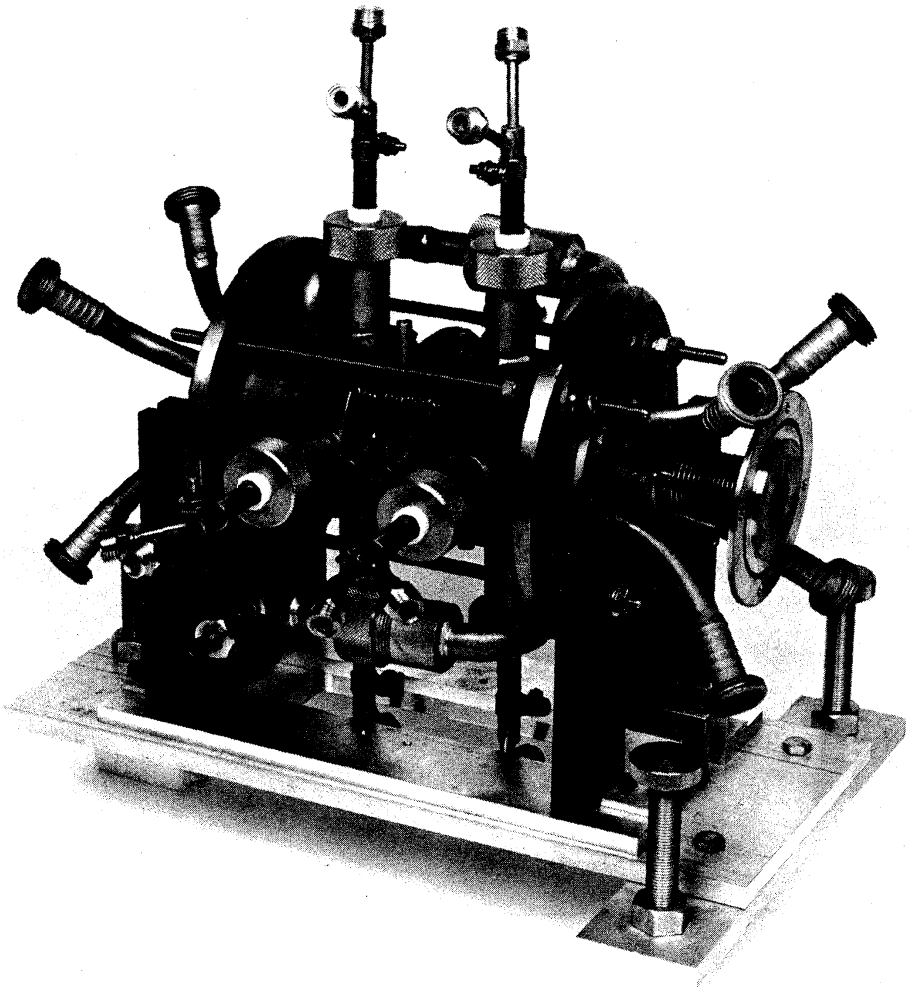

Figure 7. A photograph of the hydrogen wall-stabilized arc. This particular photograph shows gas ports in between several of the arc plates. These are not normally used in hydrogen arc radiometry but are available to admit gas impurities needed for other applications.

In summary, a high power atmospheric pressure hydrogen arc capable of operating at temperatures on the order of 20,000 K has been examined theoretically and experimentally and found to be suitable as a primary radiometric standard in the VUV. The experimental investigations have shown that at such temperatures molecular hydrogen emission below 165 nm is negligible, and the hydrogen plasma continuum emission coefficient can be measured throughout the 124-360 nm spectral range. By operating the arc at currents such that the maximum emission coefficient is reached, the uncertainties associated with various plasma diagnostics and alignment imprecisions are minimized to the one-percent range. The results of a comparison with other available standard sources are consistent with the estimated 2σ uncertainty of ±5% in the hydrogen arc spectral radiance between 140 nm and 360 nm. This uncertainty is due mainly to the uncertainty in the measurement of the arc length. Below 140 nm the Lyman α Stark broadened wing becomes significant, and the estimated uncertainty in the hydrogen arc intensities increases to about ±9% at 130 nm and ±14% at 124 nm due mainly to uncertainties in the plasma line broadening theory. These results are also consistent with a comparison standard. Finally, all experimental comparison data confirm that the hydrogen arc spectral radiance is calculable throughout the 124-360 nm range without dependence on any other radiometric standard or plasma diagnostic technique. Therefore, the high power hydrogen arc is a true primary standard.

b. Description of the Arc

The plasma source for generating the hydrogen continuum is a steady-state wall-stabilized arc operating in a flow system of pure hydrogen at 1 atm pressure. The general arc design is based on the one developed by Maecker and Steinberger[10] and is illustrated both in the schematic drawing in Fig. 4 and the photograph in Fig. 7. The 5.3 cm long discharge is formed between a set of four tungsten cathodes and four tungsten anodes (only two electrodes from each set appear in Fig. 4) and is constricted by a stack of 20 copper plates each with a central bore of 2.0 mm diameter. The thickness of the plates is limited to 2 mm in order that the arc current, which chooses the path of lowest voltage drop, passes through the resistive plasma rather than through the plates themselves. The plates must also be very closely spaced in order to avoid any kinks or asymmetries in the strongly constricted cylindrically-symmetric plasma column. As can be seen in Fig. 8, electrical isolation and uniform spacing between the arc plates are provided by a 0.3 mm thick bakelite mask surrounding a 0.5 mm thick x 20 mm diameter silicone gasket whose purpose is to seal the discharge region from the atmosphere. The four 10 mm diameter holes in the plates carry the cooling water to the arc plates and are likewise sealed by silicone gaskets.

The pile of cascade plates in Fig. 4 is terminated by two large identical end pieces which contain the cooling water connections, gas ports and connections, and radial holes for mounting the electrodes. The central cavities in these end pieces are connected by two insulated pressure equalization tubes of large cross section through which the arc gas flows. There is little flow in the arc channel itself which rather depends upon diffusion from the end sections for its source of gas. The pressure equalization tubes also serve to minimize instabilities in the gas flows which

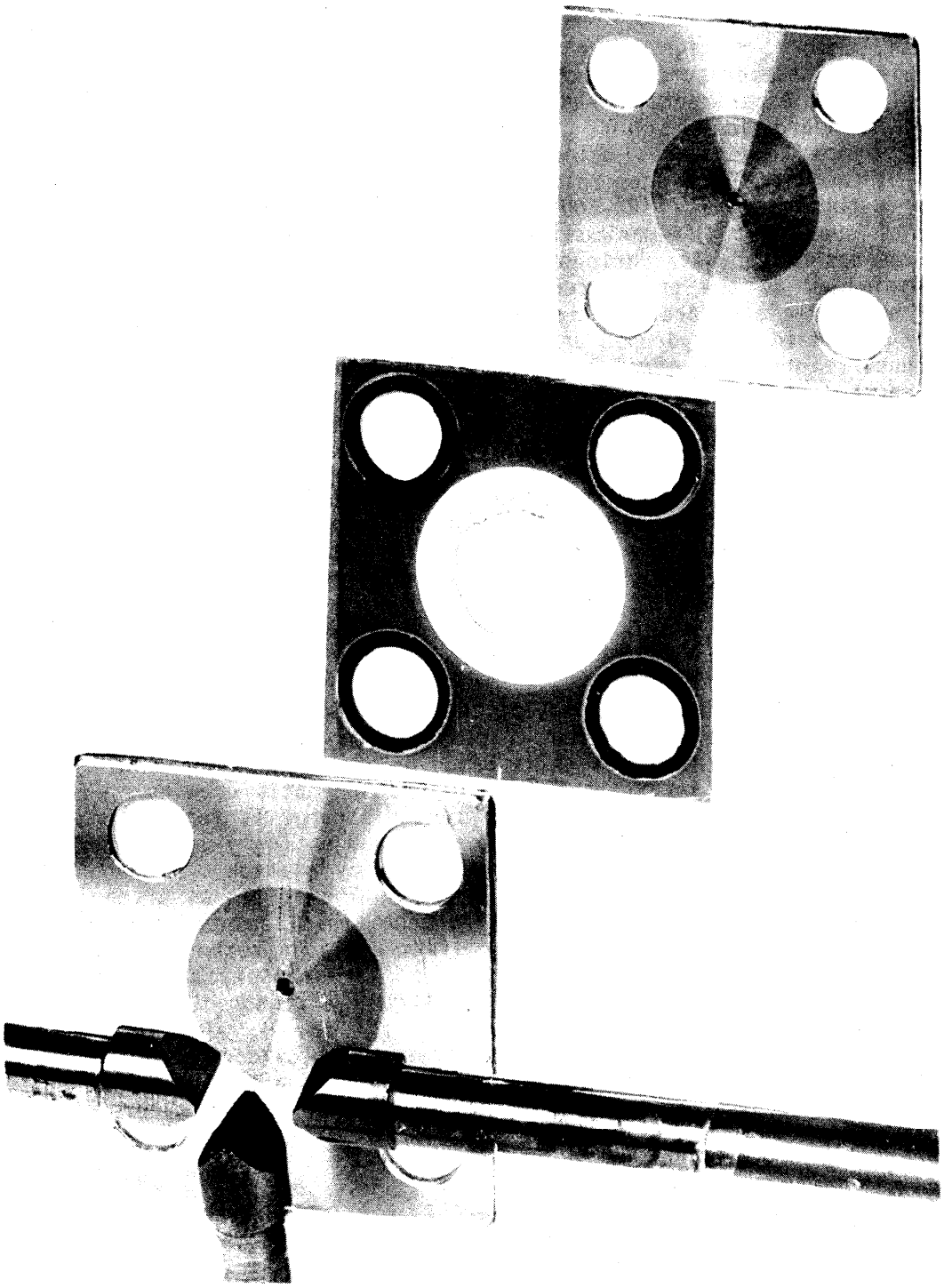

Figure 8. Exploded view of the major components of the arc: electrodes (one has been removed), two arc plates, a bakelite spacer and gaskets.

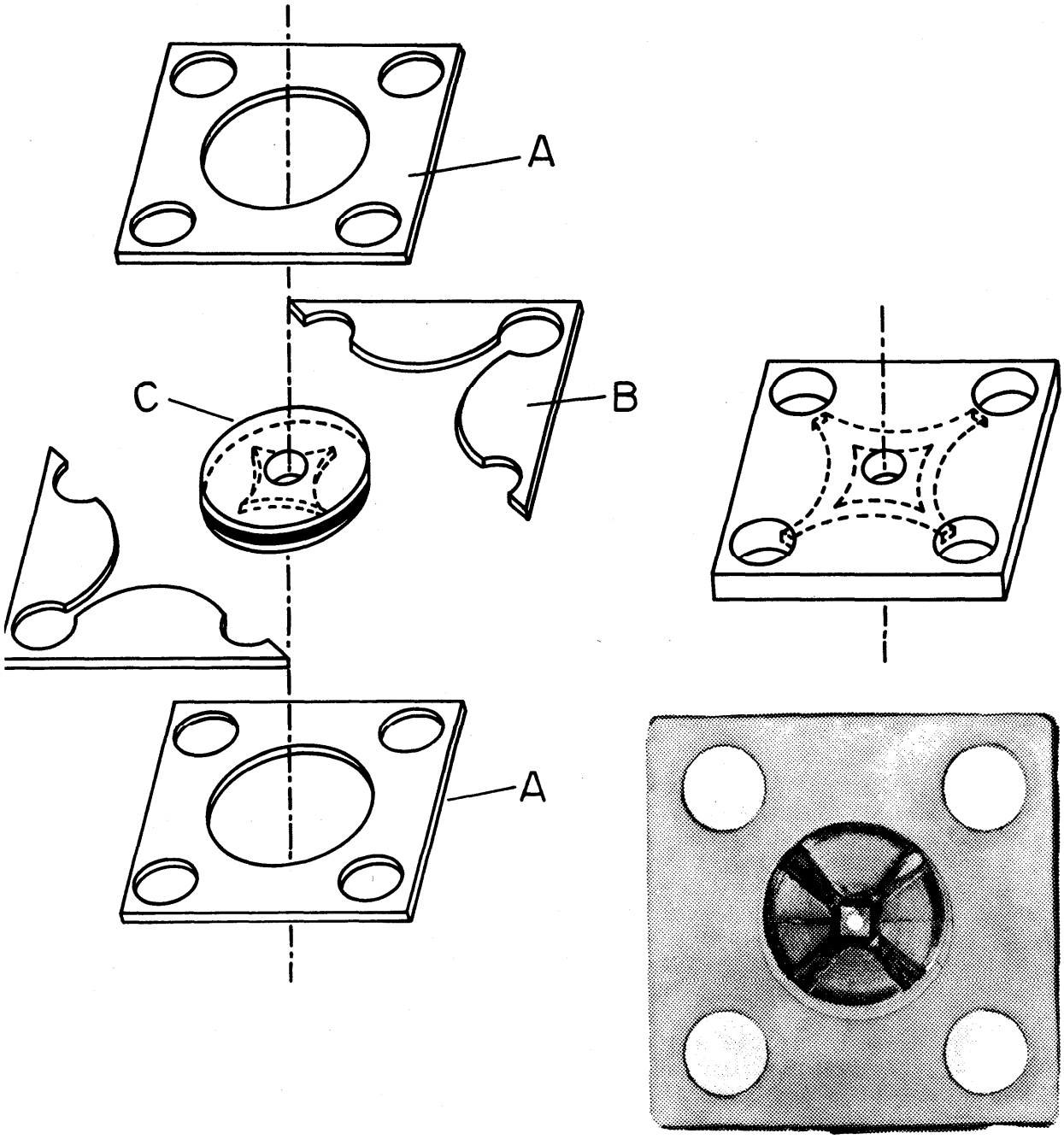

Figure 9. (a) A schematic illustrating the method of arc plate construction. (b) The assembled arc plate. (c) A photograph of an arc plate cut away in the center to expose the water channels.

may arise from small pressure fluctuations in the electrode regions due to occasional shifting of the arc termination points. If they are present, these instabilities are manifested by a varying arc length. A polycarbonate plastic extension tube is attached to the end piece on the vacuum side of the arc for the purposes of insulating the end piece from the vacuum system. It also allows remote mounting of a UV quality MgF_2 window with shutter, which doubles as an observing port for adjustment of the anodes. The window is located 17 cm from the arc because of possible degrading effects caused by heat and intense UV irradiation. Also, a gas input port directs a flow of gas onto the window and prevents it from collecting a layer of attenuating tungsten dust which is evaporated from the anodes at high power levels. The Suprasil window on the air side of the arc does not require similar precautions since the cathodes do not heat up as much as the anodes and since the window transmission, which is needed for calibrations in the near UV and visible, can be conveniently measured by simple removal during arc operation.

As can be seen in Fig. 4, the electrodes, especially insulated and sealed by o-rings, are positioned as close as possible (about 0.5 mm) to the arc plates in such a way as to form an extension of the channel. Four electrodes at each end in a cross arrangement are used in order to subdivide the heat load and to minimize arc asymmetries in the end zones near the arc termination points. The electrode cooling is provided by soldering the 48 mm long, 10 mm diameter tungsten rods which serve as the electrode tips to water-cooled copper tubes.

The arc plates themselves are of fairly complex design. Several variations, designed principally to reduce machining difficulties and increase the economy of production, have been described in the literature.[10,12] Basically, the problem is to cool the walls efficiently and to avoid the formation of vapor bubbles and consequent thermal isolation of the heated channel walls which comes about when there is poor or turbulent contact between the channel wall and the flowing water. The particular method of fabrication for our model[10] is illustrated in Fig. 9. By inserting the split brass plates labeled B in Fig. 9a into the central copper piece C, water channels are formed 4 mm wide at their ends and 1 mm wide in the bent parts near the 2 mm diameter bore as seen in Fig. 9b. In this way the water entering from two opposite sides is accelerated near the arc channel, pressed towards the hot wall, and removed through the two remaining adjacent ports. Pieces A, B and C are silver-soldered together and machined to the required thickness of 2 mm. A photograph of an arc plate assembly with the central part cut open to expose the flow channels is included in Fig. 9c.

The operation of the arc requires substantial electric, water, and gas utilities. The electric current to the arc is supplied by a 1200 V, 110 A DC power source with 0.05 percent current regulation and a ripple less than 0.2 percent of the average voltage. In order to divide the arc current equally, a 12 Ω ballast resistor is placed in series with each of the four arc anodes and cathodes. These resistors, designed for loads up to 7.5 kW, are immersed and cooled in a flowing tap water reservoir. A separate 12°C chilled water system with a total flow rate of about 80 $\ell\ min^{-1}$ at 2.5 atm pressure is used to cool the arc plates and electrodes. Since arc ignition is best performed in pure

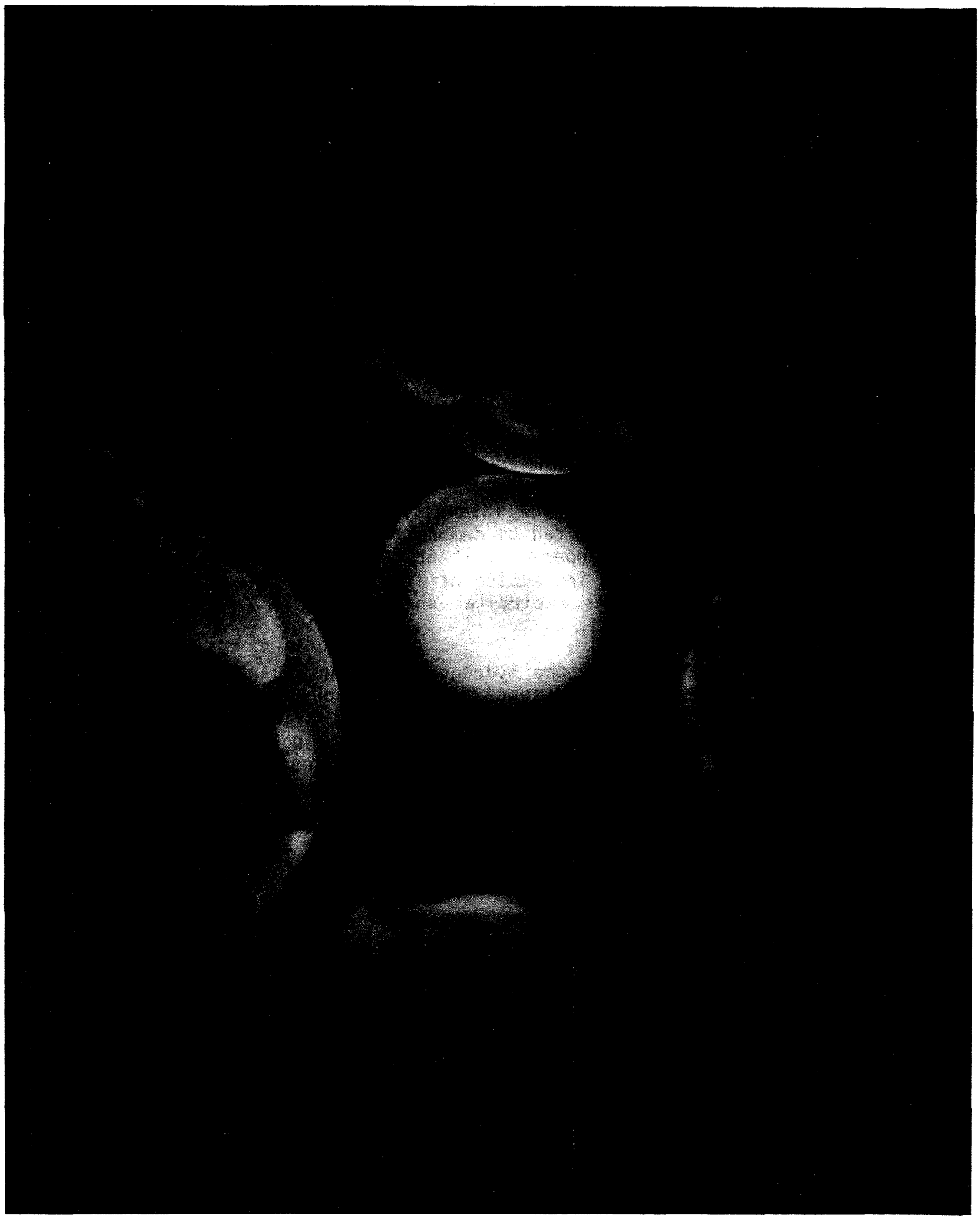

Figure 10. An end-on view of the hydrogen arc operated at 100 amperes. The temperature for maximum continuum emission has been exceeded in the vicinity of the arc axis for wavelengths in the visible. This is manifested as a slight contrast between the brighter outer edge and the darker center of the plasma.

argon gas, a simple gas handling system is required. The arc is struck at 20 A by shorting the cathode to the anode with a tungsten rod connected to the cathode potential and slowly withdrawing the rod down the axis of the arc. After adjusting the position of the electrodes and raising the current to 60 A, the argon flow is replaced by a hydrogen flow of about 5 ℓ min^{-1} through a valve and flow meter system. The high flow rate is necessary primarily to purge the extension tube between the arc and the MgF_2 window where air and water vapor absorption can affect the calibration accuracy.

As was discussed above, calibrations utilizing the hydrogen continuum are most accurate when the arc is operated at power levels such that maximum emission is achieved. The calibration procedure reduces then to a simple adjustment of the arc current for maximum signal at the wavelength of interest. At this condition the response of the system is identified with the spectral radiance calculated from the maximum continuum emission coefficient. If the arc current is increased so that the axis temperature exceeds that for maximum emission for a given wavelength, the intensity at that wavelength can be observed to decrease. This effect can be demonstrated by projecting white light from the arc onto a screen and operating it at currents well above that needed for maximum emission. A close inspection of Fig. 10 made at an angle close to the plane of the paper reveals a circular shadow about 1/3 the arc diameter and centered about the arc axis.

The long-term stability of the hydrogen arc source is excellent and depends primarily on how well one accounts for small changes in the transmission of the windows. The source stability in the air ultraviolet range of 200 nm to 360 nm is measured to be about 1 percent over a 10 hour period. However, since the vacuum ultraviolet signal of the arc with window decreases over the same period by 10-20 percent due to window degradation, calibration experiments are kept as brief as possible, and the shutter is closed between measurements to protect the VUV optics.

2. Blackbody Line Arc

The short wavelength limit of the hydrogen arc at about 124 nm is determined by the onset of the Stark-broadened, optically thick Lyman line series of atomic hydrogen that dominates the spectrum between 94 nm and 124 nm. Since the short wavelength cutoff of magnesium fluoride windows which are used in many VUV instruments is at about 115 nm, it would be convenient to have a primary standard which covers the range 115 nm to 124 nm. This need has been met with the development of the blackbody line arc.[13-15]

Blackbody radiances for a number of prominent UV spectral lines are determined in the following manner. A wall-stabilized steady-state arc source is operated at about 12,000 K in argon with small admixtures of oxygen, nitrogen, and carbon dioxide. The admixtures produce very strong emission for their principal resonance lines, which all happen to lie conveniently in the far ultraviolet, spanning a wavelength range from 115 nm to 250 nm. These extremely strong resonance lines reach the blackbody intensity limits even at very small concentrations of the elements in the plasma, i.e., they become "optically thick." More precisely, the central regions of these line profiles reach, for a small wavelength range of a few hundredths of a nanometer, the intensity a blackbody would have at the arc temperature. Thus, the arc represents, for a few narrow wavelength bands in the UV spectrum, a very high temperature blackbody. To utilize this arc as a standard source, the temperature must be accurately determined using standard plasma spectroscopic techniques including absolute radiometry in the visible region of the spectrum. Subsequently, using Planck's radiation law, absolute intensities are established for these narrow spectral bands and are utilized as calibration points. Calibrations at other wavelengths are usually found by spectral interpolation. This technique has been used in a number of experiments and has been found to be reliable, with uncertainties ranging from about 10% at 250 nm to about 25% at 115 nm. For general use, however, it has the significant deficiency that large areas of the far UV have to be covered by interpolation since very few blackbody limited lines are found outside the ranges 115 nm to 126 nm and 146 nm to 175 nm. Since we are primarily interested in the range 115 nm to 124 nm, this is no great handicap here.

The accuracy of the blackbody line method depends critically on the measurement of the arc temperature, which is applied in the Planck function to determine the intensity of the blackbody ceilings of the optically thick resonance lines. It has been estimated that no single spectroscopic method is sufficient to determine the temperature of such a plasma with small O_2, N_2, and CO_2 additions to within an uncertainty of ±2%.[13] This represents an uncertainty in the blackbody ceiling of about 10% at 250 nm and about 25% at 115 nm as was mentioned above. To reduce this uncertainty, it was recommended that several methods be applied, and the results averaged. However, a single method, which is thought to be superior, was adopted here to determine the blackbody temperature.

The blackbody ceiling of the C I emission line at 247.9 nm is measured with a UV-calibrated tungsten strip lamp. The uncertainty in the spectral radiance of the strip lamps calibrated by NBS at this wavelength is about 2%. The peak of the 247.9 nm C I line is actually calibrated in two steps:

first, the continuum emitted by the arc mixture at 250 nm is measured and calibrated at low spectral resolution using the tungsten strip lamp and the air-path predisperser and monochromator; and second, the peak of the carbon line is calibrated with respect to this continuum using the VUV instrument at high resolution. The difference in the VUV system efficiencies between 247.9 nm and 250 nm is minimal but is measured with the hydrogen arc and taken into account. Care is also taken to ensure that the contribution of the line wing at 250 nm in the low resolution air system is negligible. For a 4.7 mm diameter arc at 60 A the axis temperature of the argon plasma with admixtures of N, C, O, and H was measured to be 11,900 K. A temperature uncertainty of ±160 K is estimated due to an estimated rms uncertainty of about 6% in the blackbody intensity determination at 247.9 nm. This results in an uncertainty of 10% in the blackbody line radiances between 115 nm and 140 nm.

Besides the temperature of the plasma, the character of the blackbody limited lines is also critical. For example, if the boundary layers between the mixed plasma and the pure argon buffer are too thick, the radiation transfer may be complicated by the density and temperature gradients through the layers. Such conditions are more the rule than exception and are easily detected at high resolution as structure in the line peaks. However, by appropriate flow rate adjustments, this effect can be minimized so that the blackbody plateaus are essentially flat- topped. Referring to Fig. 6, we see that for a high power hydrogen arc the calibrated spectral radiances obtained using blackbody limited lines are consistent with the corresponding calculate quantities, as was noted above in Section III-A,1a.

B. Secondary Standards

1. Argon Mini-Arc

a. Physical Principles

After the development of the hydrogen arc as a primary standard of radiance in the VUV, it was realized that a simpler, portable, more easily operated, and lower powered transfer standard would be of great value. The hydrogen arc is complicated and difficult to operate, and requires a massive 1200 V, 110 A dc power source. A secondary standard which could be compared with our primary standard and then transported to the user's laboratory was recognized as being essential.

The most widely used transfer standard at that time was the commercially available deuterium lamp. Although the deuterium lamp has attractive properties such as its relatively strong continuum, low power requirements, and small size, it also has limitations. First, its region of applicability as a radiometric standard is restricted to wavelengths above 165 nm due to the presence of a many-line molecular deuterium band system below 165 nm. Second, the lamp exhibits a variability related to the positioning of the discharge on the electrodes following each ignition. Finally, the deuterium lamp has aging characteristics which are not well known. At the least, this means that the lamp must be frequently recalibrated to ensure accuracy.

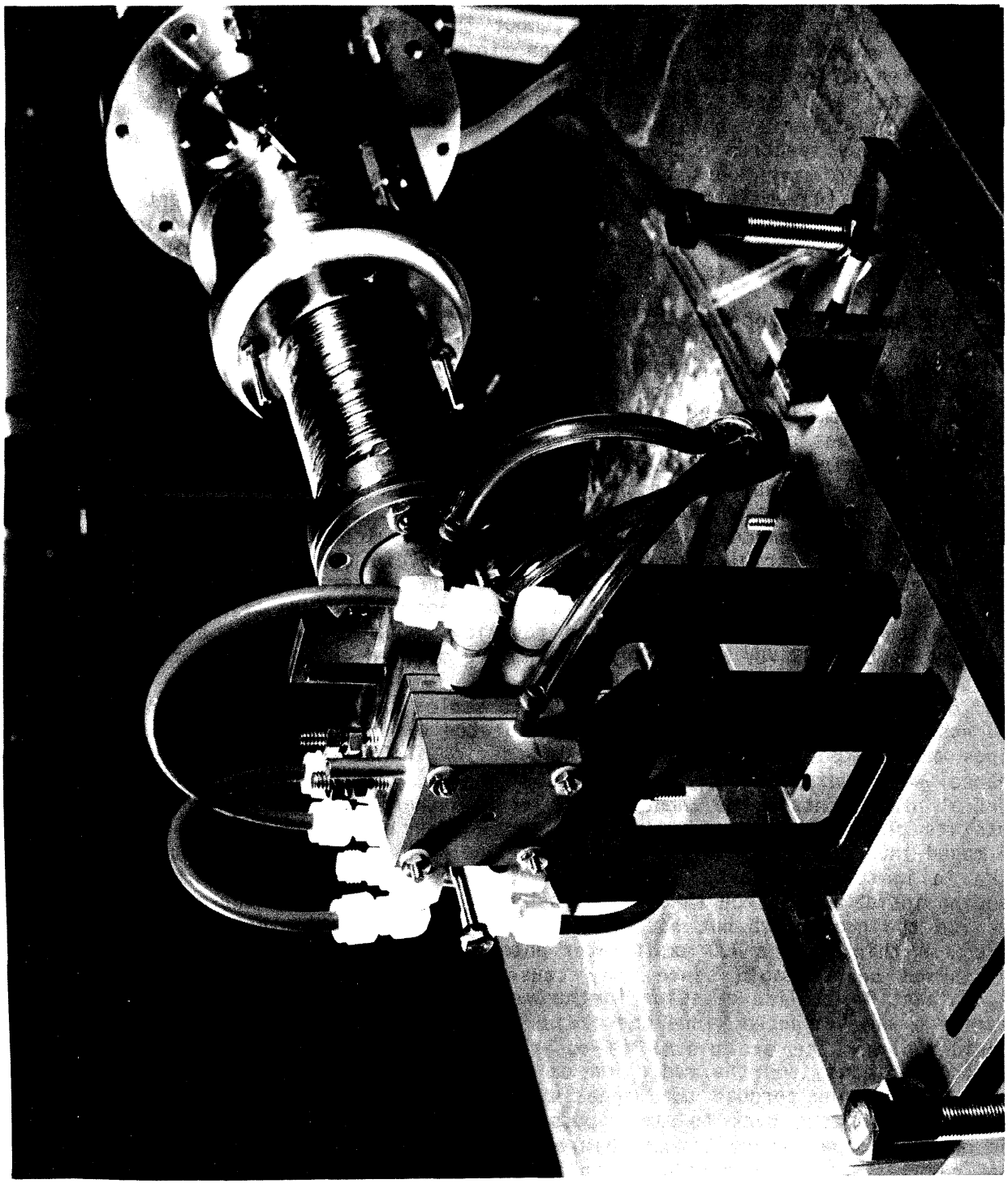

Figure 11. A photograph of the argon mini-arc mated to a monochromator.

To meet the lack of adequate transfer standards in the far UV, the argon mini-arc was developed at NBS.[16] This source can be conveniently applied as a radiometric transfer standard without the limitations of the deuterium lamp. The wavelength range of the argon mini-arc overlaps the lower range of the tungsten strip lamp in the near UV and extends beyond the short wavelength limit of the low pressure deuterium lamp at 165 nm. The mini-arc was designed to fulfill, insofar as possible, the following goals: (1) an intense line-free continuous spectrum between 115 nm and 330 nm; (2) stability and reproducibility over many hours of operation; (3) light source and power supply both portable; (4) uniform output over a large solid angle; (5) radiant power output adjustable over a range of several decades; and (6) simple alignment and operation. We now proceed to discussions of the arc construction and operating characteristics.

b. Description of the Arc

Figure 11 is a photograph of the arc source. The model described here was designed specifically for use as a secondary radiance standard and is different in some respects from arc sources previously designed for other purposes. It was developed after experimentation as the simplest model which meets the requirements listed above. Argon was chosen as the operating gas because of its suitability in providing a stable discharge and an intense, line-free UV continuum with minimal power requirements. In the photograph the arc is mated to a monochromator with a stainless steel bellows. Water cooling connections and a triple-tube manifold for supplying argon are also shown. The two vertical threaded posts on the top of the arc are the electrical connections to the anode and cathode. The arc is mounted on an adjustable table which allows precise translation and rotation about two axes. All sources utilized in the NBS VUV radiometry program are mounted on this type of table.

As shown in Fig. 12, which is drawn to scale, the arc source is constructed essentially of five copper plates separated by silicone rubber insulating rings and clamped together to form the device. The central plate forms a channel which guides and constricts the discharge. The plates adjacent to the central plate contain the anode, a 3.2 mm diam thoriated tungsten rod pressed into its plate, and the cathode, also of tungsten but mounted so that it can be moved into and out of the arc channel. The cathode was made adjustable for ease in igniting the arc. All five plates are water-cooled with the water flowing inside each piece through holes drilled in the sides. These holes are seen in the photograph but not in the diagram. The arc constricting section is 6.3 mm thick with a 4.0 mm diameter hole. Diameters smaller than this were considered unacceptable since they caused a higher plasma temperature and significant Ar II line emission in the wavelength region of interest. Larger diameters were rejected since the radiant power for a given current decreased considerably. The arc plasma is observed end-on through the holes in the electrode pieces, and the radiation calibrated is that emitted along the arc axis and emerging through the magnesium fluoride window on the cathode side. This window is set back to avoid possible contamination from the discharge. The gas purity necessary to maintain arc stability and reproducibility of the continuum emission is insured by operating with a continuous flow of argon. Maintaining a high degree of argon purity within the arc chamber also minimizes the radiant power of atomic resonance lines in the spectrum which arise from small (ppm) concentrations of oxygen, nitrogen, carbon, and hydrogen.

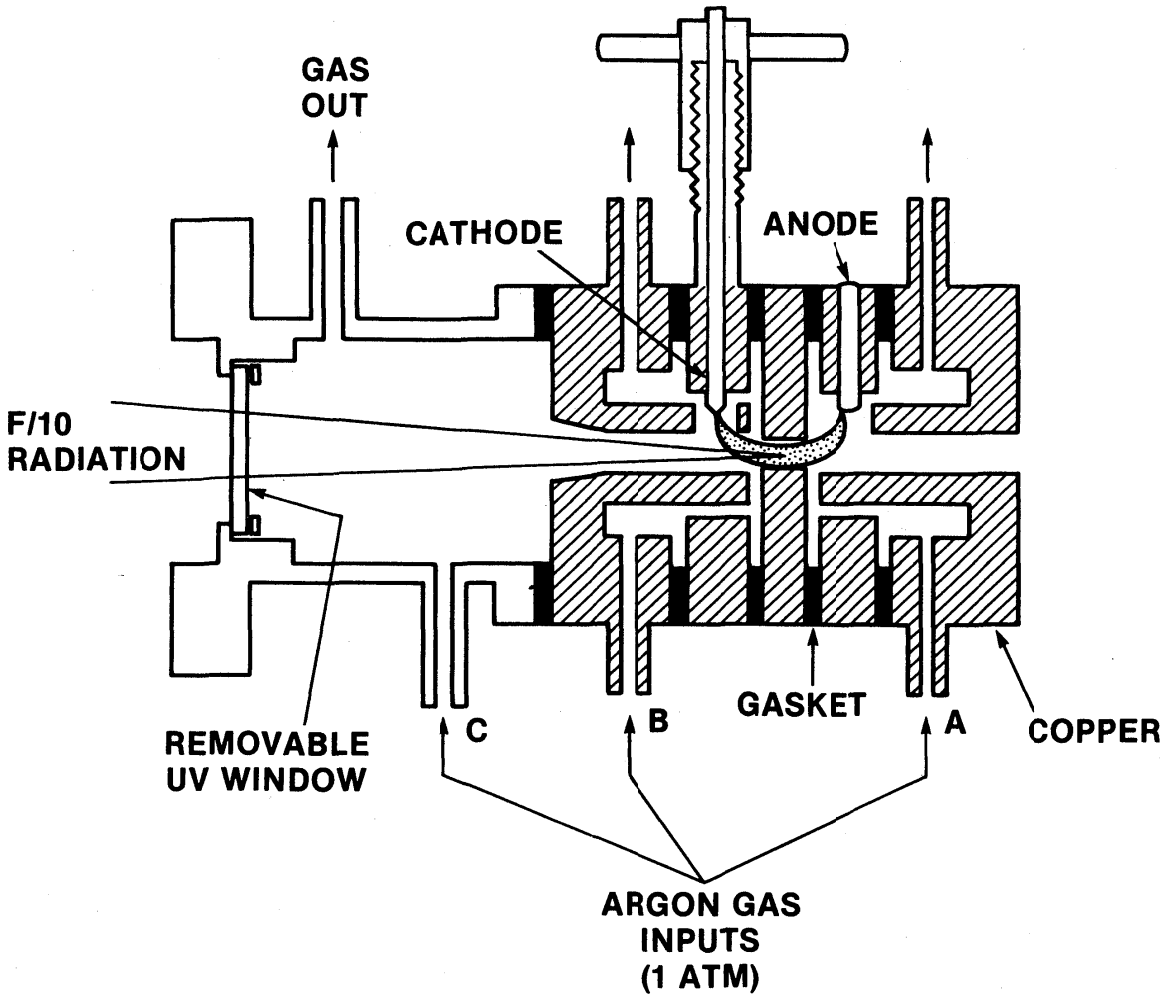

Figure 12. A schematic of the argon mini-arc light source.

These elements are present due to air and water vapor in the arc chamber and gas handling system. The positions of the gas inlet and outlet ports are chosen to keep all sections of the arc chamber thoroughly purged. The argon is admitted to the inlet ports through plastic tubing connected to a flowmeter. Under the flow rate used here, the pressure in the chamber is unchanged from the ambient atmospheric pressure. The arc may be operated most conveniently with the outlet ports open and the data given below used to account for local and temporal differences in atmospheric pressure, if necessary.

Optical alignment can be performed by sighting with a telescope or laser beam down the arc axis. The distance for proper focus should be measured to the center of the middle copper piece.

The arc discharge is initiated by applying voltage between the electrodes and then inserting a tungsten rod, which is externally connected to the anode potential, until it touches the cathode protruding into the arc channel. The discharge is transferred from the tip of the rod to the anode as the rod is withdrawn. Finally, the cathode is withdrawn from the channel as shown in Fig. 12. Power for the discharge is furnished by a current regulated supply, the size of which is determined by the current required. For example, the power supply used in some of our experiments was a 1.2 kW, high efficiency switching regulator weighing only 10 kg. For starting the arc without difficulty, it was found necessary to use a ballast resistor of about 0.5 Ω in series and to apply a potential of at least 40 V. The arc can be started at currents above 10 A, and after ignition the resistor may be shorted out if desired. For currents above 10 A the voltage drop across the arc is nearly constant at 28 V.

In developing the arc model presented here, various designs were tested. Arcs were constructed with different dimensions and numbers of confining plates; several were provided with a window for measuring the radiation emitted side-on, i.e., perpendicular to the discharge axis. Upon observing the discharge side-on midway between the electrodes, a feature in the continuous spectrum was seen which is not apparent looking end-on. This was a broad peak in the continuum centered at 130 nm, with a halfwidth of about 10 nm. By scanning across the arc diameter, this radiation was observed to be emitted most strongly from a region well away from the arc axis, where the temperature is much lower than its value at the axis. This radiation arises from a molecular argon continuum.[17] Its spatial distribution and intensity were found to be strongly dependent upon gas flow rates. For this reason, it was decided that the radiation emitted side-on was not appropriate for application as a reliable standard and that the radiation emitted end-on would be the quantity to be investigated further and finally calibrated.

Wall-stabilized arcs employed for end-on measurements usually are constructed of many constricting plates or disks, in order to obtain a nearly homogeneous plasma extending along the axis to the boundary regions near the electrodes at each end. These boundary regions emit a negligible part of the radiation emerging along the arc axis. The hydrogen and blackbody arcs which we use for primary radiance calibrations are necessarily of this type, since the lengths of the emitting plasma columns must be well defined. In such cases, however, the solid angle over which uniform radiation can be observed

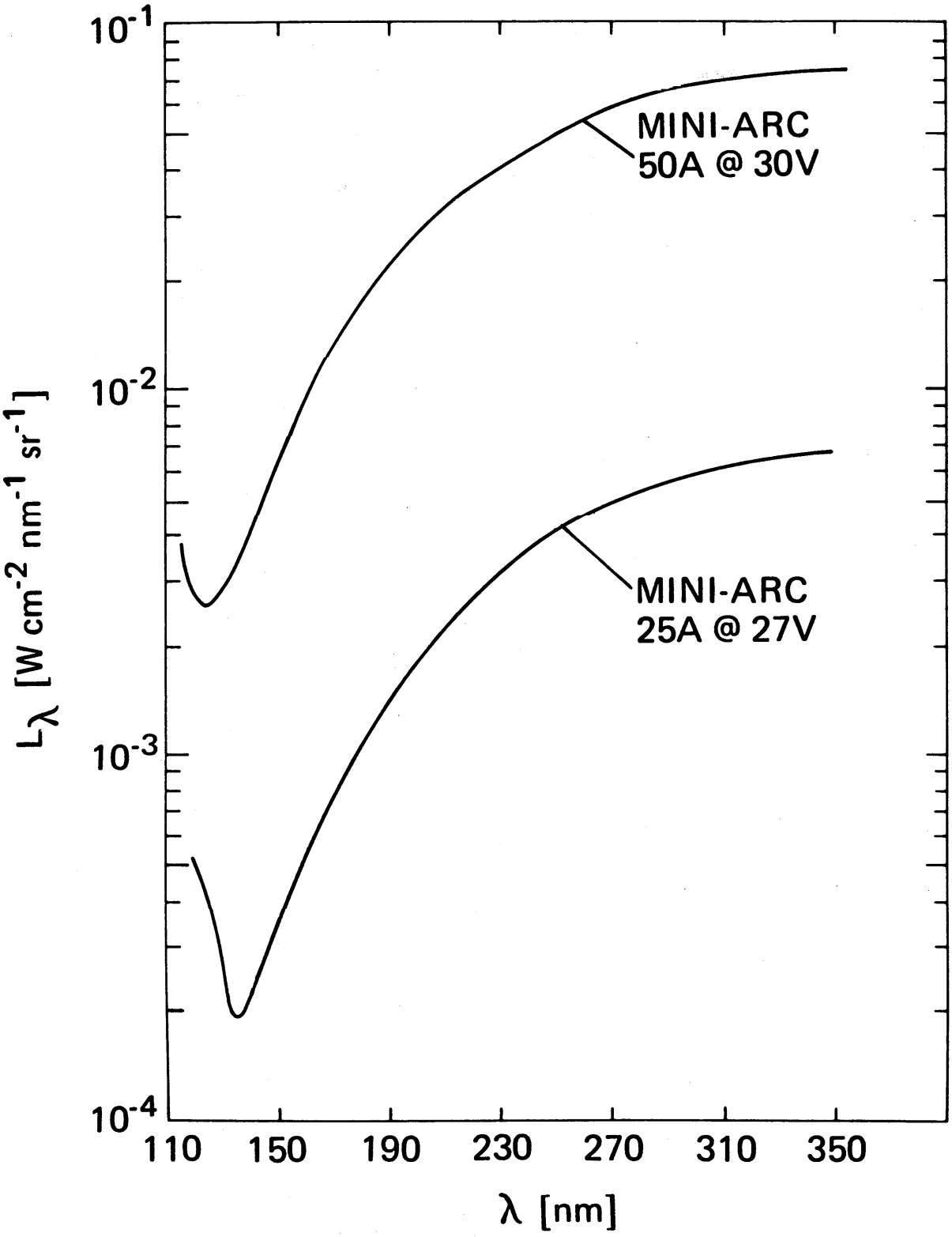

Figure 13. Spectral radiance as a function of wavelength for a mini-arc with an arc plate diameter of 4.0 mm operated at two different currents: 50.0 A and 25.0 A.

Table II. Spectral Radiance as a Function of Wavelength for a 50.0-A Argon Mini-arc Light Source with an Arc Plate Diameter of 4.0 mm[a]

λ(nm)	L_λ (mW cm^{-2} nm^{-1} sr^{-1})	T	λ(nm)	L_λ (mW cm^{-2} nm^{-1} sr^{-1})	T
330.5	70	0.945	198.0	26.6	0.900
325.5	70	0.943	192.5	24.0	0.900
320.5	69	0.942	191.0	23.5	0.894
315.5	69	0.942	186.0	20.8	0.891
310.5	68	0.941	181.0	18.4	0.883
305.5	67	0.940	176.0	16.1	0.873
300.5	66	0.939	173.5	15.0	0.870
295.5	64	0.939	170.0	13.6	0.860
290.5	63	0.938	166.5	11.8	0.850
285.5	62	0.938	165.0	11.1	0.848
280.5	60	0.938	162.0	9.9	0.840
275.5	58	0.938	159.5	9.3	0.826
270.5	57	0.937	157.0	8.3	0.810
265.5	55	0.937	155.0	7.8	0.798
260.5	54	0.937	153.5	7.3	0.785
255.5	52	0.935	151.0	6.5	0.765
250.5	50	0.933	148.5	5.9	0.740
245.5	48.1	0.932	147.0	5.4	0.724
240.5	45.2	0.931	144.0	4.73	0.700
235.5	43.3	0.928	139.5	3.81	0.672
230.5	40.9	0.925	135.0	3.38	0.655
225.5	39.1	0.922	129.5	2.77	0.662
220.5	36.3	0.920	127.0	2.65	0.642
215.5	34.6	0.917	123.5	2.54	0.626
210.5	32.4	0.914	118.5	2.77	0.597
205.5	30.3	0.910	116.0	3.34	0.530
200.5	27.9	0.900	114.5	3.74	0.439

[a] The measured transmission T of the arc window is also listed. The radiance of the plasma itself is obtained by calculating the quantity $L_\lambda T^{-1}$.

is small (f/200 is used for calibrations with the hydrogen and blackbody arcs) and not convenient for the calibration of many optical systems. For a transfer standard, on the other hand, the arc length does not need to be precisely known as long as it is a reproducible quantity. Thus, in order to provide a much greater solid angle, the argon mini-arc was made with only one constricting plate. Measurements discussed below show that this construction provides a rather large angular beam of radiation (f/10) having a practically uniform intensity distribution. This should be considered an advantage even if one does not require such a large solid angle, since having the larger available angle makes the angular alignment of the mini-arc less critical.

c. Spectrum

Figure 13 illustrates the spectral radiance of the argon mini-arc light source for two arc currents: 25.0 A and 50.0 A. The continuous spectrum of the argon arc arises primarily from atomic recombination radiation. Near the short wavelength end the molecular continuum mentioned above contributes to some degree, and below 125 nm the increased output is from the wings of the argon resonance lines at 106.7 nm and 104.8 nm. Below the MgF_2 window cutoff, one should expect to have strong emission on the wings of the resonance lines with complete absorption at their centers. Below 80 nm there should be complete resonance continuum absorption by ground state argon atoms.

The spectral radiance was determined by direct comparison to the NBS wall-stabilized hydrogen arc[1] between 130 nm and 330 nm and to a plasma blackbody line radiator below 130 nm.[1,3,13] Data were taken with a spectral resolution of 0.01 nm. The temperature of the blackbody line radiator was determined to be 11,800 K ± 100 K by directly measuring the blackbody ceilings at 193 nm, 174 nm, 165 nm, 149 nm, and 146 nm, using the hydrogen arc as a primary standard of spectral radiance. With this temperature the radiant power of other blackbody limited lines emitted below 130 nm could then be calculated. For the calibration of longer wavelengths (>210 nm), the second-order spectrum from shorter wavelengths was eliminated by purging the small volume between the arc and the spectrometer with oxygen. Below 210 nm, argon was used as the purge gas.

The spectral radiance values illustrated in Fig. 13 and listed in Table II apply to the plasma radiation emitted along the axis of the mini-arc which is imaged on a 0.30 mm diameter aperture (magnification = 1) at a solid angle f/200. The basic uncertainty in the spectral radiance is ±5% above 140 nm and ±10% below 140 nm due to uncertainties in the primary radiometric standards. Also included in Table II for reference purposes is the measured transmission of the MgF_2 window used on the mini-arc. If one wishes to know the spectral radiance of the plasma itself, the figures in the table must be divided by the transmission. Known systematic deviations or uncertainties in the radiant power due to different operating or imaging conditions are described in subsequent sections.

There are no Ar I lines in the spectrum between 114 nm and 330 nm. Below 200 nm there are several narrow Ar II lines and atomic nitrogen, carbon, and oxygen lines in the mini-arc spectrum due to air impurities in the argon gas (99.999% pure). In addition the hydrogen Lyman alpha line at 121.6 nm is

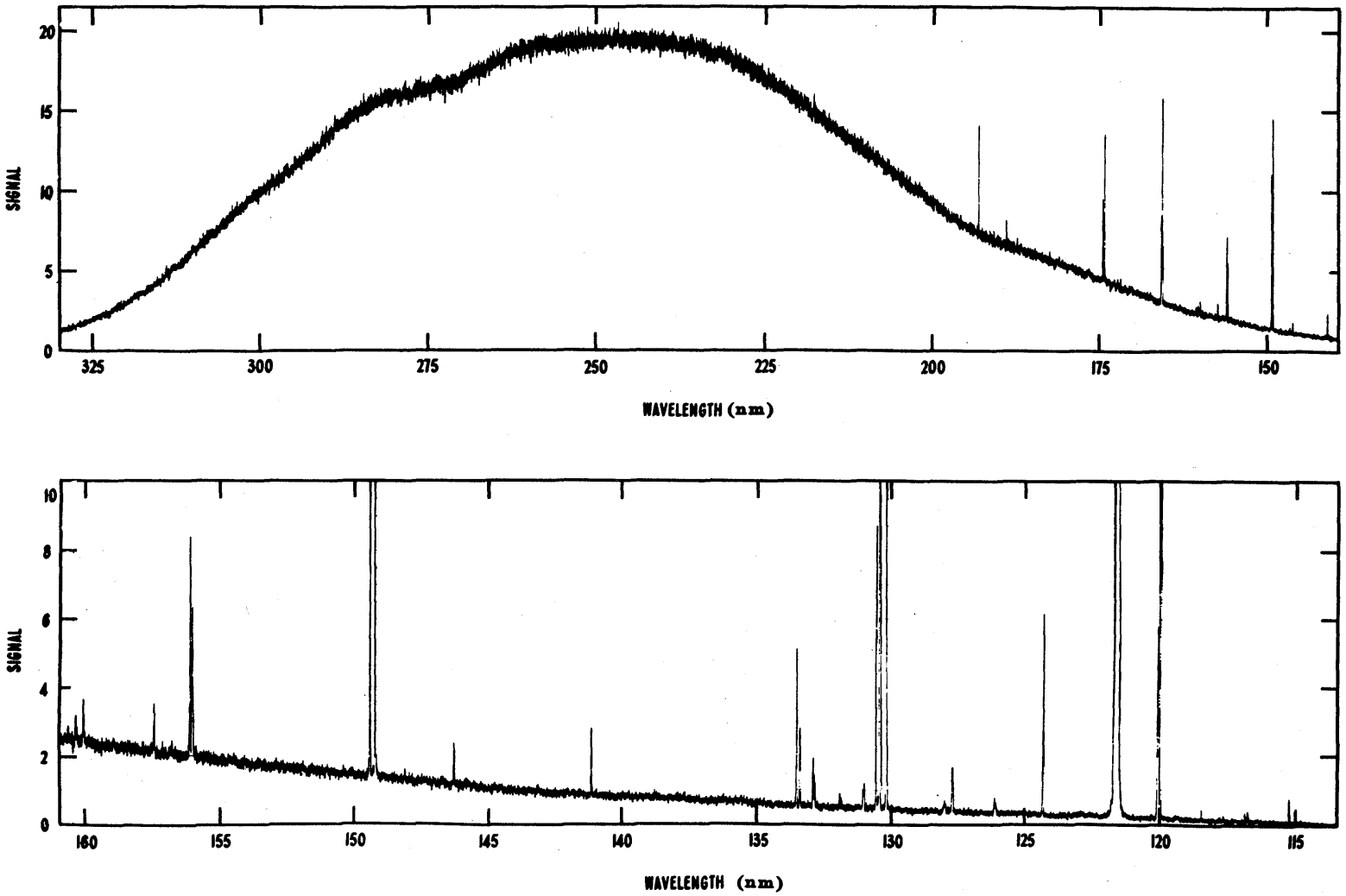

Figure 14. A photoelectric scan of the spectrum of the argon mini-arc between 115 nm and 320 nm, taken with a 0.01 nm spectral resolution and with a solar blind phototube detector.

Table III. Survey of Emission Lines Appearing in Spectrum of Mini-arc

λ(nm)	Identification	Radiance relative to continuum[a]
115.22	O I	1
116.79	N I	1
117.69	N I	0.3
118.94	C I	0.3
119.38	C I	1
119.99	N I	30
121.57	H I	100
124.33	N I	5
126.13	C I	2
127.75	C I	5
128.98	C I	1
130.22	O I	15
130.55	O I	10
131.07	N I	1
131.95	N I	0.5
132.93	C I	4
133.53	C II	8
135.58	C I	0.2
141.19	N I	0.7
143.19	C I	0.1
145.91	C I	0.1
146.33	C I	1
146.75	C I	0.1
148.18	C I	0.2
149.26	N I	4
149.47	N I	6
156.10	C I	4
157.50	Ar II	0.2
160.04	Ar II	0.2
160.35	Ar II	0.1
160.65	Ar II	0.05
165.72	C I	2
174.27	N I	1
174.53	N I	0.5
175.19	C I	0.1
187.31	Ar II	0.05
188.90	Ar II	0.1
193.09	C I	2
247.86	C I	0.05

[a] In column three are listed line radiances relative to the continuum, measured with 0.25-nm spectral resolution.

present due to trace quantities of water vapor throughout the system. These impurity lines can be seen in Fig. 14 which is a photoelectric scan of the spectrum between 115 nm and 320 nm. The halfwidths of the lines are on the order of 0.01 nm, and the lines are well separated. Their presence has no significant influence on the ability to make absolute continuum measurements except when extremely coarse wavelength resolution is used, as would be the case, for example, if the monochromator were replaced by relatively wideband filters. All lines observed in the spectrum are listed in Table III. From this list one may readily determine if, for a given wavelength and bandpass, one is free of lines. This precaution is necessary since the amount of trace impurities in the arc and the corresponding line intensities may vary somewhat from one system to another.

Figure 15 compares the spectrum of the mini-arc with several other light sources which have been applied as spectral radiance standards. Included in this figure is a representation of the spectra of the two primary standards, the hydrogen wall-stabilized arc and the blackbody line radiator, which were used to calibrate the mini-arc spectrum. The figure clearly illustrates the main advantages of the new transfer source. The mini-arc has substantially larger output and longer UV wavelength range than either the deuterium lamp or the tungsten strip lamp. Also, scattered visible light is not a significant factor, as it is when a tungsten lamp is used as a UV light source. The visible light from the argon arc is of the same order of magnitude as the near UV light, and there are less than 2 orders of magnitude difference between the radiance at 110 nm and at 330 nm.

2. Argon Maxi Arc

A recent advance in the arc standards program at NBS is the development of the argon maxi-arc. This source is essentially a high powered version of the mini-arc with three or four arc confining plates instead of one and power ratings of 5-10 kw instead of 1.5 kw. The maxi- arc with three plates has an irradiance approximately thirty times that of a mini-arc and was designed to enable calibrations to be performed at a level comparable to the solar irradiance in the near UV (250-350 nm). The discussion of the mini-arc given above generally applies also to maxi-arcs except for the powers and radiances. Figure 15 gives a comparison of the spectral radiance of the maxi-arc with that of several other UV primary and transfer standard sources. Several of these arcs have been supplied for use in calibration of space experiments.

3. Deuterium Arc Lamp

a. Introduction

A source which has advantageous properties as a radiometric standard and is quite convenient to use is the molecular deuterium arc lamp.[18] This lamp has considerable UV radiant power, is light and compact, is low-powered (30 W), and with maximum radiant power at 190 nm has a very favorable ratio of UV to visible radiant power. This last fact is important in avoiding systematic errors due to visible scattered light effects when making measurements in the UV. Its disadvantages are that it is restricted to wavelengths above 165 nm due to the presence of a many-line molecular band system below 165 nm;

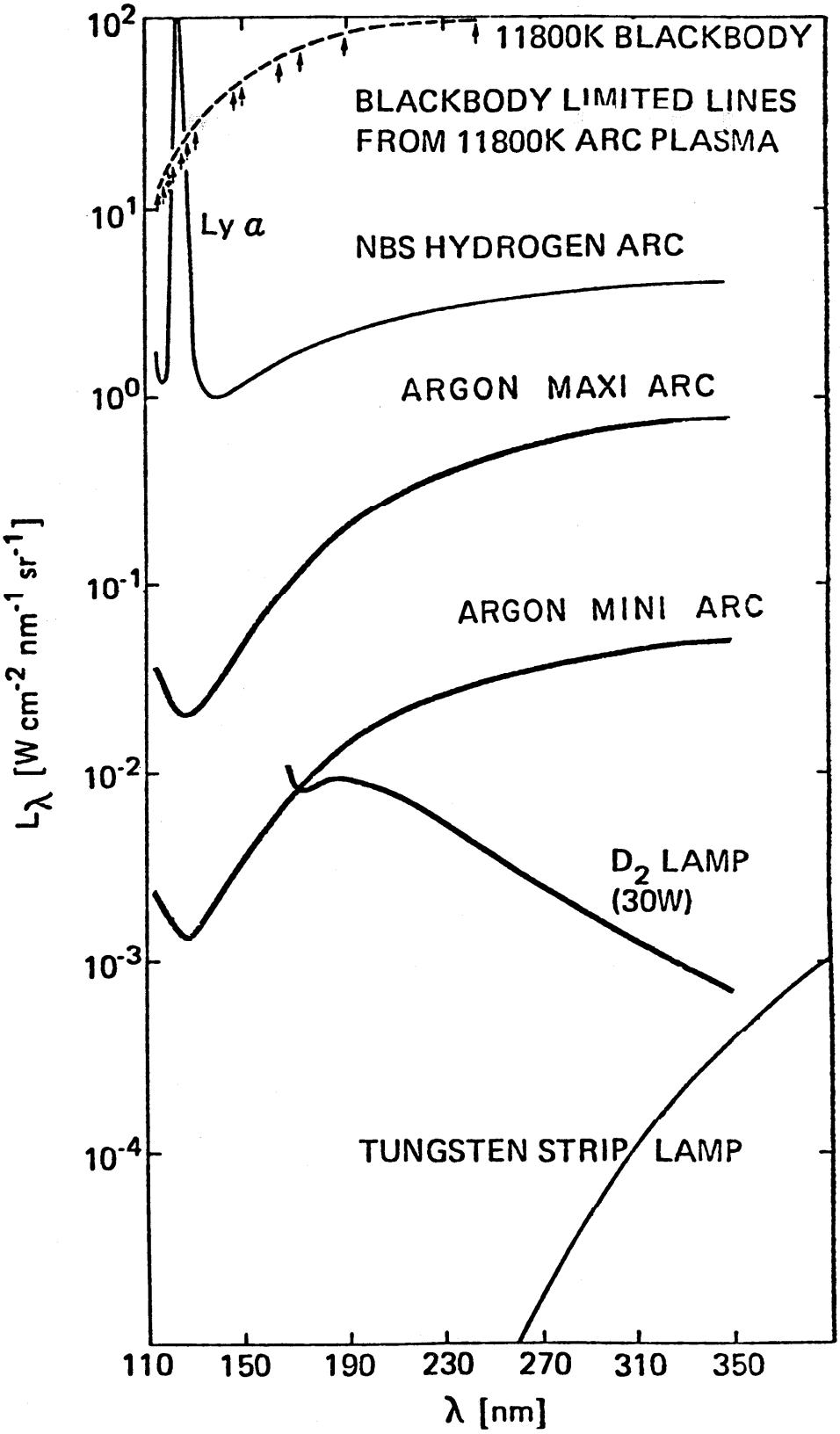

Figure 15. Comparison of the spectral radiance of several UV primary and transfer standard sources.

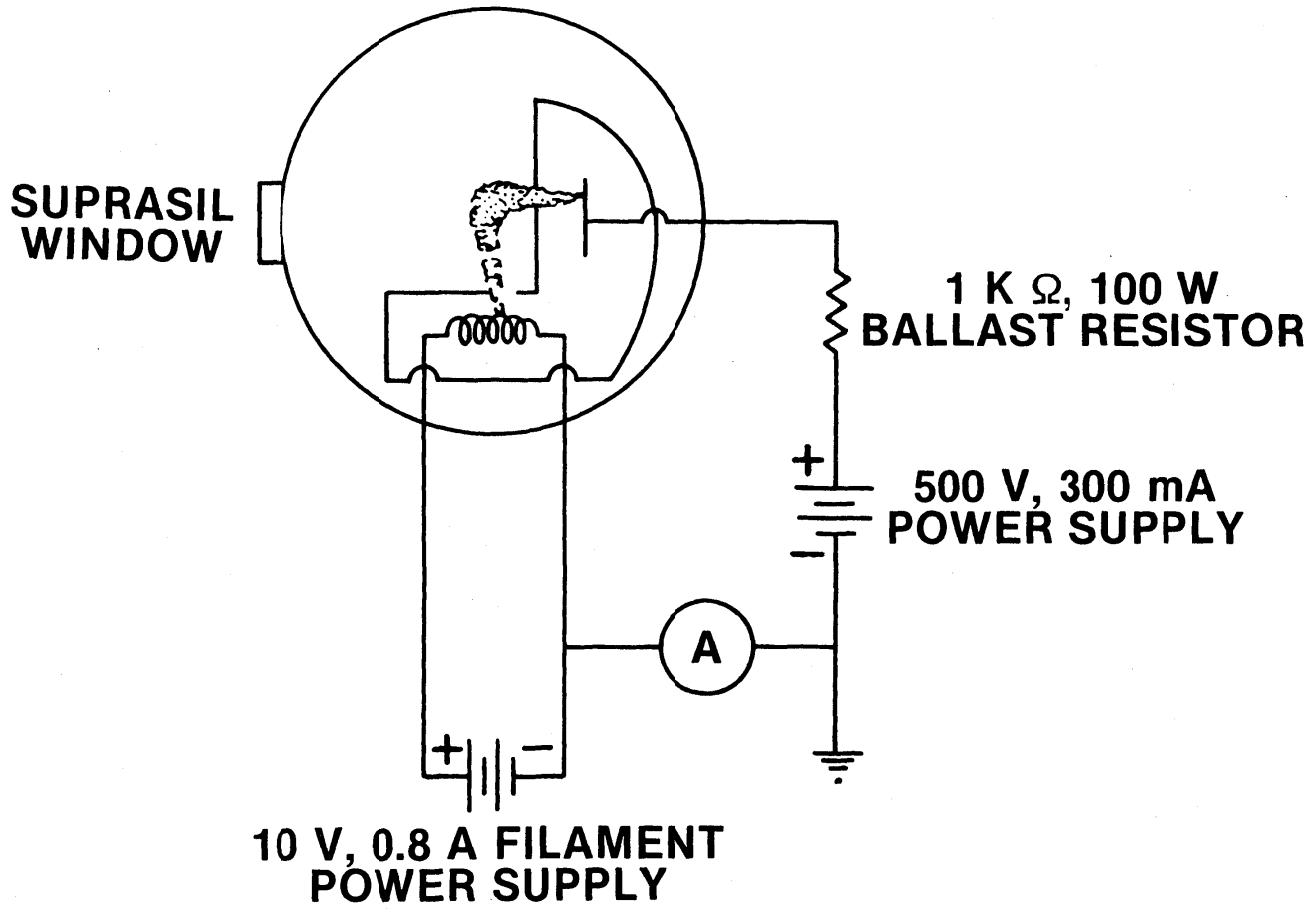

Figure 16. Schematic illustrating the operation of a deuterium lamp. The radiation is measured through the Suprasil window sealed to the quartz lamp envelope.

it may exhibit a variability in the positioning of the discharge on the electrodes following each ignition; and its aging characteristics are not well known. On balance, however, the advantages of the deuterium lamp outweigh its disadvantages making it an essential component of any program of UV radiometry. The following discussion will describe the calibration of the deuterium lamp for spectral irradiance in the range 167-350 nm.

Discussion of the spectral radiance calibration of the deuterium lamp is not presented here since it is not a standard calibration service offered by NBS. However, this type of calibration can be requested under the category "Special Tests of Radiometric Devices in the Near and Vacuum Ultraviolet."

b. Description and Operation of the Lamp

A schematic illustrating the operation of the deuterium lamp is shown in Fig. 16. In order to start the lamp, the cathode coil is first heated for 5 sec by a dc power supply (10 V at 0.8 A) in order to provide some free electrons which facilitate initiating the discharge. When a voltage of about 400 V is applied to the lamp, an arc forms between cathode and anode in the general form of an L. Most of the UV light is generated at the constricting aperture (1 mm diameter in our case) located in front of the anode. The main dc power supply is a 500 V, 300-mA constant current supply, with 0.1% current regulation. A ballast resistor (1kΩ, 100 W) is used in the anode circuit because most power supplies cannot react fast enough to maintain a constant arc. After the arc is started, the voltage across the arc drops to about 100 V. At this point the heater current is switched off, and the lamp output stabilizes in 20 minutes or less. If the lamp is switched off, it should be allowed to cool back to room temperature before restarting.

Because of variations in fabrication from one deuterium lamp to another, optical alignment of the deuterium lamp with respect to one of its physical characteristics does not necessarily result in a lamp whose radiant output is least sensitive to alignment uncertainties. Therefore, optical alignment of lamps calibrated at NBS is achieved with respect to a precision bipost base in which each lamp has been individually positioned and potted to yield maximum irradiance. Through this technique any number of deuterium lamps can be put into the system in a reproducible way such that uncertainties in the spectral irradiance due to small variations in alignment are minimized. Also, since the bipost base is identical with the one used to mount NBS calibrated tungsten-quartz-halogen lamp standards,[19] these potted deuterium lamps are compatible with calibration systems designed to accommodate the quartz-halogen lamp. Figures 17 and 18 show a line drawing of the deuterium lamp and a photograph of the deuterium lamp and the quartz-halogen lamp emphasizing their common bipost base. The orientation procedure is as follows. First, the bipost base, mounted in a kinematic support,[20] is positioned so that the optical axis of the spectroradiometer optics forms a perpendicular with the plane defined by the front surfaces of the posts and passes midway between the posts, 9.5 cm above the bottom of the posts. This adjustment was made precisely and quickly with the use of an auxiliary alignment jig made by sealing a piece of glass plate onto the posts of an identical base mounted in the kinematic support; an etched cross on the glass serves as a target for a laser beam, and the mount is adjusted so that the laser beam reflects back on itself. With the position of the base so determined, the deuterium lamp is

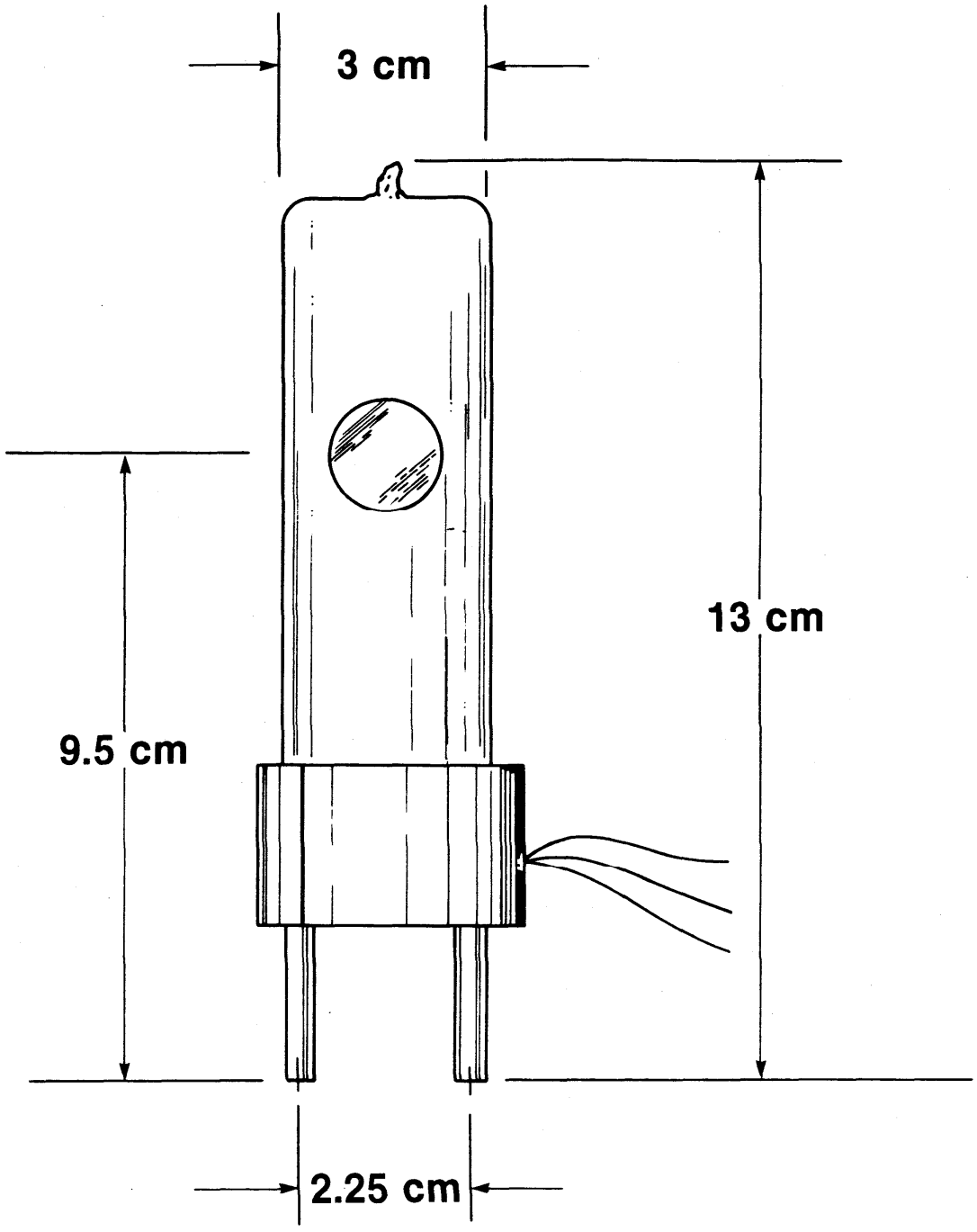

Figure 17. Line drawing of the deuterium arc lamp standard.

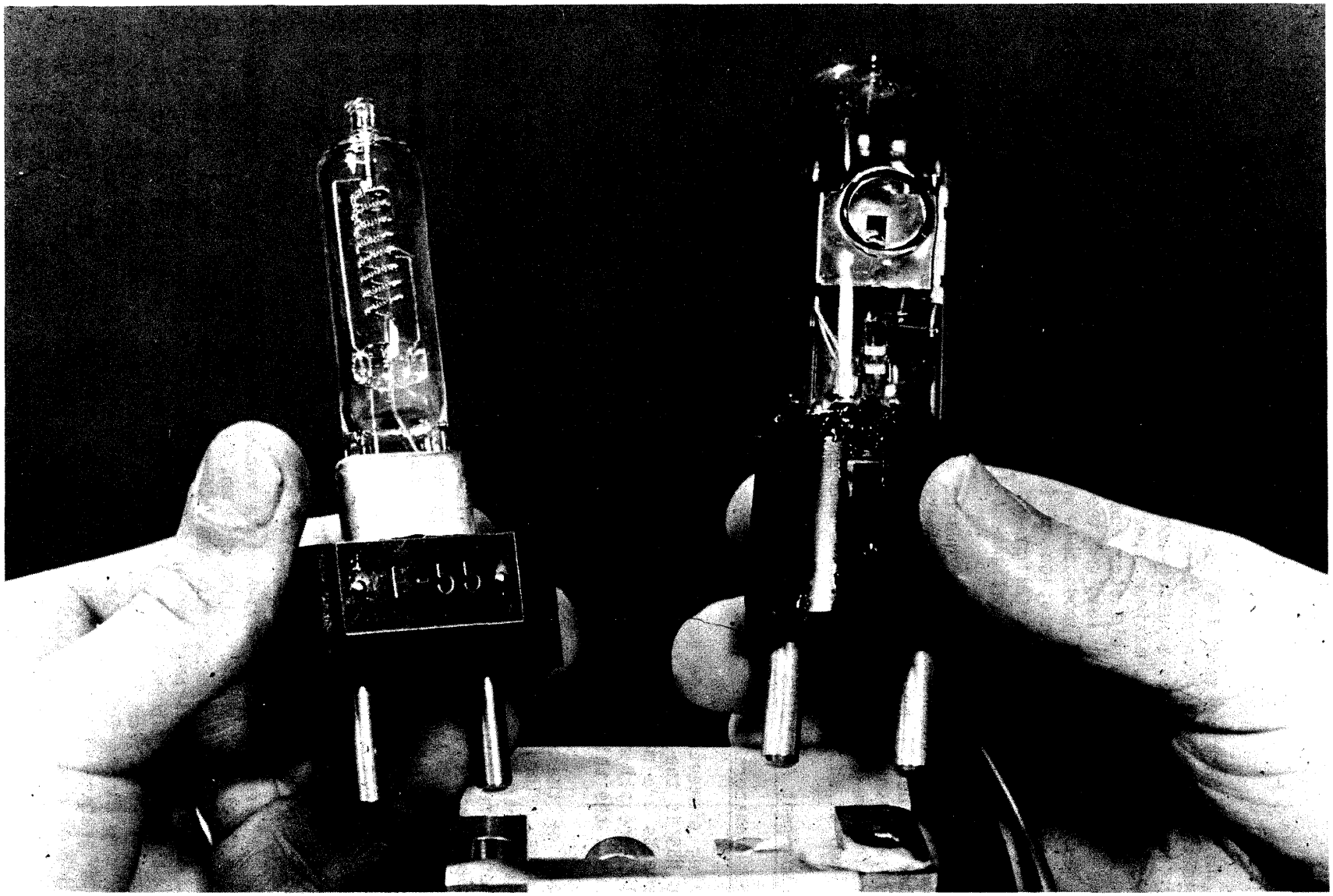

Figure 18. Photograph of the deuterium lamp and the tungsten-quartz-halogen lamp highlighting their common bipost base..

placed in the base so that the laser beam passes through the center of the 1 mm diameter discharge-constricting aperture inside the lamp. The pitch and yaw of the lamp are then adjusted about the center of the 1 mm lamp aperture for the condition giving maximum spectral irradiance at 250 nm, as measured using a 0.3 mm diameter field stop and diffusing window as the monochromator entrance slit optics. The lamp is then potted in the base. It can now be positioned in a precise, reproducible way anywhere in the optical system by properly adjusting the orientation of the kinematic support through use of laser retroreflection from the alignment jig and then substituting the potted deuterium lamp in place of the alignment jig.

The deuterium arc lamp with quartz window was calibrated for spectral irradiance using the method of collimating apertures.[18,21,22] This method is described in detail below in Sec. IV-B. Also, the spectral irradiances of several other sources were determined using this method, and the results along with two reference spectra are shown in Fig. 19. Further aspects of the deuterium lamp as an irradiance standard are covered in Sec. V-C.

C. Measurement Apparatus

1. Monochromators

A key element of the vacuum ultraviolet portable source radiometry program at NBS is the set of three monochromators on which all spectroradiometric measurements are made. The monochromators are commercial models which until recently were all available as stock items. Two of the instruments operate in vacuum with the third operating in air.

Each of the units has been generally dedicated to a specific type of measurement. The 3 m focal length vacuum instrument is set up for measurements of spectral radiance, whereas the 1 m Seya-Namioka vacuum and 1 m air instruments are usually reserved for measurements of spectral irradiance. The 3 m monochromator is equipped with a 1200 L/mm grating with a ruled area of 65 mm x 150 mm. Its first order reciprocal linear dispersion is 0.278 nm/mm with wavelength coverage from central image to 400 nm photographically and from central image to 382.5 nm photoelectrically. The use of a magnesium fluoride entrance window limits the low-wavelength cutoff to about 115 nm. The bilaterally adjustable slits have a continuous range of widths from 10 μm to 2 mm, and a synchronous motor driven gear box provides eleven scanning speeds from 0.025 nm/min to 50 nm/min.

The 1 m focal length Seya-Namioka vacuum monochromator has a 1200 L/mm grating with a ruled area of 30 mm x 50 mm. Its first order reciprocal linear dispersion is 0.83 nm/mm with a wavelength coverage from central image to 300 nm. With a magnesium fluoride entrance window the low-wavelength cutoff here is also about 115 nm. The bilateral entrance and exit slits are continuously adjustable from 10 μm to 2 mm, and twelve synchronous scanning speeds from 0.05 nm/min to 200 nm/min are provided. The 1 m air monochromator has a 1200 L/mm grating with a ruled area of 102 mm x 102 mm. Its first order reciprocal linear dispersion is 0.833 nm/mm with a wavelength range from 200 nm to 1300 nm. The bilateral slits are adjustable from 5 μm to 2 mm, and the twelve scanning speeds range from 0.05 nm/min to 200 nm/min. To reduce scattered

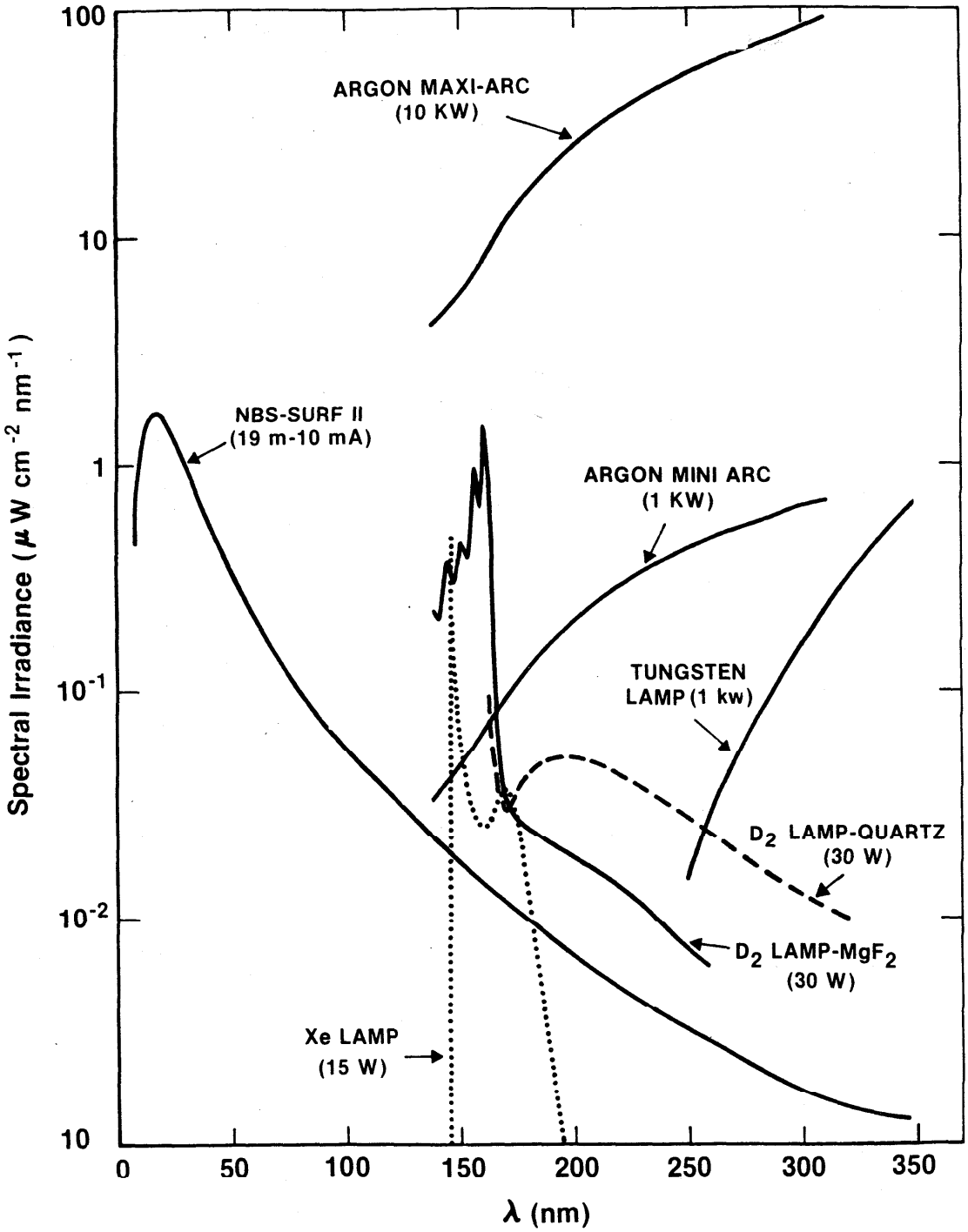

Figure 19. Absolute spectral irradiance measured as a function of wavelength at a distance of 50 cm from the field aperture for five different continuum sources with the indicated power requirements. The spectrum of the D_2 lamp with MgF_2 window below 170 nm, measured for a 1 nm bandpass, is a pseudo-continuum made up of blended lines. Shown for comparison purposes are spectra of the 250 MeV National Bureau of Standards synchrotron radiation facility, for a beam current of 10 mA and a field aperture distance of 19 m, and the tungsten-quartz-halogen lamp, for the standard 50-cm distance.

light, a 0.25 m focal length Ebert monochromator has been mated as a pre-disperser to the 1 m air monochromator. The Ebert instrument is equipped with a pair of interchangeable gratings with ruled areas of 64 mm x 64 mm. One grating with a ruling of 2365 L/mm is blazed at 300 nm for use at shorter wavelengths, and the other has 1180 L/mm with a blaze at 600 nm for longer wavelength use. The reciprocal linear dispersions are 1.65 nm/mm and 3.3 nm/mm, respectively. For irradiance measurements an integrating sphere with a 0.6 cm diameter entrance aperture is used as the diffusing element at the entrance to the pre-disperser. The inner surface of the sphere is coated with barium sulfate. For radiance measurements the integrating sphere is replaced with a 0.3 mm diameter entrance aperture.

2. System Components

a. Photomultipliers

Photomultipliers are used as detectors on our three monochromators. The two vacuum instruments are equipped with VUV-sensitive solar blind tubes, while the tube on the air monochromator has a UV-through-visible sensitivity. The solar blind tubes are operated at voltages such that the anode current does not exceed 1 nA. This is done to eliminate possible hysteresis effects which have been observed at higher currents. Scattered light is removed from the air system by the use of the previously described double monochromator setup. With the vacuum monochromators the scattered light is strongly reduced through the use of the solar blind photomultipliers.

b. Detection Electronics

The detection systems utilize picoammeters with ranges from 10^{-2} A to 3×10^{-13} A full scale as amplifiers, with the output of each picoammeter being fed simultaneously into a strip chart recorder and either a data logger or a voltage-to-frequency converter. The output of the converter is registered on an electronic counter, whereas the output of the data logger is processed by a computer. The strip chart recorder serves to monitor the data as it is being taken. The picoammeter ranges are related by factors of 3 and 10, and they are calibrated relative to one another using a "bootstrap" technique with a constant current source.

c. Specifications

The solar blind photomultipliers are end-on 18-dynode tubes having cesium telluride photocathodes and lithium fluoride windows, while the tube on the air monochromator (1P28) is side-on with nine dynodes, a cesium-antimony photocathode, and a UV transmitting glass envelope. The solar blind tubes are used over the range 115 to 360 nm, and the 1P28 is used over the range 195 to 750 nm. The solar blind tubes are potted for operation in vacuum, where one is used on the 3 m monochromator. On the Seya instrument the window on the solar blind tube serves as a vacuum interface.

The photomultipliers are operated with power supplies which show no more than 0.0025% variation in output voltage for combined line and load variations within the operating range 0 to 10mA at constant ambient temperature. The

temperature variation in voltage is within ±50 ppm/°C in the operating range 0 to 50°C after a 30 minute warmup, and the long-term drift in voltage is less than 0.01%/hr or 0.03%/24-hr at constant input line voltage, load, and ambient temperature, also after a 30 minute warmup. Finally, the output ripple is less than 15 mV peak to peak at frequencies from 5 Hz to 5 MHz.

The accuracies of the picoammeters are ±2% of full scale on the 10^{-2} to 10^{-8} A ranges and ±4% of full scale on the 3 x 10^{-9} to 3 x 10^{-13} A ranges. Zero drifts are less than 0.5% of full scale per week plus 0.02% per °C on the 10^{-2} to 10^{-12} A ranges and 1.5% per week plus 0.06% per °C on the 3 x 10^{-13} A range, with source potentials greater than 1 V and after a warmup of 10 minutes. The amplifier outputs are ±1 V for full-scale meter deflection, with noise less than 1% of full scale peak-to-peak on the 10^{-3} to 10^{-11} A ranges. The noise increases to 5% peak-to-peak on the 3 x 10^{-13} A range. Since our methods of calibration involve ratios of signals measured with a common picoammeter, we profit from the phenomenon that the systematic errors in the ratios are smaller than the systematic errors in the measured signals. This is shown by the following expression,

$$\Delta\left(\frac{S_X}{S_R}\right) = \frac{1}{S_R}\left(\Delta S_X - \frac{S_X}{S_R}\Delta S_R\right), \qquad (1)$$

where S_X and S_R are the measured signals of the unknown and standard sources and ΔS_X and ΔS_R are the corresponding systematic errors. If, for example, S_X and S_R were equal and the measurements were made on the same picoammeter range, ΔS_X and ΔS_R would be equal and the systematic error in the ratio of signals would be zero.

The strip chart recorder has an accuracy of 0.2% of full scale with resettability and linearity each 0.1% of full scale. Its full scale response time is 0.5 sec. The data logger has a range of 2 V with a resolution of 1 mV. Its accuracy is ±0.05% of the reading or ±1 count full scale, and its linearity is 0.05% of the reading. The voltage-to-frequency converter has a linearity referred to a straight line between zero and the full scale calibration point of ±0.02% of full scale. Its stability at constant line voltage and temperature is ±0.02% of full scale per day, and its line voltage effect is less than ±0.006% of full scale for a ±10% line voltage change. Its temperature coefficient is ±0.001% of reading and ±0.0005% of full scale per °C in the range 10 to 50 °C.

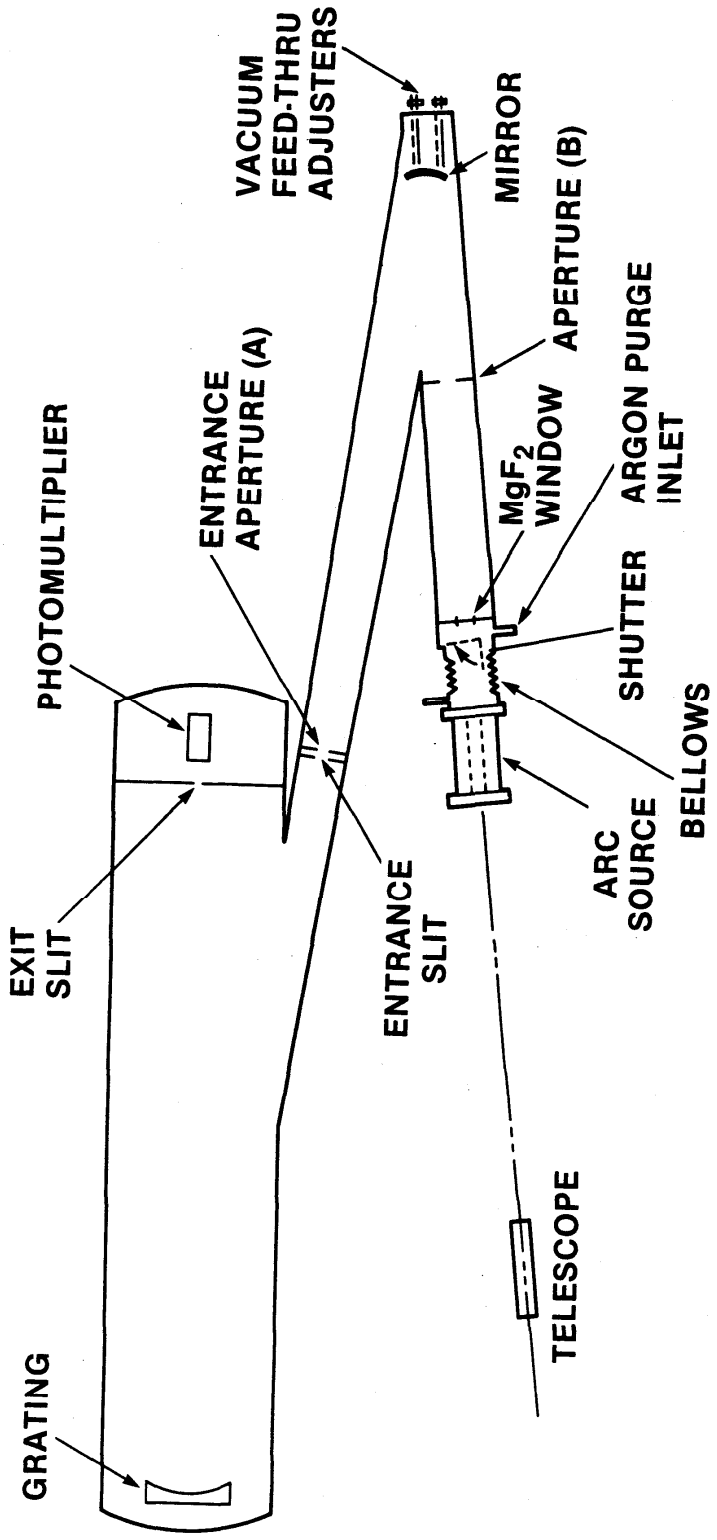

Figure 20. Schematic of the setup for comparing sources of spectral radiance in a vacuum.

IV. Calibration Methods

A. Radiance Calibrations

1. Introduction

Spectral radiance, L_λ, is defined in the Introduction as the radiant power emitted by a source per area per solid angle per wavelength interval: L_λ = [watts cm^{-2} sr^{-1} nm^{-1}]. A calibration of radiance is performed by directly comparing the source to be calibrated with a standard radiance source. An optical system is used to limit the geometrical quantities, i.e., area and solid angle and to direct the radiation to a detector. A monochromator selects the wavelength band desired. First, one source is placed in position and signals are measured at the various wavelengths. This source is then replaced by the second source and the measurements are repeated. The radiance of the source to be calibrated is then obtained from the ratio of the signals times the radiance of the standard source. In general the signal obtained from a source is

$$S\ (\text{amps}) = \varepsilon_\lambda\left(\frac{\text{amps}}{\text{watt}}\right) \cdot L_\lambda\left(\frac{\text{watts}}{\text{cm}^2\ \text{sr}\ \text{nm}}\right) \cdot A(\text{cm}^2) \cdot \Omega(\text{sr}) \cdot \Delta\lambda(\text{nm}), \quad (2)$$

where A is the area, Ω the solid angle, $\Delta\lambda$ the wavelength bandpass, L_λ the spectral radiance, and ε_λ the efficiency of the detection system. If subscript R refers to the standard source and subscript x refers to the one to be calibrated, then

$$\frac{S_x}{S_R} = \frac{\varepsilon L_{\lambda,x} \cdot A_x \cdot \Omega_x \cdot \Delta\lambda_x}{\varepsilon L_{\lambda,R} \cdot A_R \cdot \Omega_R \cdot \Delta\lambda_R}. \quad (3)$$

If A, Ω, and $\Delta\lambda$ are identical for each source, then

$$L_{\lambda,x} = \left(\frac{S_x}{S_R}\right) \cdot L_{\lambda,R}. \quad (4)$$

2. Hydrogen Arc

a. Setup

Figure 20 shows the setup for the measurement of signals from the hydrogen arc, our principal primary radiance source. The monochromator used is a 3 meter vacuum instrument with a grating of 1200 L/mm. The hydrogen arc is a standard spectral radiance source for $124 < \lambda < 360$ nm, if observed as shown, along its axis. The mirror images the arc with magnification M = 1 onto the entrance aperture of the monochromator. The aperture A, placed just outside the entrance slit of the monochromator, is 0.15 mm in diameter and limits the area observed to a circle of this diameter. The distance from the center of the source to the mirror is 150 cm. Aperture B, 0.63 cm in diameter and located 125 cm from the source center, limits the solid angle to 2.0×10^{-5} stera-

dians or f/200. These are rather small geometrical limits, but are necessary to limit the variation in radiance to 1% within the observed optical beam.

b. System Alignment

Before placing the arc in position, the position of the telescope is adjusted so that its crosshairs are coincident with both the vacuum window and aperture B. The mirror is then adjusted so that aperture A is coincident with the telescope crosshairs. The arc is next placed in position and adjusted so that its axis is coincident with the optical beam. The arc is ignited and operated as discussed in Sec. III-A, 1b. After operating the arc in hydrogen at about 40 A, the mirror is adjusted further. This is done by observing a signal with the monochromator set at 350 nm and carefully rotating the mirror to maximize this signal. This insures that the arc alignment is correct.

c. Arc Current

The arc current is increased while observing the signal at 350 nm. At about 100 A the signal reaches a maximum and decreases with further increase in current. To avoid saturation of the photomultiplier (PM) tube, the maximum signal should be limited to 1 μA by reducing the PM voltage if necessary. This value of current should be recorded since the current values corresponding to the maximum signal depend upon wavelength. In this manner a set of current values for maximum signal are obtained as a function of wavelength for use during the calibration.

These settings for arc current are determined prior to measuring any signals from the arc, because radiation from the arc gradually degrades the optical system, especially the vacuum window, by polymerization of condensed hydrocarbon molecules. Once measurements are begun, therefore, the exposure time is limited to only that necessary to obtain a good measurement at each wavelength. This is done by using a shutter to block the beam while measurement is not actually in progress, as when moving from one wavelength to another. In fact even when the exposure time is limited, some change in signal may be observed when a measurement at a given wavelength is repeated during a run. This change is a function of wavelength, with the shortest wavelengths being most affected, and thus contributes to the uncertainty of the calibration.

d. Dark Current and Scattered Light

The signal from the arc increases with increasing wavelength over our range of operation. To cover our complete wavelength region, different ranges of the picoammeter must be used. For each range, the signal with the shutter closed is taken, and this "dark current" is to be subtracted from the detected signal at each wavelength. Also necessary to be subtracted is the portion of the signal due to scattered light. Scattered light is the part of the signal which comes from radiation at wavelengths other than the wavelength being properly diffracted by the grating, i.e., other than that wavelength at which the monochromator is set. The scattered light signal may be evaluated by scanning the monochromator grating to cover the range of wavelengths near

110 nm. As the grating is scanned toward shorter wavelengths, the signal gradually decreases and finally becomes constant at a value greater than the dark current. Since no radiation is transmitted at these wavelengths below about 113 nm (the MgF_2 window does not transmit radiation beyond this wavelength), the signal is the sum of the scattered light from longer wavelengths and the dark current. It is subtracted from the detected signal to obtain the arc signal. At settings of the monochromator which transmit much longer wavelengths, the grating is at a different position, and the scattered light may be somewhat different from its value with the grating set near 110 nm. However, for these longer wavelengths the signal level is much higher than for the short wavelengths, and therefore an error in estimating the scattered light will have little effect.

For wavelengths $\lambda > 230$ nm a contribution to the signal from second order radiation is possible. To avoid second order radiation, a quartz filter is included in the optical system for $200 < \lambda < 320$ nm, and a glass filter is used for $\lambda > 320$ nm. In actuality, the second order contribution to the signal is extremely small.

In the wavelength range near 130 nm the continuum radiation from the hydrogen arc is modified somewhat by both molecular emission lines and absorption lines. The absorption occurs in the cooler transition zones near the ends of the arc column along the axis. To get a good measurement of the continuum level in this wavelength range, the monochromator is scanned and the signal observed with a chart recorder to avoid wavelengths at which lines occur.

3. Argon Arc

The hydrogen arc primary standard is generally used to calibrate an argon arc. After measuring its signals, the hydrogen arc is removed and replaced with the arc to be calibrated. The telescope is used to align the argon arc, and once it is operating, a fine adjustment in position is accomplished by translating the arc both horizontally and vertically to maximize the signal. As with the hydrogen arc, there is a volume in between the arc source and the vacuum window. This volume is purged with argon at a flow rate of 5 liters/-min. The purging must continue for at least 10 min before measurements are begun in order to sufficiently displace the air from this region. This flow rate is continued during the entire calibration. By monitoring the signal at 170 nm where air absorption is strong, the rise in signal during purging may be observed, and the time at which essentially all air is displaced can be determined. There are two cases to consider: (1) if the arc to be calibrated contains a window, the purge region is isolated from the arc, and any purge rate which is sufficient to maintain the region free of air may be used; and (2) if the arc to be calibrated is one without a window, the flow in the "purge" region is not independent of the arc, and the same flow arrangement must be used whenever the arc is used as a secondary standard. This is necessary because the flow rate in the purge region can have an effect on the arc operation and hence on the radiance of the arc. Once the argon arc is operating and the purge region is clear of all air, signals are measured at the various wavelengths as with the hydrogen arc. In addition to the wave-

lengths covered by the hydrogen arc, signals are also measured at shorter wavelengths extending to 115 nm. In this region, however, there are numerous lines in the spectrum from minute air impurities. These lines are typically resonance lines and are extremely strong even at very low concentrations. The wavelengths at which the continuum is measured are selected to avoid interference from these relatively strong lines. Table 1 of App. F-1 lists wavelengths typically included. Also, in order to avoid interference from the lines, the wavelength bandpass must be no greater than 0.2 nm (700 μm slits on the 3 m monochromator). The continuum from this short wavelength region is calibrated using a second primary standard, the blackbody line arc.

4. Blackbody Line Arc

Another primary standard source, the blackbody line arc, is used to extend the calibration to wavelengths below 124 nm. This is also a wall-stabilized arc, operated with argon but including small admixtures of H, O, C, N and Kr. These admixture elements furnish spectral lines which can be made to be optically thick, i.e., they reach a maximum radiance value at the wavelength of the line.

In practice the arc to be calibrated is subjected to measurement and then replaced by the blackbody line arc. The latter arc is then aligned using the telescope and initially ignited with pure argon. After setting the current at 40 A and completing a fine adjustment of the arc position, measurements are made at wavelengths adjacent to the positions of the black body lines to be measured. The admixture elements are next added gradually while the spectrometer is scanned slowly and repeatedly over the respective lines. Prior to measuring the lines, the spectrometer slits are reduced to 10 μm each, giving a spectral bandpass of 0.0028 nm. The elements are added by admitting H_2, CO_2, N_2 and Kr at flow rates of a few ml/min. The flow arrangement limits the admixtures to a volume near the center of the arc. Initially, a line will increase in both height and width as the admixture flow rate is increased until the top of the line becomes flattened. Further increase of the admixture increases the line width, but the height remains constant. The flow rate of the various gases should be adjusted until all lines are flat-topped, but no more admixtures should be added than necessary. This is because the addition of these gases changes the temperature of the arc slightly, thus affecting the accuracy of this calibration method, which depends upon having a nearly uniform temperature in the region where the lines are emitted. For this reason, the admixtures are limited to the central part of the arc. If they were present at the end boundaries of the arc column where the temperature is lower, self absorption would distort the flat tops of the line profiles. In practice it usually proves difficult to achieve a good flat top for each line, and a compromise must be accepted since adjusting the flow rates to improve one line may worsen another.

The process of extending the calibration to shorter wavelengths is a "bootstrap" procedure. The lines at the longer wavelengths are first calibrated relative to the hydrogen arc, and each such line furnishes a value of temperature via the Planck blackbody relation.[4] Using several lines, an average value of arc temperature is obtained. With this value the radiances of the lines below the range covered by the hydrogen arc can be obtained, thereby

extending the range of calibration down to 115 nm. By interpolation the calibration is extended to all wavelengths in between the lines. A sufficient number of lines are available to restrict the interpolations to short intervals.

Since the slits had to be greatly reduced in width to observe the blackbody lines, the line radiances cannot be directly compared to the continuum level of the argon arc or the hydrogen arc. This comparison has to be done in steps:

1. With the arc operating in pure argon, continuum levels at wavelengths adjacent to the lines are first measured with the same monochromator slit settings used for the previous two arcs.

2. With 10 μm slit settings, the radiances of the lines are measured relative to the adjacent continuum levels. This may require changes in PM voltage to get sufficient signals from the continuum.

3. The gas admixtures are stopped and the change in continuum level is measured. This will be only a slight change, but it is significant.

From these ratios, the ratio of the blackbody line peaks to the continuum levels of both the hydrogen and argon arcs may be obtained. The spectral lines used in determining the temperature of the arc have wavelengths in nm of 193.1, 174.5, 174.3, 165.7, 149.5, 149.3, and 146.3; and the spectral lines whose radiances are determined have wavelengths in nm of 126.2, 124.3, 120.0, 119.4, 118.9, 117.8, 116.8, 116.5, and 115.2.

5. Tungsten Lamp Standard

In the calibration of radiance one additional standard source, the tungsten strip lamp,[11] is applied. The tungsten lamp is used for two reasons: (1) to increase the accuracy of the calibration, and (2) to extend the calibration to longer wavelengths. The wavelength ranges of the hydrogen arc and tungsten lamp overlap in the near UV region, and although the uncertainty in the radiance of the hydrogen arc is ±5%, tungsten lamps are calibrated for radiance with an uncertainty of ±2.3% in the near UV. Therefore, the calibration of a source extending to the near UV may be increased in accuracy by comparing it directly to the tungsten strip lamp. If this is done, a calibration using the hydrogen and blackbody line arcs is considered to furnish only the relative spectral distribution of the radiance of the unknown source. A calibration with the tungsten lamp at the long wavelength end of the range of the hydrogen arc then serves to set the absolute scale of the radiance.

The calibration with a tungsten lamp is carried out on a different instrument, namely the double monochromator in air. The double monochromator is necessary because the tungsten lamp is relatively weak in the near UV compared with its output in the visible range. With only a single monochromator the scattered light level would be too high to perform precise signal measurements in the near UV region. Figure 21 shows a diagram of the double monochromator setup. The tungsten lamp is first aligned according to the procedure described in its calibration report. This is accomplished by using

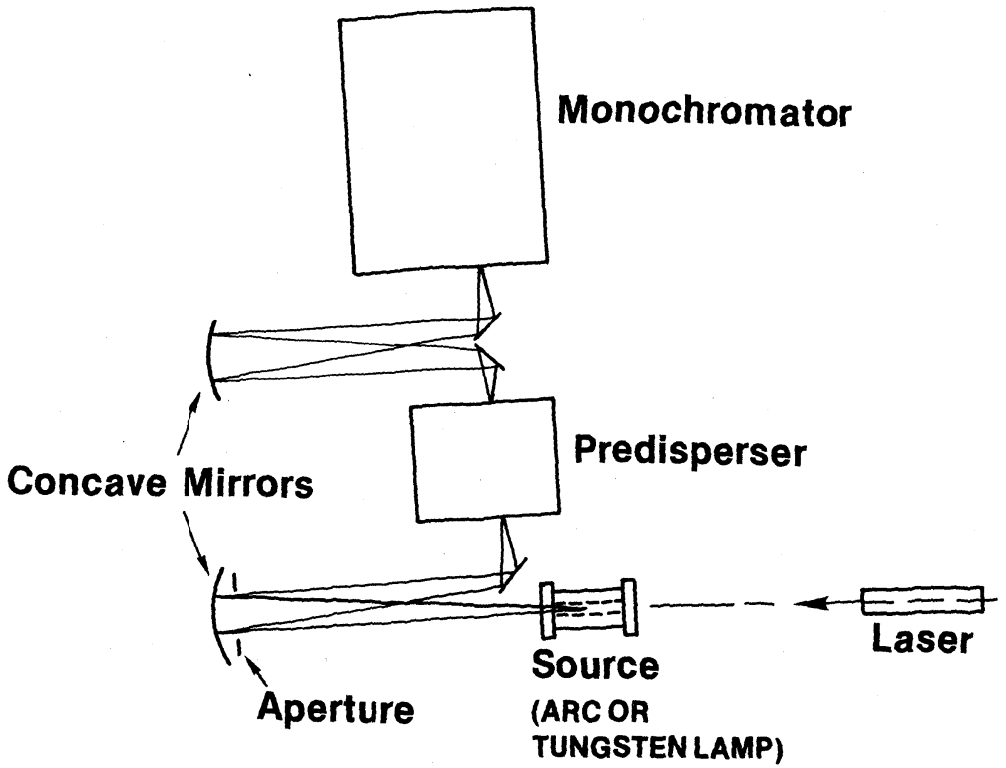

Figure 21. Schematic of the setup for comparing sources of spectral radiance in air.

a laser with an alignment device to set the angular orientation. After ignition, the lamp is translated slightly to precisely adjust the image position on the entrance aperture as specified in the lamp calibration report. Then the concave mirror between the predisperser and monochromator is adjusted to give a maximum signal at an arbitrary wavelength setting before measurements are begun. No further adjusting of this mirror should be done during the run. A 0.3 mm diameter circular aperture is used as the entrance aperture of the predisperser. Due to the fact that the tungsten lamps are calibrated using a larger area than that necessary for the arc, mapping of the lamp image is required to evaluate the slight difference in radiance due to the different areas used in the measurement. The exit slit of the predisperser and the entrance slit of the monochromator are set at 2 mm, and the exit slit of the monochromator is set at 300 μm. These settings give a bandpass of 0.5 nm. The aperture at the focusing mirror gives a beam of f/30. As with the previous setup the sources are aligned in succession, and signals are measured from each source at the various wavelengths. With the monochromator set at the wavelength of interest, the predisperser is set to maximize the signal. Usually the setting of the predisperser is sufficiently insensitive to allow the wavelength counter to be used to obtain the proper setting. The wavelength counter on the monochromator is calibrated by scanning over known spectral lines from a mercury source. Signals are usually measured in 10.0 nm increments from 250 to 320 nm. This gives an overlapping range with the hydrogen calibration, and the measurement at each wavelength in this range furnishes an absolute radiance of the unknown source at that wavelength. Although a measurement at one wavelength would in principle suffice to set an absolute scale, the results for several wavelengths are averaged to get a more accurate result.

As before, the scattered light and dark currents must be determined and subtracted from the total signals. In this setup scattered light is very weak; it is determined by measuring a signal at a wavelength beyond the response of the instrument ($\lambda < 180$ nm).

6. Calibration of Argon Arcs Relative to an NBS Argon Arc

For most calibrations the hydrogen arc and blackbody line arc are not employed, but rather calibrations are performed using a mini-arc (the NBS argon arc) as a transfer standard.

The transfer standard is employed since calibrations with the hydrogen and blackbody arcs are much more difficult and time consuming than calibrations performed relative to an argon arc. Moreover, the comparison of two similar sources (two argon arcs) can be accomplished in reasonable time with less error than is involved in a calibration involving the hydrogen and blackbody line arcs. Therefore only a slight decrease in accuracy results from employing the transfer standard. The calibration of one argon arc relative to another proceeds similarly to the calibration of an argon arc relative to the hydrogen arc. In this case the apertures A and B in Fig. 20 are changed to 0.3 mm in diameter and 1.3 cm in diameter, respectively. An exit slit of 700 μm is used, giving a bandpass of 0.20 nm. The NBS argon arc is operated without a window using a purge rate of 5ℓ/min. The arc to be calibrated usu-

ally contains a window, and thus the calibration of the arc must include a separate measurement of its transmission.

The window transmission measurement is carried out by removing the window from the arc and installing it in a holder which enables the window to be positioned in or out of the beam just in front of the arc. The window is replaced in the arc by a disc having a 1 mm aperture in its center; this reduces the difference in the gas flow within the arc produced by positioning the window in and out of the beam. The window holder is located in the region purged with argon, so it need not be vacuum tight. With the window near the arc, the area of the window for which the transmission is measured is approximately the same as the area which the radiation traverses when the window is mounted on the arc.

The transmission of the window at each wavelength is given by the ratio of the signal with the window in the beam to the signal with the window out of the beam. However, as in the arc calibrations the dark current and the scattered light contributions to the signal must be subtracted from the total signal. The scattered light levels are determined as before by measuring the signals at 110 nm with the window in and out of the beam. The window transmission at a given wavelength λ is

$$T_\lambda = \frac{(\text{Signal}_\lambda - \text{Dark Current} - \text{Scattered Light})_{\text{Window in}}}{(\text{Signal}_\lambda - \text{Dark Current} - \text{Scattered Light})_{\text{Window out}}}. \qquad (5)$$

B. Irradiance Measurements

1. Establishment of Irradiance Scale: General Method

Spectral irradiance is the radiant power incident upon a target area per area per wavelength band: $E = [\text{watts cm}^{-2}\ \text{nm}^{-1}]$. A source of radiation may serve as a standard source of irradiance by operating it at a given distance from the target area. If one had a radiance source with uniform radiance over its emitting area, the irradiance at a given distance from this source could be easily computed. In general however, radiance sources are non-homogenous, and the radiance is known only for a small portion of the source, i.e., an area element which can be approximated to be homogeneous. Thus, the irradiance at some distance from the source can be determined only if radiation from outside the calibrated area is prevented from reaching the measurement system. This can be done by the use of optical imaging or collimating apertures. For applications in the VUV, the method using collimating apertures[22] has proved to be more practical and is the basis for the measurements described here.

The collimating aperture method is as follows. A radiation source that is homogeneous over a certain emitting area and whose spectral radiance has been previously determined is situated a given distance from a monochromator. A pair of apertures, one at the entrance slit of the monochromator (the field aperture) and the other as close to the source as possible (the source aperture), is chosen so that only the radiation from the homogeneous portion of the source is measured. The spectral irradiance at the field aperture is given by the product of the known spectral radiance of the source and a geo-

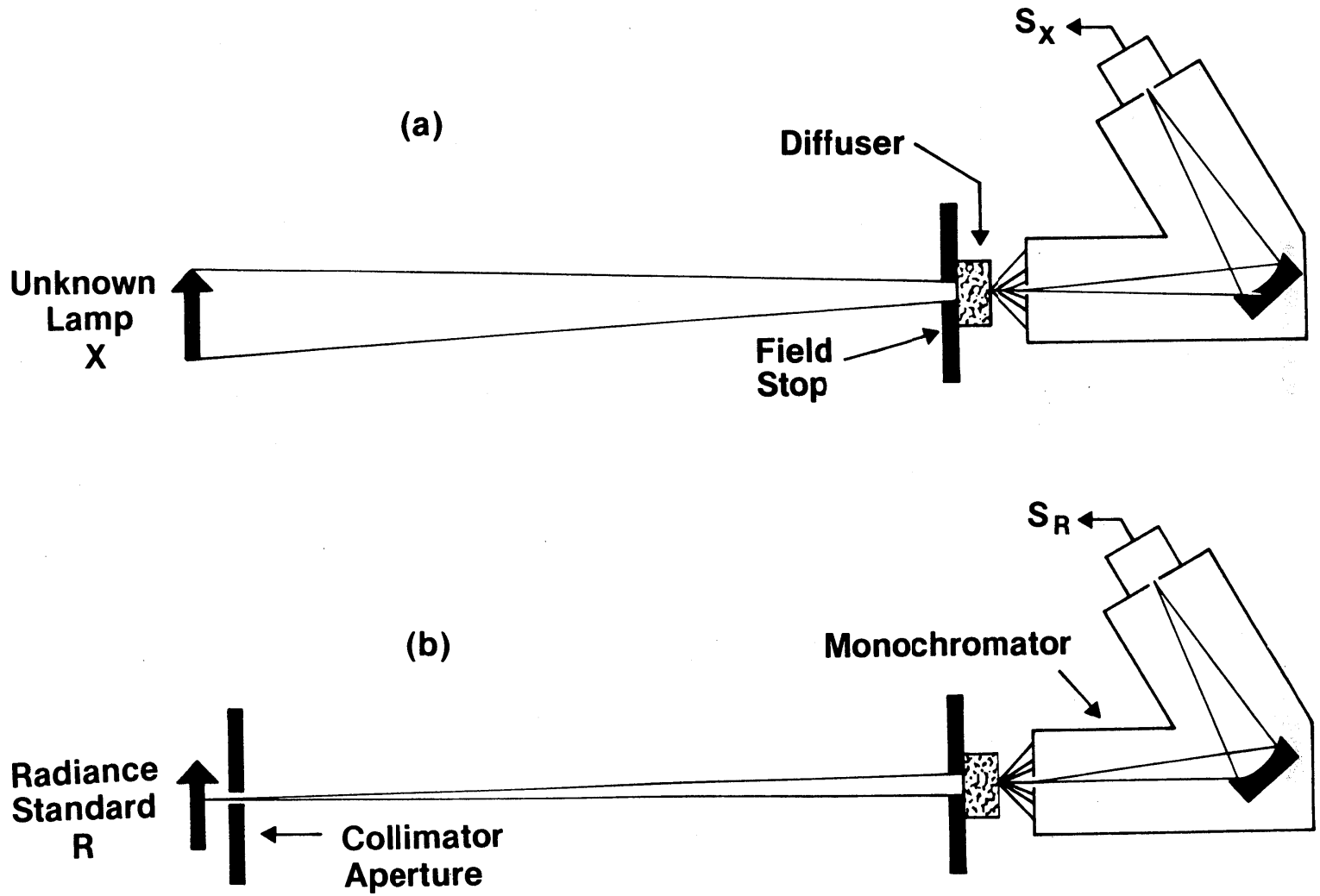

Figure 22. Schematic of calibration procedure. (a) Spectroradiometer is irradiated by the lamp whose spectral irradiance is to be evaluated; (b) efficiency is determined on a relative scale by irradiation with a stopped-down radiance standard.

metric factor dependent on the aperture dimensions and their locations relative to the lamp. This geometric factor contains the information on the effective area of the emitting source, the solid angle of the radiation beam incident upon the field aperture, and the irradiated area.

In principle, these quantities can be determined by measurement. However, a direct determination of the geometric factor is unnecessary, as is shown by the following discussion. The response of a spectroradiometer as a function of wavelength to a suitably collimated radiance standard is essentially a measure of the system detection efficiency on a relative scale. If the same spectroradiometer is irradiated with an unknown source and the response is measured again, the spectral irradiance of the unknown source can be determined, also on a relative scale. Then, provided that the wavelength range of calibration extends to the visible or near-UV region in which standard sources of irradiance are available, the absolute spectral irradiance of the unknown source can be determined at one wavelength within the calibrated wavelength range. This absolute value can then be used to normalize the relative scale of irradiance to an absolute scale.

The calibration procedure is illustrated in Fig. 22. If $E_X(\lambda)$ is the spectral irradiance at wavelength λ of the source whose irradiance is to be determined, the response $S_X(\lambda)$ of the spectroradiometer to this radiation source [see Fig. 22(a)] is

$$S_X(\lambda) = E_X(\lambda)\alpha(\lambda), \tag{6}$$

where $\alpha(\lambda)$ is the spectroradiometer system efficiency. The response $S_R(\lambda)$ to the apertured radiance standard [see Fig. 22(b)] is

$$S_R(\lambda) = L_R(\lambda)\alpha(\lambda)\gamma, \tag{7}$$

where γ is the geometric factor discussed above and $L_R(\lambda)$ is the spectral radiance of the radiance standard. The relative spectral irradiance can then be determined:

$$E_X(\lambda) = \gamma\frac{S_X(\lambda)}{S_R(\lambda)}L_R(\lambda). \tag{8}$$

The absolute spectral irradiance is determined by comparing the unknown source with an already existing irradiance standard at some convenient wavelength. If it is more suitable, this can be done on a separate spectroradiometer setup, for example, one that is dedicated to spectral-irradiance measurements in the air. The responses of this system (primed) both to the source to be calibrated, S'_X, and to the already existing irradiance standard, S'_I, are measured at one wavelength, λ_0, so that the spectral irradiance of the unknown source, $E_X(\lambda_0)$, is given by

$$E_X(\lambda_0) = \frac{S'_X(\lambda_0)}{S'_I(\lambda_0)}E_I(\lambda_0), \tag{9}$$

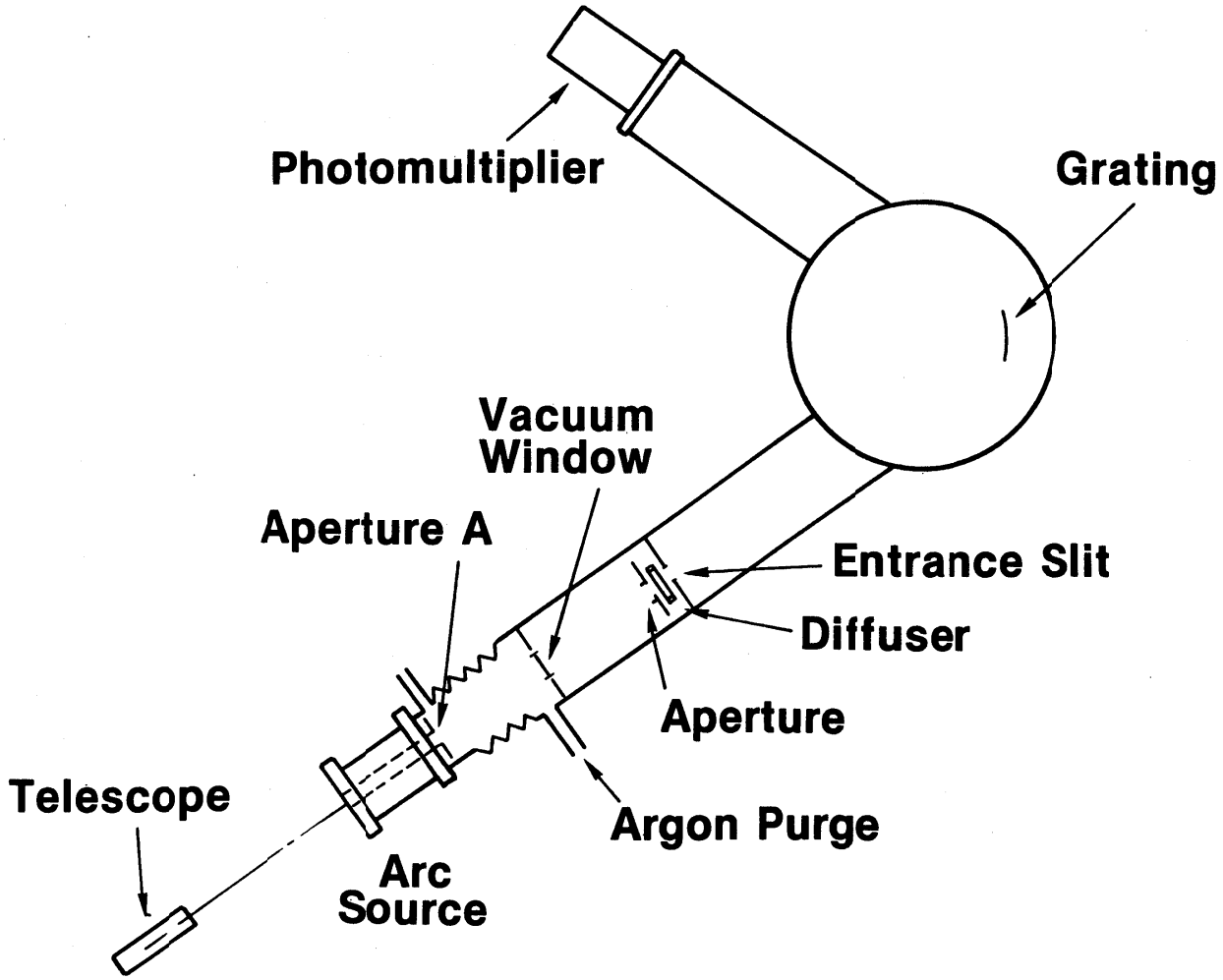

Figure 23. Schematic of the setup for comparing sources of spectral irradiance in a vacuum.

where $E_I(\lambda_0)$ is the spectral irradiance of the standard source.

If Eq. (8), with $\lambda = \lambda_0$, is combined with Eq. (9), γ can be eliminated to give

$$E_x(\lambda) = \frac{S'_x(\lambda_0)}{S'_I(\lambda_0)} \frac{S_R(\lambda_0)}{S_x(\lambda_0)} \frac{E_I(\lambda_0)}{L_R(\lambda_0)} \frac{S_x(\lambda)}{S_R(\lambda)} L_R(\lambda). \qquad (10)$$

From Eq. (10) the absolute irradiance of the unknown source can be determined over the complete wavelength range of the radiance standard.

The considerations given above assume first that the system efficiency of the spectroradiometer employed does not depend on the angle at which radiation enters. A diffuser located directly behind the field aperture is usually necessary to ensure that this assumption is correct.

2. Argon Arc Calibrations

Two types of sources are calibrated as irradiance standards, the argon mini-arc and the deuterium lamp. Calibration of an argon arc will be discussed first.

The light source used as a standard of spectral radiance in the VUV and near UV is an argon mini-arc previously calibrated by the hydrogen arc. This source is used according to the method discussed above to calibrate a second mini-arc as an irradiance standard. The measurements in the VUV spectral range are performed using the SEYA monochromator described above in Sec. III-C,1.

Figure 23 is a diagram of the setup. The telescope is first aligned with the optical path through the entrance slit and the center of the grating. The monochromator must be brought to atmospheric pressure temporarily to accomplish this. A 2-mm diameter aperture mounted on a ground MgF_2 diffusing window is then positioned on the optical axis 5 cm in front of the entrance slit. The entrance and exit slits are set at 0.5 mm, giving a spectral bandpass of 0.4 nm. The arc source is connected to the system with a bellows as shown to permit alignment. A 0.5 mm diameter aperture is used in place of the arc window. After alignment, the arc is ignited, and the volume in front of the arc is purged for 10 minutes. Signals are then measured at wavelengths listed in Table 1 of App. F-2. For $\lambda < 138$ nm the signal/noise is too small (mainly due to the diffuser) to obtain a useful measurement, so 138 nm is usually the lower wavelength limit in irradiance calibrations. The arc is then removed, and replaced by the arc to be calibrated. This second arc is aligned with the telescope as before. The unknown arc should be operated as it is intended to be used, e.g., with a window instead of the aperture used with the transfer standard arc above. Signals are then measured from the second arc at the respective wavelengths. The irradiance from the unknown source at each wavelength is proportional to the ratio of signals from the two sources times the radiance of the standard source (see. Eq. 8 above).

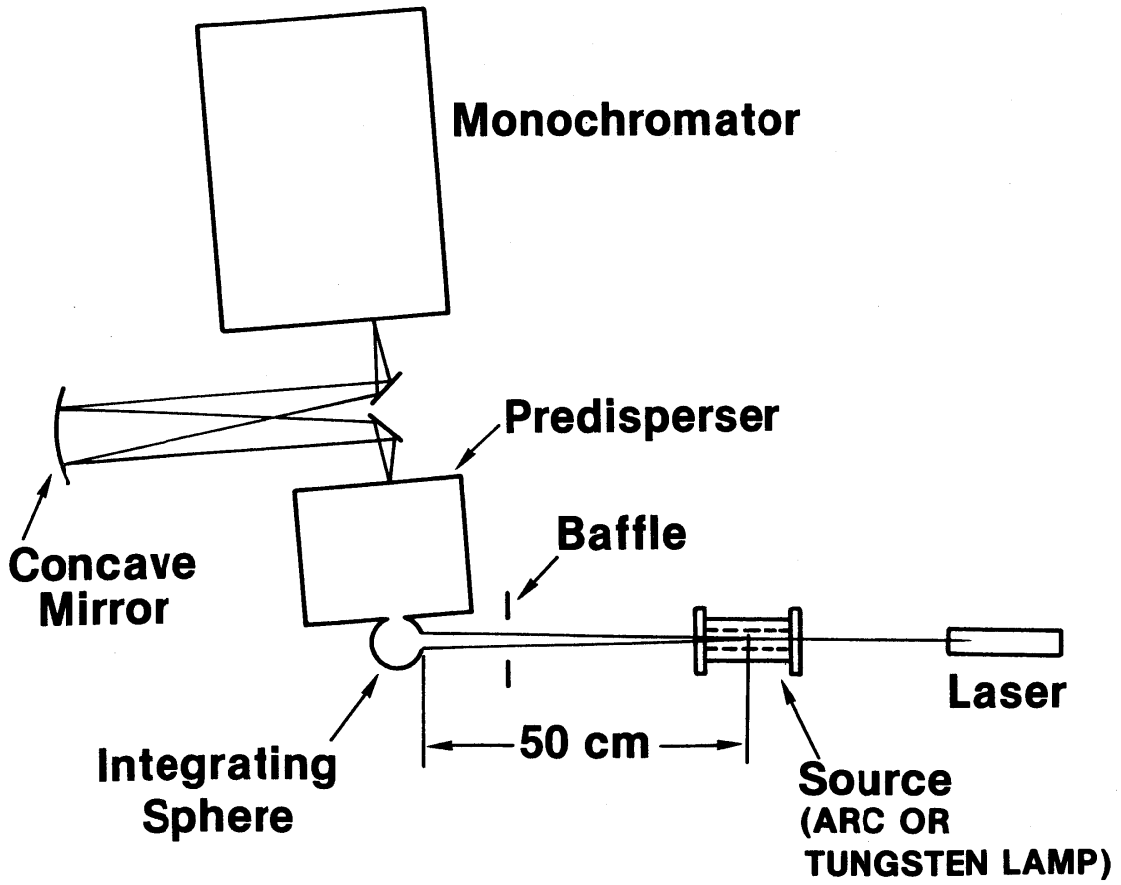

Figure 24. Schematic of the setup for comparing sources of spectral irradiance in air.

Thus, the above measurements determine the irradiance of the unknown source, but only on a relative scale as long as the value of the constant γ in Eqs. 7 and 8 is unknown. To obtain an absolute scale, the irradiance of the unknown source is compared in the near UV region to that of a calibrated tungsten-quartz-halogen irradiance standard.[19] This measurement is carried out on the double monochromator, with an integrating sphere used as its entrance aperture. For this measurement this setup has two advantages. First, the double monochromator greatly reduces scattered light which otherwise would be a serious problem for the quartz-halogen source. Second, the integrating sphere serves as a better method of rendering the signal insensitive to the direction of radiation from the source. This is important in comparing the small sized arc source with the much larger quartz-halogen source area.

Figure 24 is a diagram of the double-monochromator setup for irradiance measurements. On this setup the arc is operated with the front of its window exposed to air, since all measurements are for $\lambda \geq 200$ nm. Using the laser, the arc is aligned with the integrating sphere aperture which is 0.6 cm in diameter. The baffle shown is ≈10 cm from the source; it is an aperture 3 cm in diameter. The arc is positioned so that its center is 50 cm from the aperture of the integrating sphere. Measurements are carried out on this setup as described in Sec. IV-A,4. The quartz-halogen lamp is aligned and operated according to the instructions included in its calibration report supplied by the Radiometric Physics Division of NBS. With this type of lamp light is emitted in all directions, so it is especially important to prevent light from entering the integrating sphere or predisperser by reflection from some object. This is accomplished by positioning baffles to avoid any possible reflecting paths.

3. Deuterium Lamp Calibration

Deuterium lamps are calibrated as spectral irradiance standards in the near UV range $200 \leq \lambda \leq 350$ nm by another calibration group in the Radiometric Physics Division of NBS. The lamps calibrated are of the side-on type. Prior to calibration they are potted in a base identical to that of the tungsten-quartz-halogen lamps. Our calibrations of such lamps usually consist of extending the spectral range in the vacuum UV down to 165 nm. The measurements are performed on the SEYA monochromator setup, using the same method as was described in the previous section for calibrating an argon arc as an irradiance source. The deuterium lamp is placed inside a stainless steel container which is purged with argon during the measurements. The container is constructed so as to isolate to a large degree the upper (emitting) portion of the lamp from the potted base. This helps to keep the volume through which the radiation passes free of impurities so as to minimize absorption. The deuterium lamp is aligned with the spectrometer in the same manner as is the quartz-halogen lamp, i.e., an alignment fixture is substituted for the lamp and aligned with a laser beam as described in the quartz-halogen lamp calibration report. In this procedure the alignment device is first translated until the laser beam intersects the designated position on the device; the alignment device is then rotated to reflect the laser beam back along its path. The alignment fixture is then removed and the deuterium lamp is inserted in the base. This technique aligns the lamp in the orientation in which it was calibrated for $\lambda > 200$ nm. Since the measurements to be made are only to deter-

mine the relative spectral distribution, the exact distance from the lamp to the entrance aperture is not critical. This distance is set at approximately 50 cm. The lamp is ignited and operated for 10 minutes with an argon purge of at least 10 ℓ/min. This purge rate is essential because of the possibility of radiation absorption due to air contamination in the radiant heated purge chamber between the lamp and the vacuum system window. After this warm-up signals are measured at the following wavelengths in nm: 260, 200, 195, 190, 187, 184, 182, 180, 178, 176, 174, 173, 172, 171, 170, 168, 167, and 166.

The lamp output is highly sensitive to changes in wavelengths near 165 nm. Therefore, measurements are made for small increments in wavelength in this region, so that the shape of the spectrum near 165 nm depends somewhat on the wavelength bandpass. For calibrations a bandpass of 0.4 nm is used. This is the full width at half maximum of a triangular slit profile obtained by setting the monochromator entrance and exit slits both at 0.5 mm.

After signals are measured from the deuterium lamp, the lamp is removed and replaced by the argon arc transfer standard source previously calibrated by the hydrogen arc. This argon arc is set up and operated as described in the previous section: a 0.5 mm aperture is used in place of a window, the arc is aligned with the telescope, and the volume between the arc and the spectrometer window is purged with argon. After igniting the arc, signals are measured at the same wavelengths as was done with the deuterium lamp. Then the irradiance of the deuterium lamp at each wavelength is given by Eq. 8 above, i.e., the ratio of signals from the two sources times the radiance of the standard source. This gives the irradiance of the deuterium lamp to within a constant factor γ. The value of γ is found by applying Eq. 8 with λ = 260 nm. This then enables the relative irradiance values at all wavelengths to be put on an absolute scale. Table 1 of App. F-3 lists the values of spectral irradiance determined for a typical 30 W deuterium lamp.

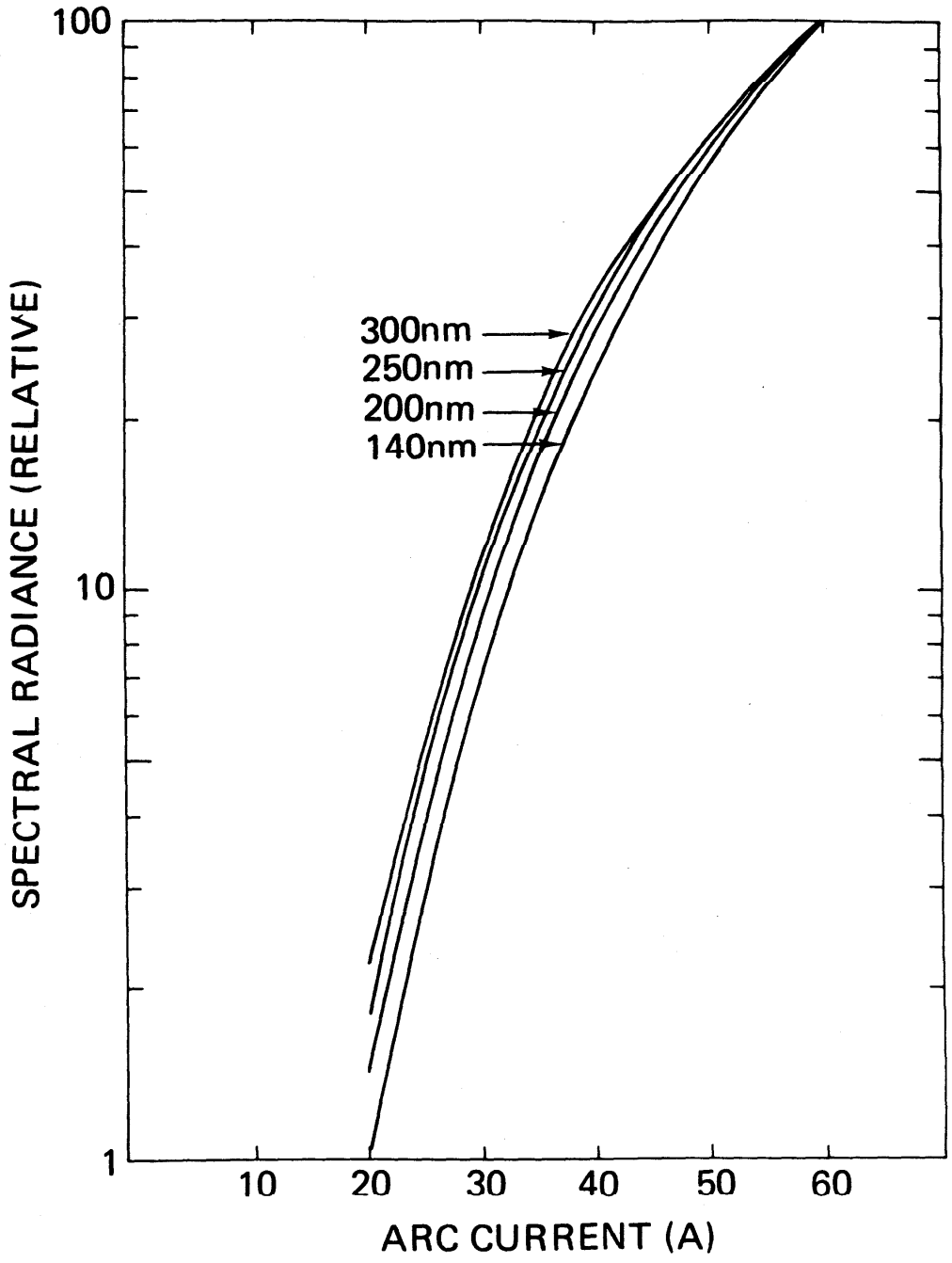

Figure 25. The dependence of the mini-arc spectral radiance on arc current for several representative wavelengths.

V. Uncertainties

A. Argon Mini-Arc Radiance Standard

1. Primary Standards

The basic uncertainties in the spectral radiance of the mini-arc are due to uncertainties in the primary radiometric standards. As was discussed in Secs. III-A,1 and 2, the hydrogen arc contributes a 2σ uncertainty of ±5% to the mini-arc radiance between 140 nm and 330 nm,[1] while the blackbody line arc is responsible for a 10% contribution between 114 nm and 140 nm.[16]

2. Arc Current

As the arc current and consequently the input power to the discharge are changed, both the electron density and temperature change. For an atmospheric pressure argon arc with a 4.0 mm diameter channel, the electron temperature varies from about 14,000 K to 11,000 K and the electron density from about 1.5×10^{17} cm^{-3} to 3×10^{16} cm^{-3} as the arc current is decreased from 60 A to 20 A.[23] Since the continuum radiation varies as the electron density squared, a large variation in intensity is expected. The measured dependence of the mini-arc radiance on arc current is shown in Fig. 25 for four representative wavelengths. The radiance, normalized to unity at 60 A, varies smoothly over a factor of about 100 for a 40 A current range. The wavelength (λ) dependence is due primarily to $\xi(\lambda, T)$,[24] a quantity which depends on the photoionization cross sections of the various Ar I energy levels and which enters as a multiplicative factor in theoretical calculations of the emission coefficient of a plasma in thermal equilibrium at temperature T.

The uncertainty in the spectral radiance due to an uncertainty in the arc current measurement can be obtained from Fig. 25. In general, there is generated approximately a 4% uncertainty in the spectral radiance due to an uncertainty of 1% in the arc current. Using a 0.1% current regulated power supply, a calibrated shunt and digital voltmeter, the current may be set typically to within 0.02 A, giving an uncertainty in radiance of 0.4% or less for currents above 20 A.

The ability to vary the radiance over such a wide range by a simple adjustment of arc current suggests another mode for applying the arc as a radiation standard, namely, as a source of constant spectral radiance over the complete wavelength range. Table IV shows the arc current values required at several representative wavelengths such that the spectral radiance is constant at 2.7×10^{-3} W cm^{-2} nm^{-1} sr^{-1} for each wavelength. Similarly, the arc current could be adjusted so that one's spectrometer response would be equal to its response to the unknown source or experiment being calibrated. In this way scaling difficulties and problems with the linearity of the detection system may be avoided.

3. Gas Flow

The arc is stable over a wide range of argon flow rates. Relatively large flow rates are preferred since the degree of purity in the arc chamber

Table IV. Mini-arc Current Required to Produce a Constant Spectral Radiance of 2.70×10^{-3} W cm^{-2} nm^{-1} sr^{-1} at Various Wavelengths in the 115–330-nm Range

λ(nm)	Arc current (A)
330	20.0
310	20.4
290	21.0
270	21.7
250	22.7
230	24.1
210	26.0
190	28.5
170	32.3
150	39.6
140	45.5
130	49.5
120	50.0
115	47.0

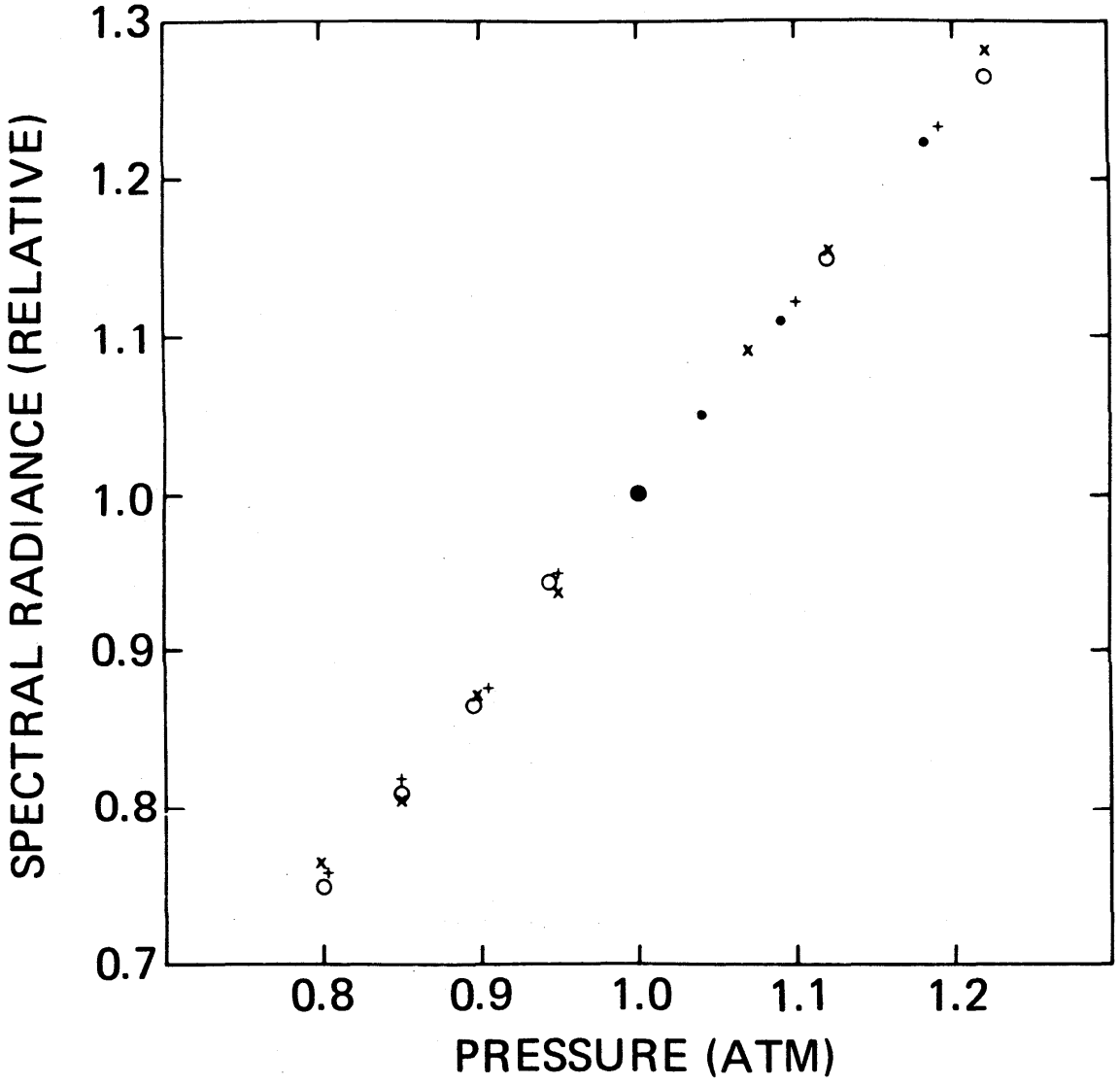

Figure 26. The dependence of the mini-arc spectral radiance on the arc chamber pressure. The arc chamber pressure, in the absence of an exhaust manifold, is equal to the local atmospheric pressure. Data are shown for the following wavelengths: 300 nm (+); 250 nm (o); 200 nm (x); and 140 nm (•).

is greater when the purge rate is high. However, too large a flow rate can cause changes in the spectral radiance of the continuum. It can cool the plasma (an effect which tends to decrease the radiant power) or cause a pressurization of the arc chamber (an effect which tends to increase the radiant power), or it may cause a slight shift in position of the constricted discharge or even an instability.

The total argon flow rate used for the arc calibration is 5 ℓ min^{-1} divided equally among the three input ports in Fig. 12. This rate was chosen because an increase beyond this amount resulted in little further decrease in the gas impurity level. Also, a change in the flow rate of a factor of 2 in either direction from this amount resulted in no significant change in the radiance of the arc. Thus the possible effects of flow rate changes were either negligible or compensated for each other to within our measurement precision.

4. Pressure

If the arc is operated open to the air, the radiative properties of the arc discharge will depend somewhat on the prevailing local atmospheric pressure. To first order, a change in pressure is expected to be relatively significant since the continuum depends directly on the square of the electron density. However, there are other effects which tend to compensate; for example, the electron temperature increases as the pressure is lowered thus increasing the ionization fraction. Deviations from local thermodynamic equilibrium may also become significant. To obtain some experimental data, an exhaust port manifold was used to vary the pressure over a range from 0.8 atm to 1.2 atm. Figure 26 shows the measured dependence of the spectral radiance on the pressure for four different wavelengths. The data are normalized to unity at one standard atmosphere. There is no significant wavelength dependence, but there is a linear relationship between spectral radiance and pressure over the 0.80 - 1.2 atm range. A linear fit to the data in Fig. 26 gives $L(p) = (1.57p - 0.57)\, L(o)$, where $L(p)$ is the spectral radiance at pressure p in atmospheres, and $L(o)$ is the radiance at one standard atmosphere. Since pressure measurements in this range can be easily made to within uncertainties of 1%, the uncertainty in the spectral radiance can be made negligible with reasonable care in monitoring the pressure.

5. Alignment

Figure 27 illustrates the results obtained by translating the arc across a 0.300 mm diameter spectrometer entrance aperture for four different wavelengths at 50 A. All data are normalized at the point of maximum signal when the discharge is properly centered on the optical axis. Only a weak dependence on wavelength is seen in that the arc appears slightly narrower at shorter wavelengths. At 300 nm the results are also given for a current of 20 A. No significant dependence on arc current is observed.

These data give the sensitivity of a calibration to possible translational alignment errors. It can be seen, for example, that an error in the arc alignment of ±0.20 mm, i.e., 5% of the radius of the central plate, would lead to a decrease of about 2% from the calibrated spectral radiance shown in

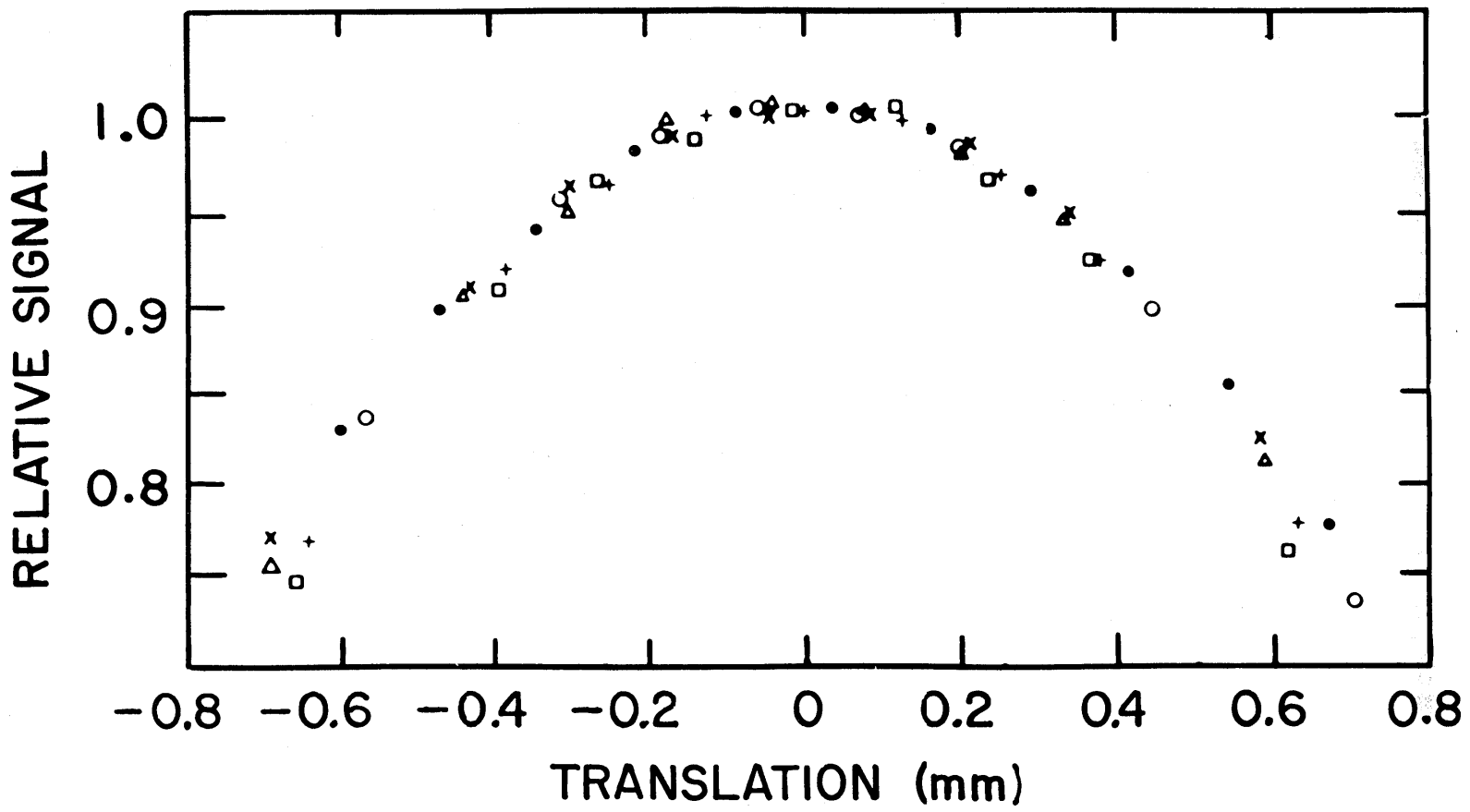

Figure 27. The dependence of the mini-arc spectral radiance on translational alignment for several field stops, arc currents, and wavelengths. The zero indication on the translation scale corresponds to the case where the arc axis is exactly aligned with the optical axis. Data are shown for the following conditions: 0.300-mm diam field stop, 50-A current, and wavelengths of 300 nm (·), 250 nm (o), 200 nm (+), 140 nm (□); 0.300-mm diam field stop, 20-A current, and 300 nm (Δ); 0.015-mm^2 field stop, 50-A current, and 250 nm (x).

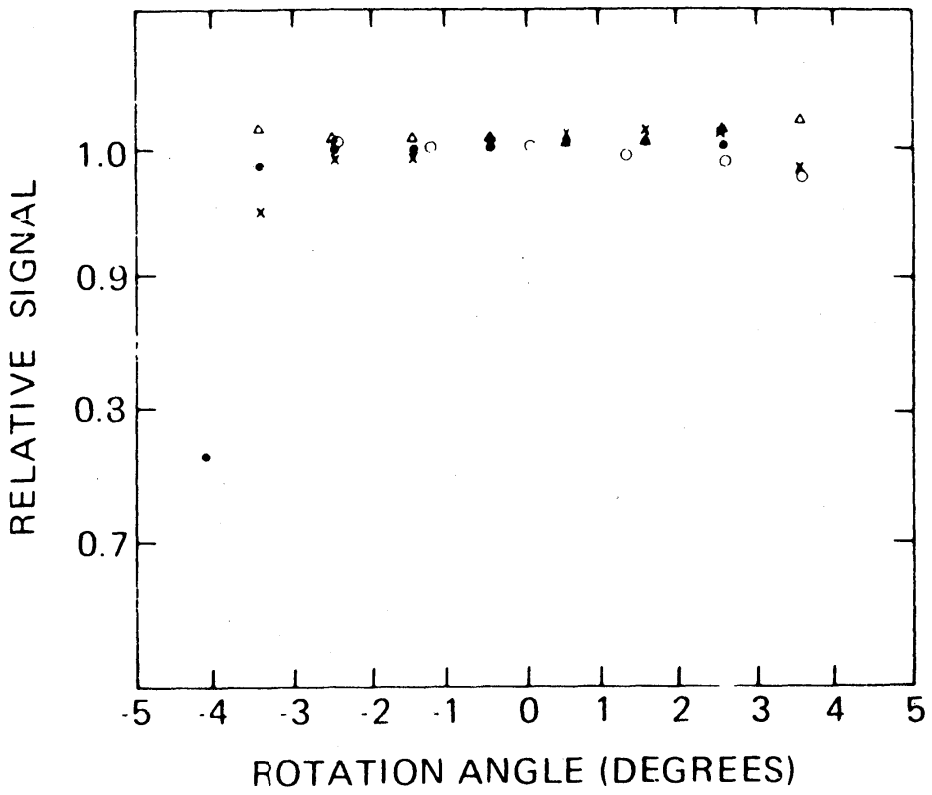

Figure 28. The dependence of the mini-arc spectral radiance on rotational alignment (pitch and yaw) for several arc currents and wavelengths. The zero indication on the rotation angle scale corresponds to the case where the arc axis is exactly aligned with the optical axis. Data are shown for the following conditions: yaw variation, 50-A arc current, and wavelengths of 300 nm (•) and 140 nm (Δ); yaw variation, 20-A arc current, 300 nm (x); pitch variation, 50-A arc current, 300 nm (o).

Fig. 13 and Table II. However, this uncertainty usually can be avoided entirely by providing fine adjustments for maximum signal, for example, by translation of the light source itself or of the arc image through use of an adjustable reflecting mirror which can be incorporated into the optical system. The latter technique was used in obtaining the absolute intensities in Table II, and therefore no translation alignment uncertainty needs to be included in the error budget for the calibration.

If one must observe a somewhat larger portion of the arc than the homogeneous 0.3 mm diameter circle, a correction to Table II must be made. A translational scan across a 0.015 mm x 0.15 mm rectangular aperture, also illustrated in Fig. 27, was indistinguishable from the other data. This implies that the data are not limited by spatial resolution and that they can be taken to represent the actual radial distribution. Using these data and knowing that the discharge is cylindrically symmetric, one can readily calculate the spectral radiance over a larger area.

Figure 28 illustrates for two wavelengths and currents the results obtained by tilting the arc through an angle of 0.1 rad (5.7°) with respect to the optical axis. Referred to a Cartesian coordinate system centered at the arc with the z axis defined as the arc axis, the terms pitch and yaw correspond to rotation about the x and y axes, respectively. The data were taken with a 0.300 mm entrance aperture and an f/200 optical beam. All these data show no significant dependence on angle, indicating that most of the radiation comes from the region of the central constricting plate. Tilting in two mutually perpendicular planes (pitch and yaw) resulted in slight differences attributable to the nonsymmetric, unconfined portions of the arc discharge near the electrodes.

In addition to the above measurement of the angular distribution of the arc radiant power, the radiant power measured over larger solid angles was compared to the radiation from a flat-filament, tungsten strip lamp as a function of the solid angle of observation. The comparison was made for arc currents of 20 A and 50 A at a wavelength of 250 nm. The ratio of signals from the arc and tungsten filament was constant within 1% for apertures smaller than f/9. For f/7 this ratio decreased by about 2% and for f/6 by 8%. Data taken at 20 A and 50 A showed no difference. Assuming that the tungsten strip lamp is a good Lambertian source, we conclude that the arc emission is indeed uniform over quite a large solid angle. This property is important since calibration of the arc is done at f/200 due to restrictions on the primary standard, whereas applications for the arc usually require larger aperture beams.

6. Reproducibility and Stability

To test the reproducibility of the arc, it was ignited ten times; after each ignition the current was set at 50.00 A ± 0.05, and the radiance at 200 nm was measured. The standard deviation of these measurements was 0.5%. This variation can be accounted for almost entirely by the uncertainty in our measurement of the arc current (see Fig. 25). Thus to within the precision to which the current was set, no reproducibility problems were encountered.

In addition, both short and long term stability must be considered to evaluate the reliability of the mini-arc as a secondary radiation standard. Short term instabilities might be caused, for example, by electrode effects in which the arc termination points on cathode and anode shift slightly, by an excessive amount of air leaking into the discharge, by too large a flow rate, or simply by poor current regulation by the dc power supply. With the operating conditions described in connection with Table II, the radiance at 200 nm was monitored photoelectrically over periods of 10 sec, 1 min, and 1 hour. With a 0.1 sec time constant for the recording system, the SNR was 100, and any shifts in the signal level were measured to be less than 1%. The behavior at all currents between 60 A and 10 A is essentially the same until the arc extinguishes at a current of about 5 A.

Long term stability is influenced primarily by the aging of the UV window. Changes in the local atmospheric pressure also have an effect, of course, but these can be monitored or controlled to the accuracy desired. The spectral radiance of the mini-arc was measured every 3 hours over a 24 hour period for several representative wavelengths: 325, 300, 275, 250, 225, 200, 178, 153, 139 and 125 nm. A shutter between the argon mini-arc and the vacuum spectrometer shielded the vacuum optics and detector system from illumination by the arc except during the actual measurements. The sensitivity of the measuring system, thus protected against possible radiation damage, was measured at the beginning and end of the experiment using the hydrogen arc primary standard. No change in sensitivity was detected to within the ±1% precision of the calibration procedure. The result of the aging test was that no systematic changes in the arc radiance were observed to within ±1% over the 24 hour test period. However, it is important to realize that the 2 mm thick MgF_2 arc window, through which observations were made, was exposed on the outside surface to a constant flow of argon at atmospheric pressure and not to the vacuum environment. An additional window, usually protected by the shutter, was used to make the vacuum seal. In this way, any possible decrease in transmitted radiant power due either to radiation damage to the arc window or accumulated tungsten evaporate on the window surface could be distinguished from a possible decrease due to contamination of the vacuum side of the sealing window. This latter effect is caused by UV photodissociated hydrocarbons which are present in trace amounts in most oil pumped vacuum systems. It was purposely uncoupled from other aging effects because it is a characteristic not of the lamp but rather of the system used to measure the radiance of the lamp.

Although no aging effects were noticeable, it should be noted that it is possible also to calibrate and operate the argon mini-arc with no window, thus eliminating any risk of window contamination. The open end then acts simply as an additional exit port for the flowing argon gas. Under these conditions and for a total flow rate of 5ℓ min^{-1} at 1 atm pressure, the arc remains stable, the continuum spectral radiance is unchanged, and the strengths of the impurity lines are not increased. The main reason for retaining the window in the basic mini-arc design is to make the light source compatible with VUV measuring systems.

7. Gas Impurity

It was standard procedure during the various experiments described here to use ultrahigh purity argon (99.9995% pure). If commercial grade argon (99.9990% pure) is used, the continuum intensities are unchanged, the only effect being an increase in the strength of the impurity resonance lines. This increase is not as much as one would expect from an analysis of the gas cylinder impurity content because there are usually impurity contributions due either to small air leaks or to outgassing of materials within the arc chamber or within the gas handling system. In our case, this impurity content was on the order of 5 ppm or about the same as that of the argon gas cylinder.

In order to investigate the effect on the continuum due to the presence of larger impurity concentrations which conceivably might be encountered in a worst case situation, air and hydrogen were mixed with the argon to produce impurity concentrations as high as the 0.1% level. If air is mixed with the argon flowing into all three gas ports, as might be the case if a large leak developed in the gas handling system, there can be obvious problems in making VUV radiance measurements because of molecular oxygen absorption in the gas volume between the cathode and the UV transmitting window. With an air impurity concentration of about 1/3000, there was no measurable effect on the continuum intensities above 200 nm. With a higher concentration of 1/1000, the continuum signal increased by not more than 3% above 200 nm, but the radiant power at 140 nm was observed to decrease by 60% due to absorption. When air was mixed only with the argon flowing into the arc plate ports (A and B in Fig. 12), the absorption effect was much smaller, 16% at 140 nm.

The effect of adding hydrogen is of interest mainly because there is always a residual hydrogen impurity which is due to trace amounts of water vapor throughout the system. Unless a bakeable system is used, this impurity content will be a function of the local relative humidity. Since even small quantities of hydrogen can alter the arc properties, it is important to estimate the effect of variations in the hydrogen impurity concentrations. Indeed, when hydrogen is added to the argon to form a 0.2% mixture, the continuum spectral radiance is increased about 10% with a slight wavelength dependence. With a 1% admixture, an increase of 30% was observed. From relative measurements of the intensity of the optically thin far line wing of the hydrogen Lyman alpha line, it was estimated that the normal residual hydrogen impurity concentration in our experiments was 0.02%. By interpolation using the above figures, it is estimated therefore that the spectral radiance figures in Table II are about 1% or 2% higher than they would be if there were no hydrogen impurities at all. Because the local humidity in the NBS laboratory is controlled to a rather normal value of about 45% and because no extraordinary drying techniques were used, it is not expected that large variations from this figure will be encountered in the field. Therefore, the effect of residual hydrogen impurities will be included as an additional uncertainty of ±1% affecting the spectral radiance determinations.

8. Summary

An argon mini-arc has been designed, tested, and operated as a transfer source of spectral radiance for the wavelength range from 114 nm to 330 nm.

Table V. Error Budget for the Spectral Radiance Calibration of the Argon Mini-Arc

Source	Contribution (%)
Primary Standard (s)	
above 140 nm	5
below 140 nm	10
Arc current (r)	0.4
Gas flow (r)	-
Pressure (r)	-
Alignment (r)	-
Reproducibility (r)	-
Short term stability (r)	<1
Long term stability (r)	1
Gas impurity (r)	1
Combination of errors in quadrature	
above 140 nm	5.3
below 140 nm	10.1

Random and systematic errors are denoted by (r) and (s).

Calibration has been performed using two primary standard sources: the hydrogen arc from 130 nm to 330 nm and the blackbody line radiator from 114 nm to 130 nm. The mini-arc has the following principal features: (1) a steady-state reproducible source with dc power requirements of less than 1.5 kW; (2) an intense continuum which is line- free between 194 nm and 330 nm and which has only a few narrow and widely spaced impurity lines between 114 nm and 194 nm; (3) a uniform output over a solid angle as large as f/9; (4) negligible aging effects over at least a 24 hour period; and (5) uncertainties (2σ) in the absolute spectral radiance of 5.3% above 140 nm and 10.1% between 114 nm and 140 nm. A budget of the errors contributing to these uncertainties is given in Table V. The radiant power emitted by the mini-arc is influenced primarily by the arc diameter, the arc current, and the transmission of the UV window material.

B. Argon Mini-Arc Irradiance Standard

The determinations of spectral irradiance are based on the assumptions that the system efficiencies of the measuring spectroradiometer are independent of the angle at which the radiation enters and that diffraction effects are not significant. Since the monochromator grating used must be assumed to have a nonuniform reflection efficiency, a diffuser located directly behind the field aperture is used to ensure that the first assumption is met, as is shown in Fig. 22. A magnesium fluoride window, ground on one side, was used as the diffusing element. Although it cannot be expected to be as good a diffuser as an integrating sphere, it was shown to be suitable, at least over a relatively small range of angles. For the argon mini-arc the uncertainty in the spectral irradiance that is due to the nonideal properties of the diffusing window can be as high as 6%.

The possible effects of diffraction must also be considered. For an extended homogeneous radiation source whose dimensions are large compared with the source aperture, it can be shown that Frauenhofer diffraction effects introduce no wavelength dependence and that the geometric factor γ in Eq. (7) is wavelength independent. This can be understood qualitatively by realizing that some percentage of the radiation from each radiating point does not pass through the field aperture because of diffraction. However, a complementary point can always be found in the domain of the extended homogeneous source that exactly makes up for such a loss. As will be discussed below, by substituting a different-sized aperture we show that the inhomogeneity of the mini-arc is insufficient to cause any measurable effects due to diffraction.

The vacuum spectroradiometer, as indicated schematically in Fig. 22, consists of a solar blind photomultiplier and a spectrometer with a 2-mm diameter field aperture. This aperture is mounted on a MgF_2 diffusing window located 50 mm in front of the entrance slit. The diffuser was located some distance in front of the entrance slit so as not to overfill the grating and thereby increase the scattered light, which was less than 2% of the weakest signal.

The light source used as a standard of spectral radiance in the near and vacuum ultraviolet was an argon mini-arc calibrated with respect to a primary standard, the NBS wall-stabilized hydrogen arc. Both sources have been sub-

Table VI. Error Budget for the Spectral Irradiance Calibration of the Argon Mini-Arc

Source	Contribution (%)
Standard (s)	5.3
Diffuser (s)	<6
Diffraction (s)	0.5
Spatial resolution (s)	4
Wavelength dependence from above effects (s)	0-4
Arc curent (r)	0.4
Gas flow (r)	-
Pressure (r)	-
Alignment (r)	-
Reproducibility (r)	-
Short term stability (r)	<1
Long term stability (r)	1
Gas impurity (r)	1
Combination of errors in quadrature	9-10

Random and systematic errors are denoted by (r) and (s).

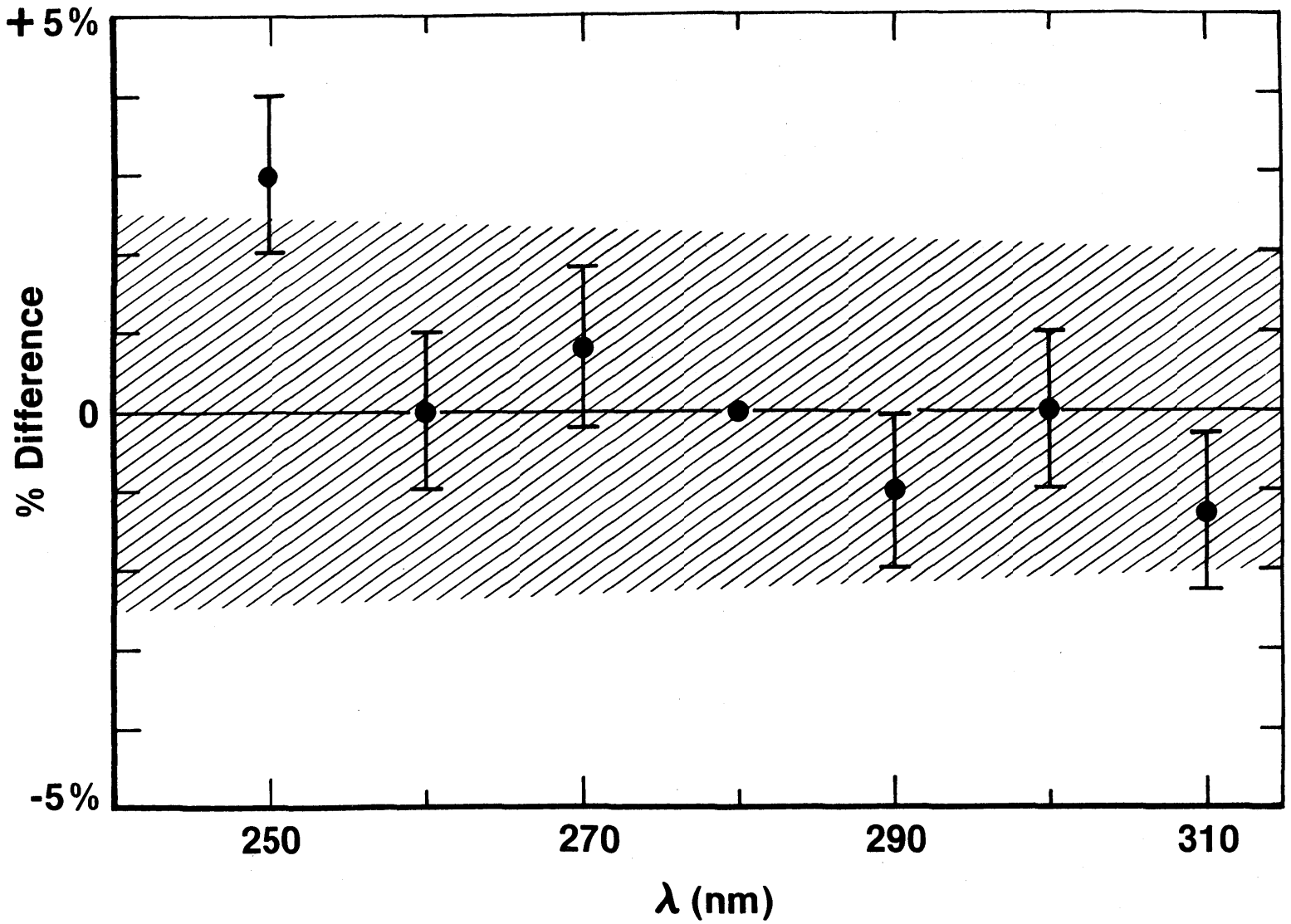

Figure 29. Percentage difference in the near UV between spectral-irradiance calibrations using conventional techniques (essentially using a tungsten-quartz-halogen irradiance standard and integrating sphere) and the method here introduced for VUV calibrations (essentially using a mini-arc radiance standard and diffusing window). The shaded area represents the uncertainty in the tungsten-lamp calibration. The error bars represent the imprecision in the measurements. The measurements were normalized at 280 nm.

jected to radiometric scale intercomparisons, both internal [1,18] and international.[25] The 2σ uncertainty in the absolute spectral radiance of the mini-arc has been determined in Sec. V-A to be 5.3% between 140 and 330 nm. The mini-arc was located 50 cm from the field stop, and a 0.3 mm diameter aperture placed 5 cm from the mini-arc center was used to restrict the size of the radiating area to about 0.5 mm in diameter.

The total uncertainty in the irradiance calibration of an argon mini-arc, including uncertainties in the primary source calibration and the transfer procedure, is estimated to be ≈10%. A budget of the errors contributing to this uncertainty is given in Table VI. Although the arc emits radiation at shorter wavelengths than that shown in Fig. 19, the short wavelength limit is taken to be 140 nm because of the low signal obtained from the stopped-down mini-arc radiance standard at shorter wavelengths. The bandpass for the radiance-to-irradiance transfer here was set at 1 nm. Not shown in Fig. 19 are several lines in the argon arc spectrum that are due to residual gas impurities.[16] The irradiance of the mini-arc was put on an absolute scale by determining its absolute spectral irradiance at 280 nm, using a tungsten-quartz-halogen lamp as an irradiance standard. A separate spectroradiometer utilizing a $BaSO_4$-coated integrating sphere, a predispersing monochromator, and an analyzing spectrometer was used for this measurement. As can be seen from Eq. (10), one measurement of this type is sufficient to determine the absolute irradiance at all wavelengths.

As a check on the method, it is possible to carry out tungsten-lamp calibrations at other wavelengths between 250 and 350 nm and thus overdetermine the system of measurements. Figure 29 illustrates the percentage difference between the spectral irradiance of the deuterium lamp based on the tungsten-lamp measurements (on the integrating-sphere-double-dispersion spectroradiometer) and the spectral irradiance based on the argon mini-arc measurements (on the diffusing-window-vacuum- monochromator spectroradiometer). The measurements are in agreement within 3%. However, perhaps because the point at 250 nm is a little high, one can perceive a slight trend toward an increasing difference at the shorter wavelengths, i.e., the radiance-based values seem to go lower than the tungsten-lamp based values. Such a trend would be expected if diffraction played an important role. In order to check on whether the argon-arc plasma was being sufficiently resolved by the collimating system and whether diffraction effects were indeed being accounted for by virtue of the extended nature of the source, additional measurements were taken with a 1-mm aperture used as the field aperture. These measurements should be more sensitive to possible diffraction effects since a smaller percentage of the diffracted beam from each radiating point passes through the field aperture. The spectral distribution of the signal was exactly the same as it was with the 2 mm diameter aperture, indicating that the data are not significantly affected by diffraction. The measurements also indicate that the spatial resolution was sufficient to define a relatively homogeneous region about the arc axis and that the radiance values applied to the data were appropriate. Thus, if there is a trend in the data of Fig. 29, diffraction effects do not seem to be the cause of it. Our irradiance scale is presently being compared with that of the NBS synchrotron ultraviolet radiation facility (SURF II) to check the consistency of the two scales.

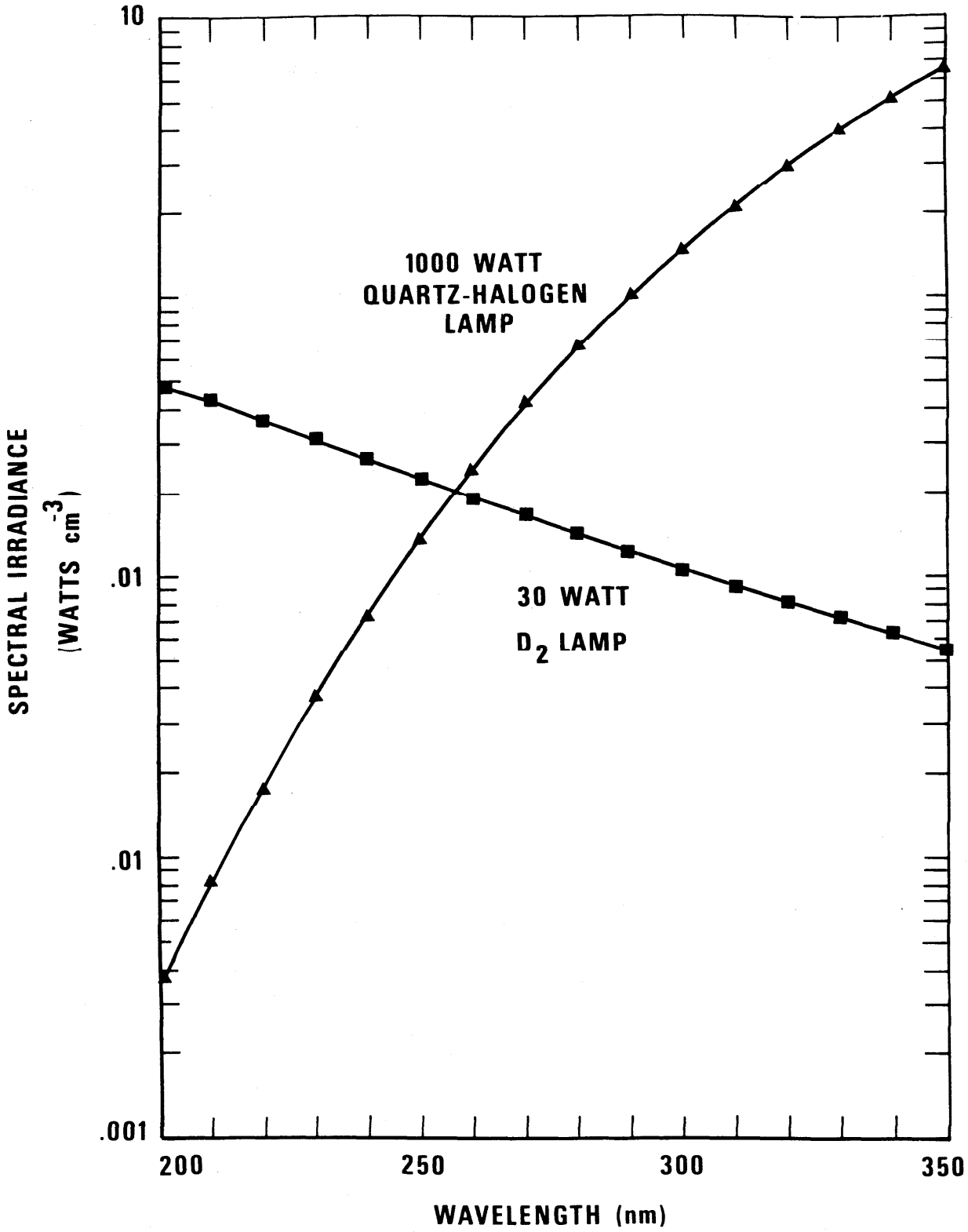

Figure 30. Typical spectral irradiance of a 1000 W quartz-halogen lamp and a 30-W deuterium lamp.

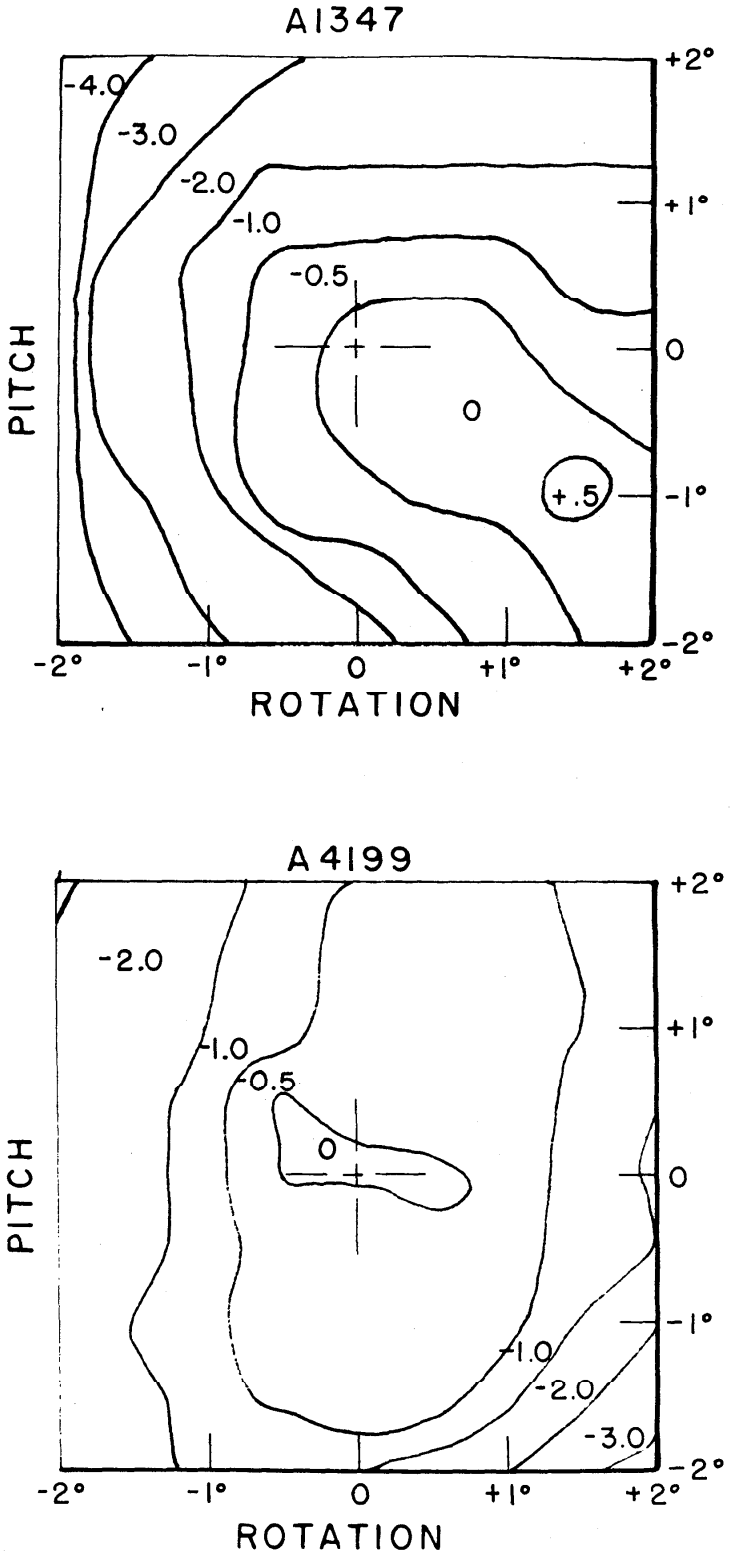

Figure 31. The dependence of the spectral irradiance upon pitch and yaw of a deuterium lamp located 50 cm from a 1-cm^2 aperture. A 2° angular change is equivalent to a 1.75-cm translational change.

C. Deuterium Lamp Irradiance Standard

1. Spectral Irradiance Calibration

Figure 30 illustrates the spectrum of a typical deuterium lamp as compared with a calibrated 1000-W tungsten quartz-halogen lamp. The spectral irradiance of the two types of lamps is equal at about 260 nm. At 350 nm the quartz-halogen lamp is stronger by a factor of 100. At 200 nm, the converse is true, the deuterium lamp being a factor of 100 stronger than the quartz-halogen lamp. The spectrum of the deuterium lamp above 350 nm is not illustrated, but is a continually decreasing continuum, about a factor of 10 lower at 550 nm than at 350 nm. Superimposed on the continuum there is an atomic hydrogen line at 486 nm and a combination of emission and absorption line structure in the region between 550 and 700 nm. However, the dominant feature in the spectrum is the intense UV continuum.

Since the shapes of the spectra of the two lamps illustrated in Fig. 30 are so different, a critical test of a spectroradiometer's performance at some specific wavelength can be applied by irradiating the instrument with each lamp. If the ratio of signals from the two lamps is not equal to the ratio of their calibrated spectral irradiances, it would follow that a systematic source of error is present in the measuring system such as scattered light, second order radiation, poor out-of-band rejection characteristics, or detector nonlinearity. We have experienced such an inconsistency which was eventually traced to fluorescence of a particular integrating sphere coating formerly used in our system.[26]

2. Alignment

The sensitivity of the spectral irradiance to lamp position is illustrated in Fig. 31 for two different lamps. The measurements were made for a wavelength of 250 nm. The contours were obtained by changing the pitch and yaw of the lamps in 0.5° increments over a ±2° grid. A $BaSO_4$-coated integrating sphere with a 1-cm^2 diameter aperture 50 cm from the lamp served as the field stop located at the entrance to the monochromator. Over such a small range of angular changes the contours may also be considered a measure of the sensitivity of the spectral irradiance to vertical and horizontal positioning over a grid range of ±1.75 cm. The two sets of contours are shown to illustrate the typical variation from lamp to lamp. Lamp A4199 appears to be more uniform since it exhibits a falloff of 2% or less through most of the grid. This is due mostly to the fact that the lamp was positioned very well for maximum irradiance when it was being potted. It can be seen that the center of maximum irradiance for the A1347 lamp is not at the 0,0 grid position but rather in the fourth quadrant. The potting procedure in this case was not as precise as for the A4199 lamp. Nevertheless, the results for both lamps indicate that if the lamp can be mounted so that the 0,0 position can be reproduced within ±0.9 cm, the alignment error will be no more than ±1%.

3. Lamp Current

The dependence of the spectral irradiance on lamp current is illustrated in Fig. 32. Below 100 mA, the lamp is not stable. Above 1 A the lamp over-

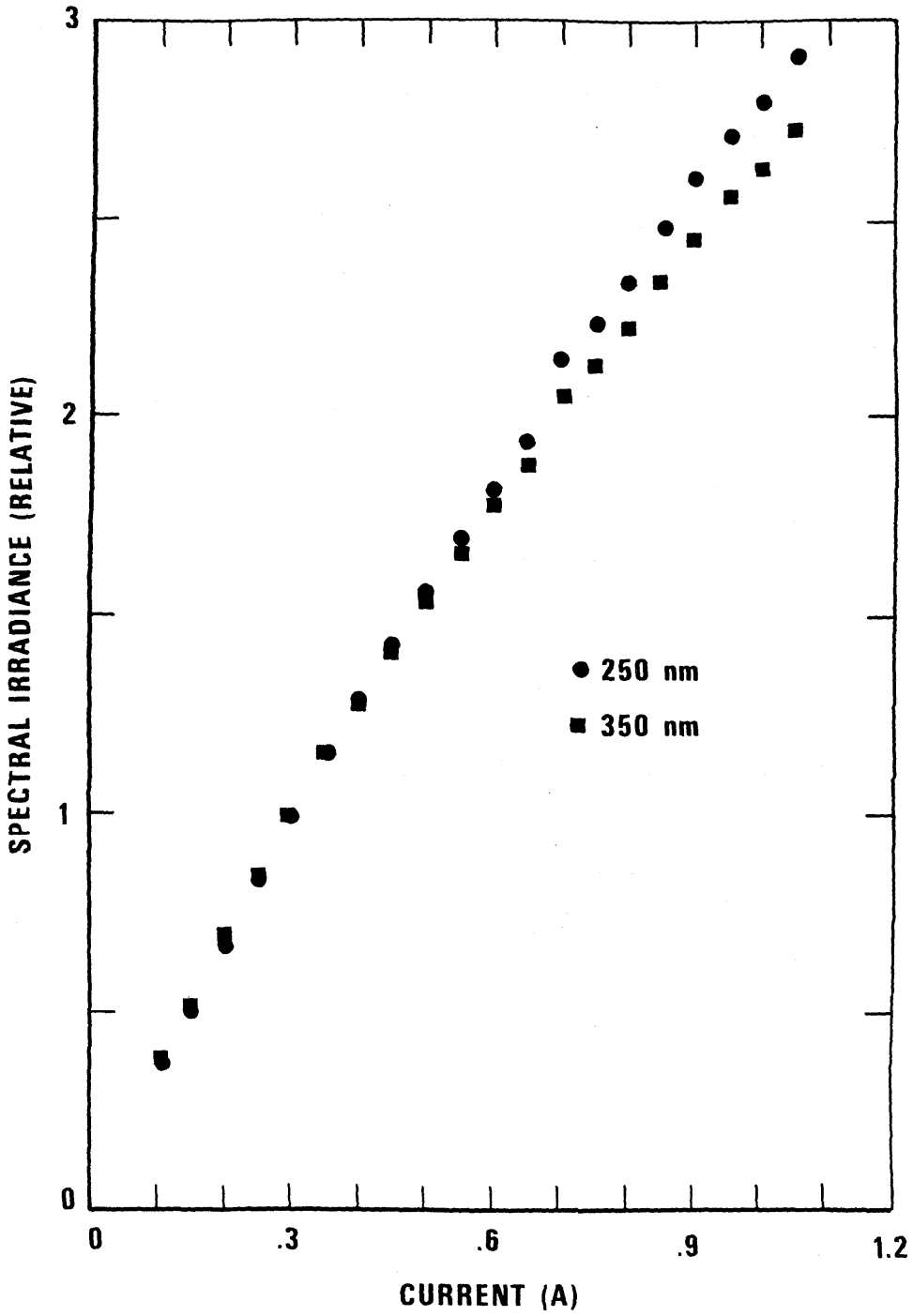

Figure 32. Spectral irradiance as a function of lamp current for two representative wavelengths. The values are normalized to the spectral irradiance at a current of 0.3 A.

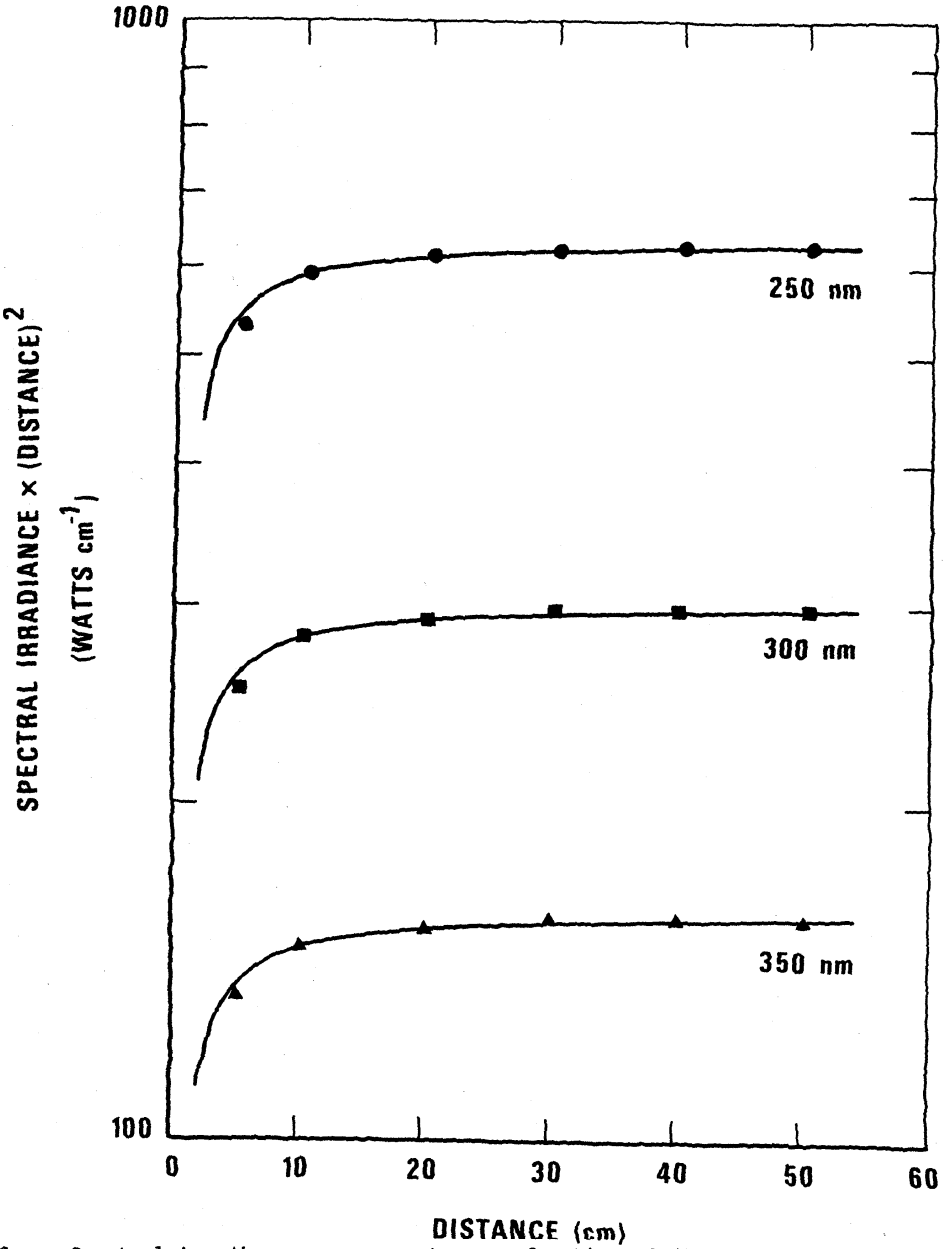

Figure 33. Spectral irradiance measurements as a function of distance between the deuterium lamp envelope and a 1-cm^2 field stop. Results expected by assuming the inverse square law and taking into account the finite size of the field stop and the position of the radiation center (determined by least squares fitting) are illustrated by the solid line. The data are taken at three representative wavelengths.

heats and is in danger of failure. Between these limits, the spectral irradiance can be varied about a factor of 10 and is nearly linear with current, with a slope weakly dependent on wavelength. It can be seen that high precision current measurements are not required in order to maintain lamp accuracy. For example, a precision of 1 mA at a lamp current of 300 mA causes an uncertainty of only 0.3% in the spectral irradiance.

4. Solid Angle

Figure 33 illustrates the dependence of the spectral irradiance of a deuterium lamp on solid angle. The field stop was a circular 1-cm^2 aperture on the entrance port of a $BaSO_4$-coated integrating sphere. If the source and this aperture were infinitely small and distance measurements were made between the aperture and the precise radiation center rather than the lamp pins, the data points on this plot would be expected to fall on a straight horizontal line. As can be seen, when the distance between the deuterium lamp and the field stop is reduced from 50 cm to 5 cm, the irradiance gradually departs from the ideal inverse square dependence. For distances greater than 20 cm, the deviation is less than 2%. The curve in Fig. 33 represents the results one expects strictly from geometric considerations when the finite aperture size and radiation center are taken into account. Because the radiation center is inside the sealed lamp and cannot be precisely measured, a least squares fitting of the curve to the data was carried out. Although the 50 to 10 cm data fit the curve to within 1%, the 5 cm datum does not. This is expected in view of the variation with position illustrated in Fig. 31. Thus, when the detector aperture size and radiation center are properly accounted for, the calibrated deuterium lamp may be operated at distances as close as 10 cm, i.e., at solid angles up to f/10 (0.008 sr), with an uncertainty in spectral irradiance of no more than 1%.

5. Variability

Because there was a fairly large variation in the stability, reproducibility, and aging characteristics from one lamp to another, much of the discussion in this section is in the form of observations rather than generalizations.

Warmup time varied from lamp to lamp. Some required none at all; others required up to 20 minutes. For the latter, typically the signal would rise to a maximum during the first minute and then slowly decrease, reaching an equilibrium value about 20% lower than the maximum after about 20 minutes. Because of this variation, it was decided that the lamps should be switched on routinely for 30 minutes prior to application. With this precaution, the radiative output of lamps, already aged for 100 hours, was measured to be stable at all wavelengths to within 1% over a 24 hour period of continuous operation.

Aging over the first 100 hours was more significant, amounting in general to a decrease of about 15% from the initial values. However, a slight wavelength dependence was observed in some lamps, and the ability of several lamps to recover from their diminished values during the first 100 hours implied that the aging process was not simple. Consequently, this study does not

attempt to generalize on the lamp behavior during the first 100 hours of its lifetime.

There was also a variation associated with striking the lamps. Some lamps would produce more signal if, after the normal warmup time, they were switched off and on again. Because the magnitude of this effect was not reproducible and certainly not characteristic of all lamps, it was decided always to start the lamp when it was at room temperature. The reproducibility of twelve lamps was tested by igniting the lamps every 2 hours for a total of 100 hours. After 30 minutes of warmup the spectral irradiance of the lamp was measured between 200 nm and 350 nm. The lamp was then turned off and allowed to cool down before the next ignition. Six of the lamps were reproducible with a standard deviation from their respective mean values of 1%. The worst of the twelve lamps had a standard deviation of 5%. For this particular lamp, the values of spectral irradiance seemed to cluster into two distinct groups, indicating that the lamp may have been bistable. Significantly, the relative spectral distribution of all the lamps tested was constant to within a standard deviation of 1%, i.e., the absolute values may have changed by about 5%, but the shape of the spectral irradiance vs wavelength curve did not vary by more than 1% on the average. From these tests, it is concluded that the standard deviation of a single measurement of a typical deuterium lamp may be as large as 5%, although one may preselect for greater dependability.

6. Calibration Checks and Accuracy

As a check on the accuracy of the method, it was standard procedure to compare the calibration of a deuterium lamp between 200 nm and 330 nm immediately after it was obtained using the argon mini-arc with a calibration of the same lamp between 250 nm and 350 nm obtained with a high accuracy calibrated quartz-halogen lamp. The uncertainty in the absolute values based on the argon mini-arc is 6%; based on the quartz-halogen lamp, it ranges from 3% at 250 nm to 2% at 350 nm. The variability of the deuterium lamp does not enter as a factor in this comparison since all measurements were done consecutively during the same run. On the average, the values based upon the arc calibration were 2% lower than those based upon the quartz-halogen lamp. The standard deviation of the differences was 3%. We interpret this agreement, to within the calibration uncertainties of the standards, to indicate that the radiance-to-irradiance calibration method used was free of significant systematic error and that the scale traceable to the hydrogen wall-stabilized arc (through the mini-arc) is consistent with the scale traceable to blackbody based methods. Confident that the scales are consistent to within 3%, we can effect a reduction in the overall deuterium lamp uncertainty by normalizing the mini-arc based values at 250 nm to the higher accuracy tungsten lamp values. Since most of the mini-arc uncertainty is traceable to a 5% uncertainty in the measurement of the hydrogen arc plasma length, the normalization essentially means that the hydrogen arc length is being determined more precisely, to within an uncertainty of 3%, based upon a radiometric measurement instead of a physical measurement. Thus, if we sum in quadrature the first six uncertainties given in Table VII, we find the total 2σ uncertainty in the deuterium lamp calibrations above 200 nm to be 6%. Below 200 nm we have an additional contribution due to the possibility of absorption by air contamination in the purge chamber between the deuterium lamp and the vacuum window. This contamination is apparently caused by outgassing from the chamber wall, which is

Table VII. Error Budget for the Spectral Irradiance Calibration of the Deuterium Arc Lamp

Source	Contribution (%)
Standard (s)	3
Diffuser (s)	<3
Alignment (r)	1
Lamp current (r)	0.3
Solid angle (r)	1
Variability (lamps preselected) (r)	4
Absorption by air contamination (195 nm to 167 nm) (r)	1-8
Combination of errors in quadrature	
above 200 nm	6
195 to 167 nm	6-10

Random and systematic errors are denoted by (r) and (s).

heated by radiation from the deuterium lamp. The inclusion of this final contribution which is given in Table VII gives an uncertainty of 6% to 10% in the wavelength region from 195 nm to 167 nm.

7. Summary

A set of commercially available deuterium lamps was calibrated for spectral irradiance in the 167-350 nm spectral range. At 250 nm and above the spectral irradiance values were obtained using a tungsten-quartz-halogen lamp whose calibration is based on an NBS blackbody. Below 250 nm the relative spectral distribution of the deuterium lamps was determined through the use of an argon mini-arc spectral radiance transfer standard whose calibration is based upon the NBS wall-stabilized hydrogen arc. The absolute values assigned to the deuterium lamps were then obtained by normalizing to the spectral irradiance values at 250 nm and above. Confidence in this procedure was established by comparing the absolute spectral irradiance of the deuterium lamps as determined independently by the argon mini-arc radiance standard and the tungsten-quartz-halogen irradiance standard in the 250-330 nm range. The agreement was within 3%. The large UV flux and high stability of the mini-arc are the properties which make possible the calibration below 250 nm.

The deuterium lamps are aligned and potted in bipost bases identical to those used in mounting tungsten-quartz-halogen lamps. The two standards are thus interchangeable in a given optical system. Since the shapes of the spectral distributions of these lamps are so different, the presence of systematic errors in a measurement system may be detected by intercomparing the two sources. The spectral irradiance of the 30 W deuterium lamp is equal to that of the 1000 W quartz-halogen-lamp at about 260 nm, 100 times stronger at 200 nm, and 100 times weaker at 350 nm.

The uncertainties in the absolute values of the deuterium lamp spectral irradiance are: 200 nm and above, 6%; 171 nm to 195 nm, 7%; and 170 nm and below, 10%. A major contribution to each uncertainty is the variability associated with the striking of the deuterium lamps. As a result all calibrated deuterium lamps supplied to customers by NBS are preselected for variabilities of 4% or less. For higher accuracy and confidence, one may take advantage of the result that the relative spectral distribution of the deuterium lamps is reproducible to within about 1%. Thus, the uncertainty may be reduced by renormalizing the absolute scale with a quartz-halogen lamp after each ignition to eliminate any variability in the strike. This procedure makes possible a reduction in the uncertainties of about 3%.

Additional work has shown that under certain conditions the deuterium lamp with an MgF_2 window may be used as a radiometric standard down to 115 nm.[27] This effort was directed at determining the circumstances under which portions of the many-line molecular spectrum below 167 nm can be used as a continuum. See App. A for a discussion of this investigation.

VI. Quality Control Through Intercomparisons

A. Introduction

In radiometric work the demonstration of the consistency of independent primary standards is essential to the foundation of valid systems of calibration. This process involves both internal and external comparisons of primary standards. At NBS the independent internal primary standards to be compared are a wall stabilized hydrogen arc discharge and a gold-point blackbody. The external comparison of primary standards involves the NBS hydrogen arc and radiation from the DESY synchrotron in Hamburg, Germany. A comparison of the NBS hydrogen arc with the SURF II synchrotron at NBS is in process, but no results are as yet available.

B. The Hydrogen Arc Versus the Gold-Point Blackbody

1. Tungsten Strip Lamp

A calibration of the spectral radiance of the hydrogen arc obtained using an NBS-calibrated tungsten strip lamp was compared to the same quantity determined from the calculated maximum hydrogen continuum emission coefficient.[1] The spectral radiance calibration of the tungsten strip lamp was based on an NBS gold-point blackbody and was carried out for twenty wavelengths in the range 230 nm to 800 nm. The uncertainties in the twenty measurements range from 2% at the shortest wavelength to 0.7% at the longest wavelength. To determine the spectral radiance of the hydrogen arc, the transmission of the arc end-window must also be measured. This contributes an additional uncertainty of 4%. Figure 6 shows a plot of the spectral radiance of the hydrogen arc as a function of wavelength as determined by several methods. The curve in the figure is the theoretical spectral radiance, which is the product of the theoretical maximum hydrogen plasma emission coefficient and the arc length. The curve is graphed as a shaded area which represents the rms uncertainty due to the previously described uncertainties in both the calculated emission coefficient and the arc length. The solid circles represent the measured continuum values obtained using the calibrated tungsten strip lamp for spectral radiance normalization. The discontinuity in the wavelength scale is due to the interruption of the hydrogen spectrum by the Balmer line series of atomic hydrogen, which dominates the high temperature arc spectrum above 360 nm except for a small region around 560 nm between H_α and H_β. The solid circles are the average of ten runs performed on different days, and the error bars represent uncertainties associated not with the hydrogen arc but with the tungsten strip lamp. As can be seen from Fig. 6, the theoretical values and the experimental results based on the tungsten strip lamp are in excellent agreement, thus showing consistency between calibrations based on the hydrogen arc theory and those based on a gold-point blackbody for a wavelength range 360 nm to 250 nm.

2. Tungsten Strip Lamp with Blackbody Line Arc

In the preceding comparison of the hydrogen arc and the tungsten strip lamp, the minimum wavelength was determined by the short wavelength cutoff of the tungsten lamp at 230 nm. By use of the blackbody line arc along with the

tungsten strip lamp, the minimum wavelength can be lowered to about 124 nm.[1] In the present comparison a wall stabilized arc discharge is seeded with C, N, and O atoms to produce optically thick blackbody limited resonance lines in the UV and VUV. The calibration of one of the lines in the UV with the tungsten strip lamp permits the calibration of others at wavelengths shorter than the low wavelength cutoff of the tungsten strip lamp. These calibrated blackbody limited lines can then be used to calibrate the hydrogen arc at their wavelengths. In particular, the blackbody ceiling of the C I optically thick emission line at 247.9 nm is calibrated with the tungsten strip lamp. This calibration is applied to the Kirchhoff-Planck function to determine the temperature of the blackbody line arc. For a 4.7 mm diameter arc at 60 A, the axis temperature of the argon plasma with admixtures of N, C, O, and H was found to be 11,900 K. A temperature uncertainty of ±160 K is estimated due to an estimated rms uncertainty of about 6% in the blackbody intensity determination at 247.9 nm. The temperature was then used with the Kirchhoff-Planck function to obtain the radiances of the following blackbody limited lines: C I, 193.1 nm; N I, 174.3 nm; C I, 165.6 nm; N I, 149.2 nm; C I, 146.3 nm; O I, 130.2 nm; C I, 126.1 nm; and N I, 124.3 nm. Finally, these line calibrations were used for the spectral radiance normalization of the hydrogen arc, the results of which are plotted as open circles in Fig. 6. Each point is the average of ten runs, and the error bars represent uncertainties associated with the tungsten strip lamp and the blackbody line arc. We see that the open circle points based on a gold-point blackbody are in excellent agreement with the shaded curve of theoretical results, and thus calibrations based on the hydrogen arc and gold-point blackbody primary standards are seen to be consistent in the wavelength range 200 nm to 124 nm.

3. Argon Mini-Arc and Tungsten-Quartz-Halogen Lamp with Deuterium Lamp

In the initial calibration of the deuterium lamp, the argon mini-arc and the tungsten-quartz-halogen lamp were used as calibrating secondary standards of spectral radiance and irradiance, respectively.[18] The mini- arc is calibrated against the hydrogen arc, whereas the calibration of the quartz-halogen lamp is traceable to a gold-point blackbody. Thus, the calibration of the deuterium lamp by the above secondary standards gives information on the radiance-to-irradiance transfer method and the consistency of the hydrogen arc and blackbody as primary standards.

Using the radiance calibrated mini-arc, the procedure for radiance-to-irradiance transfer given above was applied to calibrate the deuterium lamp for spectral irradiance in the range 200 nm to 350 nm. Immediately thereafter, the deuterium lamp was calibrated in irradiance in the range 250 nm to 350 nm using the irradiance-calibrated quartz-halogen lamp. The 2σ uncertainty in the radiance-to-irradiance calibration using the mini-arc is estimated to be less than 10%,[22] while the uncertainty in an irradiance calibration using the quartz-halogen lamp ranges from 3% at 250 nm to 2% at 350 nm. Comparing the results, the values based on the mini-arc were found to be about 2% lower than those based on the quartz-halogen lamp, and the standard deviation of the differences was about 3%. We interpret this agreement, to within the uncertainties in the two methods, to indicate that the radiance-to-irradiance transfer procedure is valid and that the scale traceable to hydrogen arc is consistent with the scale traceable to a gold-point blackbody.

C. The Hydrogen Arc versus the DESY Synchrotron

1. Deuterium Lamp

In this section we compare the UV radiometric scales of three laboratories through the spectral radiance calibration of deuterium lamps.[25] The laboratories are the Max Planck Institut für Astronomie (MPI), the Physikalisch Technische Bundesanstalt (PTB), and NBS. As fundamental radiometric standards the NBS group used the optically thin continuum radiation from its wall-stabilized hydrogen arc, whereas both the MPI and PTB groups used the DESY synchrotron radiation facility in Hamburg. Although the MPI and PTB groups used the same primary standard, their instrumentation and measurement methods were different. Because of the differing experimental requirements of the groups, the area of the deuterium lamp calibrated by each group is different. This affects the absolute values obtained by each group but not the relative spectral distribution, which is essentially independent of spot size. Thus this intercomparison is a direct check of the consistency of the relative scales between 165 nm and 350 nm.

The deuterium lamps used here were of the end-on type, Model D-15.[25] Such lamps have been flown in rocket spectroradiometers for calibration purposes[28] and have operating characteristics very similar to those of the side-on type which has been described above. The lamps were subjected to extensive aging and reproducibility tests and preselected to minimize any short term variations in radiative output and undesirable wavelength aging characteristics. Following are the relevant operating conditions:

1. lamp current: 200 mA;

2. lamp orientation: the lamp was translated and rotated for maximum signal at 220 nm;

3. cooling conditions: there was no lamp housing, and the lamp was exposed to normal room temperature and ventilation;

4. lighting procedure: with the lamp at room temperature the filament power was switched on for 5 sec and switched off after the application of the anode voltage and lamp ignition;

5. area calibrated: NBS, 0.07 mm^2 circular; PTB, 0.64 mm^2 circular; and MPI, 0.05 mm^2 circular. A detailed investigation of the lamp properties is published elsewhere.[29]

The primary standard of spectral radiance used in the MPI and PTB calibrations was synchrotron radiation.[30,31] The electron synchrotron provides intense, continuous radiation over a wide spectral range. The instantaneous power radiated by an electron accelerated in a synchrotron can be accurately calculated[32] and depends on measurable machine parameters, the final energy of the electrons, the mode of acceleration, the radius of the electron orbit, and the solid angle used for measurements. The total flux emitted from the synchrotron in a given direction is proportional to the number of circulating electrons.

The PTB calibration facility at DESY allows the simultaneous measurement of synchrotron radiation in the visible and VUV spectral regions with a two-monochromator system. One monochromator looks at the visible radiation from the synchrotron and compares it with a tungsten strip lamp. The other monochromator operates throughout the near and vacuum UV and compares the synchrotron radiation with that of the deuterium lamp to be calibrated. A detailed description of the principle of calibration and the instrumentation is given elsewhere.[33] The rms uncertainty (σ) in the absolute spectral radiance of the calibrated deuterium lamp is estimated to be $\leq$2%. This uncertainty is made up of the following individual contributions: uncertainty of the parameters of the synchrotron 0.4%, uncertainty in the determination of the current of accelerated electrons 1.2%, and uncertainty in the experimental device 1.3%. The calibrated spectral radiance of the deuterium lamp was checked by a comparison with the spectral radiance of the tungsten strip lamp in the wavelength region 290 nm to 340 nm using a different spectroscopic system. The agreement was within ±1.5%.

The MPI calibration facility at DESY has been described previously,[34] although the spectroradiometer used in these measurements was a modified version of the one described. Additional baffling and stray light precautions were necessary to overcome a systematic measurement error that was evident in an earlier calibration above 260 nm.

The MPI spectral radiance calibration, besides depending on the spectral radiance of a tungsten strip lamp in the visible and the known spectral distribution of the synchrotron radiation, depends upon measurements of the reflectivity of one mirror and the polarization characteristics of the spectroradiometer. The total rms uncertainty in the measurements is estimated to be ±3%. The absolute scale was compared separately at MPI by calibrating the D_2 lamp with a tungsten strip lamp above 250 nm. The agreement was within ±4%.

The primary standard of spectral radiance used in the NBS calibration was the wall-stabilized hydrogen arc discharge described above. The hydrogen arc provides an almost completely ionized hydrogen plasma for which the continuum emission coefficient can be very accurately calculated. By operating the arc at a current for which the spectral radiance reaches a maximum at a given wavelength, the absolute value of the spectral radiance depends only on the arc length, the atmospheric pressure, and the condition of local thermodynamic equilibrium.[1] The rms uncertainty in the absolute spectral radiance of the hydrogen arc is estimated to be ±5%.

The NBS calibration facility has been described above. The radiation of the sources is focused, with magnification M = 1, on the entrance aperture (0.300-mm diam) of a vacuum monochromator. A mask in front of the focusing mirror restricts the radiation to an f/200 beam. The possibility of second order radiation is eliminated through the use of a cutoff filter inserted in front of the solar blind photomultiplier for wavelengths longer than 220 nm. The UV end-window of the hydrogen arc serves as the vacuum seal and remains in the system for all measurements. Thus, both the primary and transfer sources illuminate the UV window, the optical surfaces, and the detector photocathode in the same way, eliminating possible sources of systematic error. The short chamber which separates the deuterium lamp from the UV vacuum window was

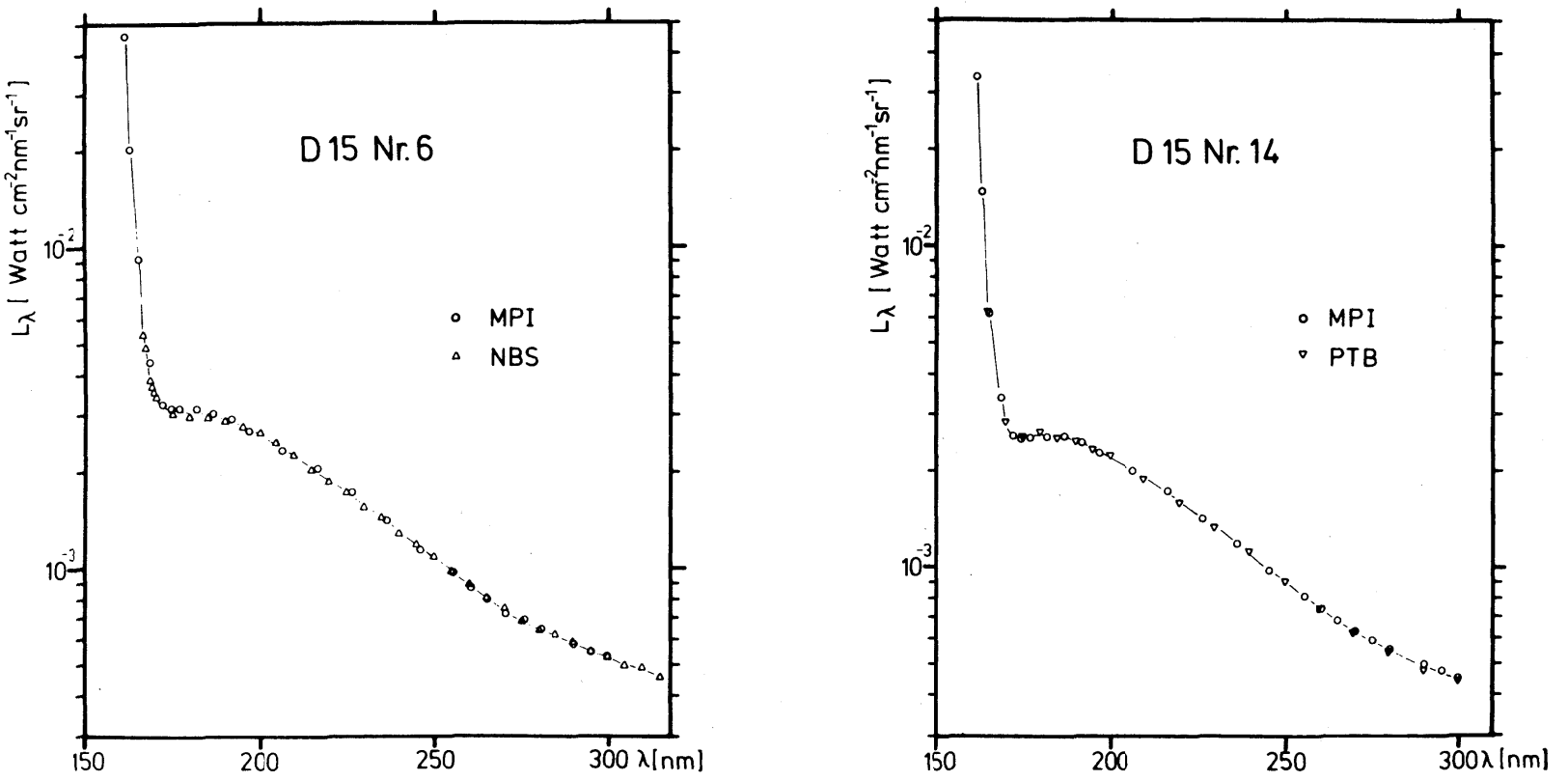

Figure 34. Results of the interlaboratory comparisons of spectral radiance calibrations of deuterium lamps between NBS and MPI (No. 6) and between PTB and MPI (No. 14). The MPI spectra were normalized to the other data to show only the wavelength dependent part of the deviations, which is within ±3%.

purged with high purity argon gas, thus protecting the lamp window from possible deterioration due to condensation of UV photo-dissociated hydrocarbons.

Following the calibration of the lamp on the vacuum UV calibration facility, the lamp was calibrated on a different spectroradiometric system using a tungsten strip lamp as the spectral radiance standard. This was done in air in the 250-350 nm wavelength range. Since the two calibrations gave the same results, one has increased confidence that the deuterium lamp alignment was proper and that no significant systematic errors were present in the measurements.

The intercomparison was performed using two lamps: No. 6 was calibrated by NBS and MPI, and No. 14 was calibrated by PTB and MPI. Figure 34 shows the absolute spectral radiance of the two calibrated lamps as determined by NBS and PTB. The MPI measurements, illustrated by circles, have been normalized to give a best fit to the NBS and PTB results. No emphasis was placed on a comparison of the absolute scales since the calibrated area of the D_2 lamp was different for each group.

The agreement everywhere is within ±3% except below about 170 nm, where several blended emission lines (not shown in the figure) belonging to the molecular deuterium Lyman band system appear in the spectrum. Similar results have been obtained by Einfeld et al.[35] in a separate intercomparison with the Technische Universität in Munich. Our agreement indicates that the spectral radiance scales based upon the DESY synchrotron and the NBS hydrogen arc are consistent, at least in a relative sense. Since each of the calibrations was repeated in the near UV using calibrated tungsten strip lamps, it may also be inferred that the absolute scales are consistent since the tungsten lamps calibrated by PTB and NBS have been shown to be consistent.[36,37] Furthermore, because the spectral distributions of the synchrotron radiation and the hydrogen arc radiation are so different, one increasing toward shorter wavelengths and the other increasing toward longer wavelengths, the agreement indicates that the three calibration facilities are reasonably free of systematic sources of error such as scattered light, second order radiation, nonlinearity effects, and fluorescence phenomena.

VII. Acknowledgments

The authors are grateful for the suggestions made by Wolfgang L. Wiese, Chief of the Atomic and Plasma Radiation Division, James R. Roberts, Group Leader of the Plasma Radiation Group, and the CALCOM committee members who reviewed this Document. The members of this committee were: Dale D. Hoppes, Donald McSparron, William R. Ott, and Bert G. Simson. Special thanks are due Dr. Ott, who served as chairman of the CALCOM committee. The helpful suggestions of Lois S. Gallahan and Helen R. Felrice in preparing this manuscript are also gratefully acknowledged. Finally, the authors wish to acknowledge the continuing support of the VUV Radiometry program at NBS by the NASA Solar and Heliospheric Physics Branch. Most of the work described here was carried out under partial funding by this agency.

VIII. References

1. W. R. Ott, K. Behringer, and G. Gieres, Appl. Opt. 14, 2121 (1975).

2. J. R. Roberts and P. A. Voigt, J. Res. Nat. Bur. Stand. 75a, 291 (1971).

3. W. R. Ott, P. Fieffe-Prevost, and W. L. Wiese, Appl. Opt. 12, 1618 (1973).

4. W. R. Ott and W. L. Wiese, Opt. Eng. 12, 86 (1973).

5. W. L. Wiese, in Methods of Experimental Physics, B. Bederson and W. L. Fite, Eds. (Academic, New York, 1968), Vol. 7B, p. 307.

6. R. W. Larenz, Z. Phys. 129, 327 (1951).

7. K. Behringer, Z. Phys. 246, 333 (1971).

8. S. Steinberger, Z. Phys. 223, 1 (1969).

9. P. Kepple, Report 831, Dept. of Physics and Astronomy, Univ. of Maryland (1968).

10. H. Maecker and S. Steinberger, Z. Angew. Phys. 23, 456 (1967).

11. J. H. Walker, R. D. Saunders, and A. T. Hattenburg, Spectral Radiance Calibrations, Nat. Bur. Stand. (U.S.) Spec. Publ. 250-1; 1986.

12. J. Uhlenbusch and G. Gieres, Z. Angew. Phys. 27, 66 (1969).

13. G. Boldt, Space Sci. Rev. 11, 728 (1970).

14. J. C. Morris and R. L. Garrison, J. Quant. Spectrosc. Radiat. Transfer 9, 1407 (1969).

15. D. Stuck and B. Wende, J. Opt. Soc. Am. 62, 96 (1972).

16. J. M. Bridges and W. R. Ott, Appl. Opt. 16, 367 (1977).

17. J. A. R. Samson, Techniques of Vacuum Ultraviolet Spectroscopy, (Wiley, New York, 1967).

18. R. D. Saunders, W. R. Ott, and J. M. Bridges, Appl. Opt. 17, 593 (1978).

19. J. H. Walker, R. D. Saunders, J. K. Jackson, and D. A. McSparron, Spectral Irradiance Calibrations, Nat. Bur. Stand. (U.S.) Spec. Publ. 250-20; 1987.

20. E. F. Zalewski, J. Opt. Soc. Am. 62, 1372 (1972).

21. W. R. Ott, J. M. Bridges, and P. A. Voigt, in Proceedings of the 5th International Conference on Vacuum Ultraviolet Radiation Physics,

M. C. Castex, M. Pouey, and N. Pouey, eds. (Centre National de la Recherche Scientifique, Meudon, France, 1977), Vol. 3, p. 123.

22. W. R. Ott, J. M. Bridges, and J. Z. Klose, Opt. Lett. 5, 225 (1980).

23. J. C. Morris, J. Quant. Spectrosc. Radiat. Transfer 9, 1629 (1969).

24. J. Richter, in Plasma Diagnostics, W. Lochte-Holtgreven, Ed. (North-Holland, Amsterdam, 1968), p. 36.

25. J. M. Bridges, W. R. Ott, E. Pitz, A. Schulz, D. Einfeld, and D. Stuck, Appl. Opt. 16, 1788 (1977).

26. R. D. Saunders and W. R. Ott, Appl. Opt. 15, 827 (1976).

27. J. Z. Klose, J. M. Bridges, and W. R. Ott, Extended Abstracts of the VI International Conference on Vacuum Ultraviolet Radiation Physics, Charlottesville, Va., (June 2-6, 1980), p. III-52.

28. C. Leinert, E. Pitz, H. Link, and N. Salm, Space Sci. Instrum. 5, 257 (1981).

29. D. Einfeld and D. Stuck, Opt. Commun. 19, 297 (1976).

30. K. Codling and R. P. Madden, J. Appl. Phys. 36, 380 (1965).

31. D. Lemke and D. Labs, Appl. Opt. 6, 1043 (1967).

32. J. Schwinger, Phys. Rev. 75, 1912 (1949).

33. D. Einfeld, D. Stuck, and B. Wende, Proceedings of the 9th Annual Synchrotron Radiation Users Group Conference, Univ. of Wisconsin (1976).

34. E. Pitz, Appl. Opt. 8, 255 (1969).

35. D. Einfeld, D. Stuck, K. Behringer and P. Thoma, Z. Naturforsch 31a, 1131 (1976).

36. M. Suzuki and N. Ooba, Metrologia 12, 123 (1976).

37. R. D. Lee et al., in Temperature, Its Measurement and Control in Science and Industry, H. H. Plumb, Ed. (Instrument Society of America, Pittsburgh, 1972), Vol. 4, p. 377.

38. G. H. Mount, G. Yamasaki, Walter Fowler, and W. G. Fastie, Appl. Opt. 16, 591 (1977).

39. J. Z. Klose, Radiometric Calibration of the Space Telescope Vacuum Optical Simulator (calibration report for Martin Marietta Denver Aerospace), October, 1984.

40. J. Z. Klose, Portable UV Radiometric Standards (contract report for the National Oceanic and Atmospheric Administration), September, 1981.

41. J. Z. Klose, J. M. Bridges, and W. R. Ott, J. Opt. Soc. Am. 72, 1804 (1982).

42. R. T. Brackmann, W. L. Fite, and K. E. Hagen, Rev. Sci. Instrum. 29, 125 (1958).

43. W. E. Kauppila, W. R. Ott, and W. L. Fite, Rev. Sci. Instrum. 38, 811 (1967).

44. K. Watanabe, E. C. Y. Inn, and M. Zelikoff, J. Chem. Phys. 21, 1026 (1953).

45. J. Z. Klose, J. M. Bridges, and W. R. Ott, Appl. Opt. 24, 2263 (1985).

IX. Appendices

A. The Deuterium Lamp as a Radiometric Standard Between 115 nm and 167 nm

At NBS an investigation has been carried out with the aim of extending the VUV range of spectral irradiance of the deuterium lamp down to the MgF_2 cutoff at 115 nm.[27] The effort was directed at determining under what conditions portions of the blended line spectrum below 167 nm can be used as a continuum. In this connection computer recorded continuous scans of the spectrum of a D_2 lamp with a side-on MgF_2 window were made over the wavelength range 115-177 nm at several different bandpasses. The data from these scans were recorded as intensities at intervals of 0.25 nm and stored in a computer as a function of bandpass for each wavelength. All measurements were made with identical entrance and exit slits. Figure 35 shows computer generated plots of intensities versus wavelengths for the extreme bandpasses of 0.83 nm (1 mm slits) and 4.98 nm (6 mm slits). The traces were normalized in the pure continuum region above 170 nm. Below 170 nm the curves are contrasted by the presence in one case and complete absence in the other of spectral line structure. Additional measurements were made at bandpasses of 1.66, 2.49, 3.32, and 4.15 nm to investigate the fading of the line structure with increasing bandpass.

In order to quantify the deviations of the spectral distributions at the various bandpasses from the spectral distribution of the broadband pseudo-continuum, a procedure of analyzing the data by comparing the normalized ratios of the intensities at the narrower bandpasses to the intensities at the broadest bandpass was adopted. The computer was therefore programmed to produce such ratios, listing them for each wavelength in columns according to their bandpass ratios. If the intensity ratio for each column is 1 over some wavelength interval, the spectral region can be treated as pure continuum. If the maximum difference in the intensity ratios over the columns is 10% for a certain wavelength region, that spectral region can be regarded as a continuum only to a precision of 10%. By comparing the intensity ratios as a function of bandpass ratio for each wavelength, one can determine wavelength intervals over which the intensity ratios vary less than a chosen amount. For example, over the range 139.75 nm through 153.75 nm the maximum difference in the intensity ratios is 15% for the set of bandpass ratios 1/6, 2/6, 3/6, 4/6, 5/6, and 6/6. Figure 36 shows the wavelength ranges over which the maximum differences in the intensity ratios are 10, 15, and 20%. From the figure one sees a significant extension of the ranges in going from a difference of 10% to a difference of 15% and ranges added, especially one near 120 nm, in going from 15% to 20%. As an experimental check several intensity ratios obtained by the continuous scans were compared with ratios obtained by static measurements at given wavelengths and found to be in good agreement.

In conclusion, the maximum differences given in Fig. 36 can be taken as indications of how closely the blended line spectrum approaches a pure continuum throughout the different wavelength ranges. Thus, the figure shows different combinations of precision and wavelength for which this deuterium lamp can be used as a continuum source for calibration in the VUV. Similar graphs can be constructed for any such D_2 lamp to determine the wavelength ranges for any desired maximum difference.

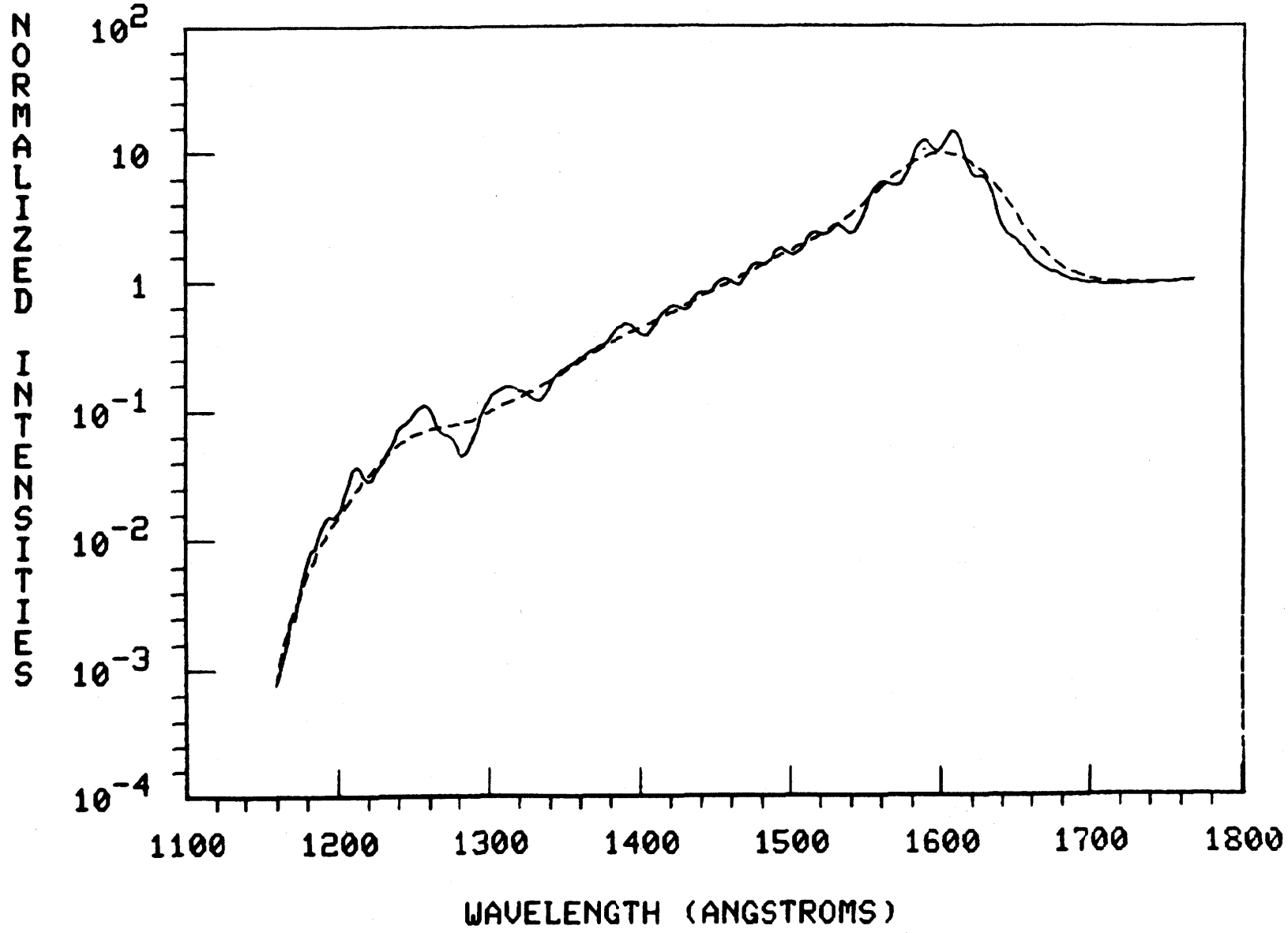

Figure 35. Intensities versus wavelength for 1-mm entrance and exit slits (solid curve), and the same quantities for 6-mm entrance and exit slits (dashed curve).

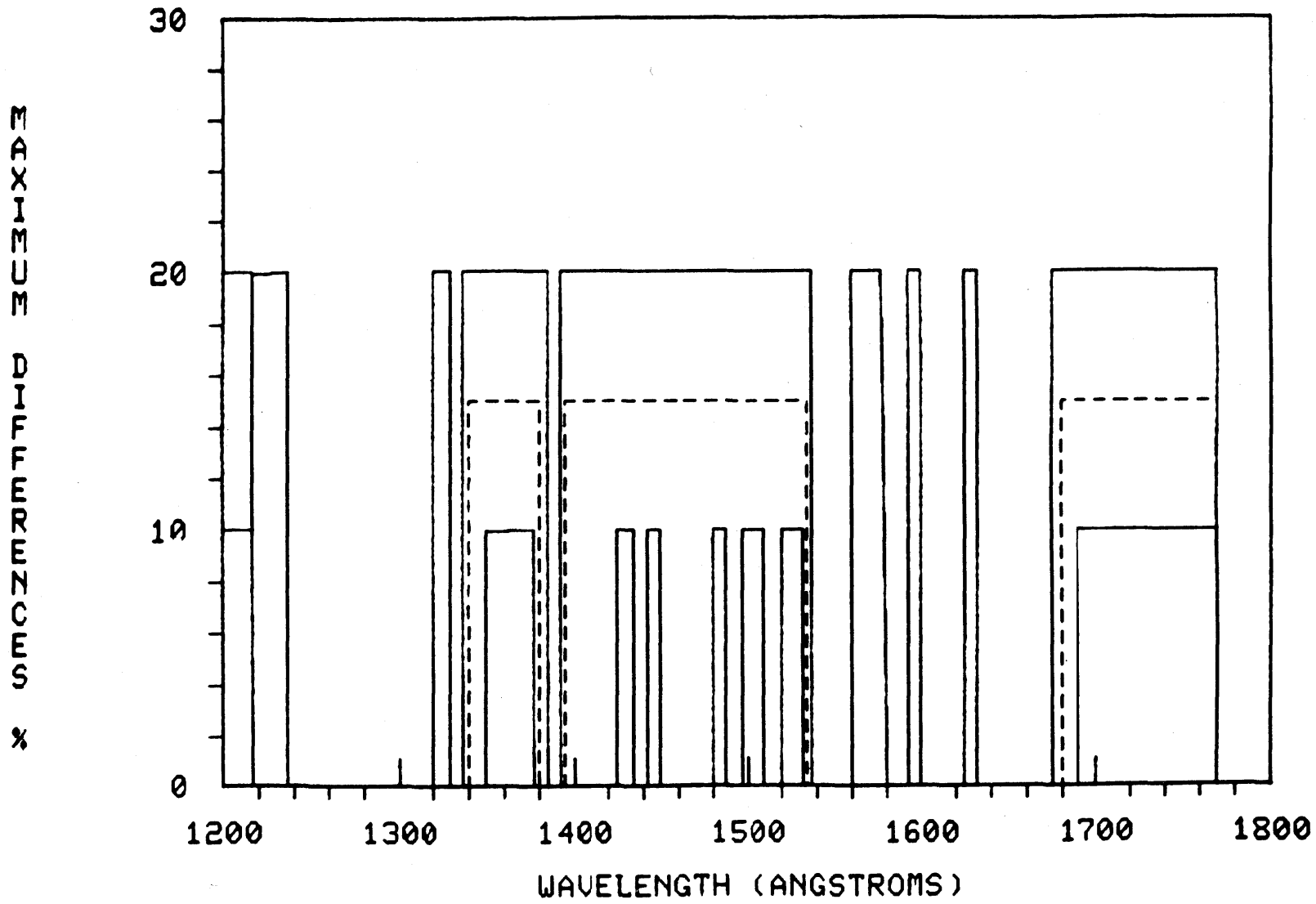

Figure 36. Maximum differences in the intensity ratios over the range of bandpass ratios versus wavelength.

B. Hollow Cathode Lamps

A source which is gaining in favor for the calibration of space experiments is the metal rare gas hollow cathode discharge lamp. Two versions of this lamp having a platinum or platinum-chromium cathode and a filling of neon gas[38] are being used to calibrate two instruments on the Space Telescope. These lamps with MgF_2 windows are spectral line sources which cover the wavelength range from the VUV at 115 nm to the infrared at 878 nm. Figure 37 shows a portion of the spectrum of a Pt-Cr-Ne lamp. Sets of the lamps were calibrated at NBS and were then used for preflight calibrations of the Faint Object Spectrograph (FOS) in wavelength and irradiance[39] and the High Resolution Spectrograph (HRS) in wavelength only. Two Pt-Cr-Ne lamps will be on board the FOS to monitor its operation and serve as inflight wavelength standards, while two Pt-Ne lamps will be on board the HRS as inflight wavelength standards. Sets of these NBS-calibrated lamps are also being used in preflight throughput tests of the Space Telescope with all of its instruments installed. The additional instruments are the Wide Field/Planetary Camera (WF/PC), the Faint Object Camera (FOC), and the High Speed Photometer (HSP).

These lamps have excellent physical characteristics for inflight use in that they are rugged, dependable, small, light, and low powered (4 W). They are also readily available commercially at reasonable prices. The VUV radiometry group at NBS is investigating these types of lamps further for the purpose of determining their suitability as secondary radiometric standards.

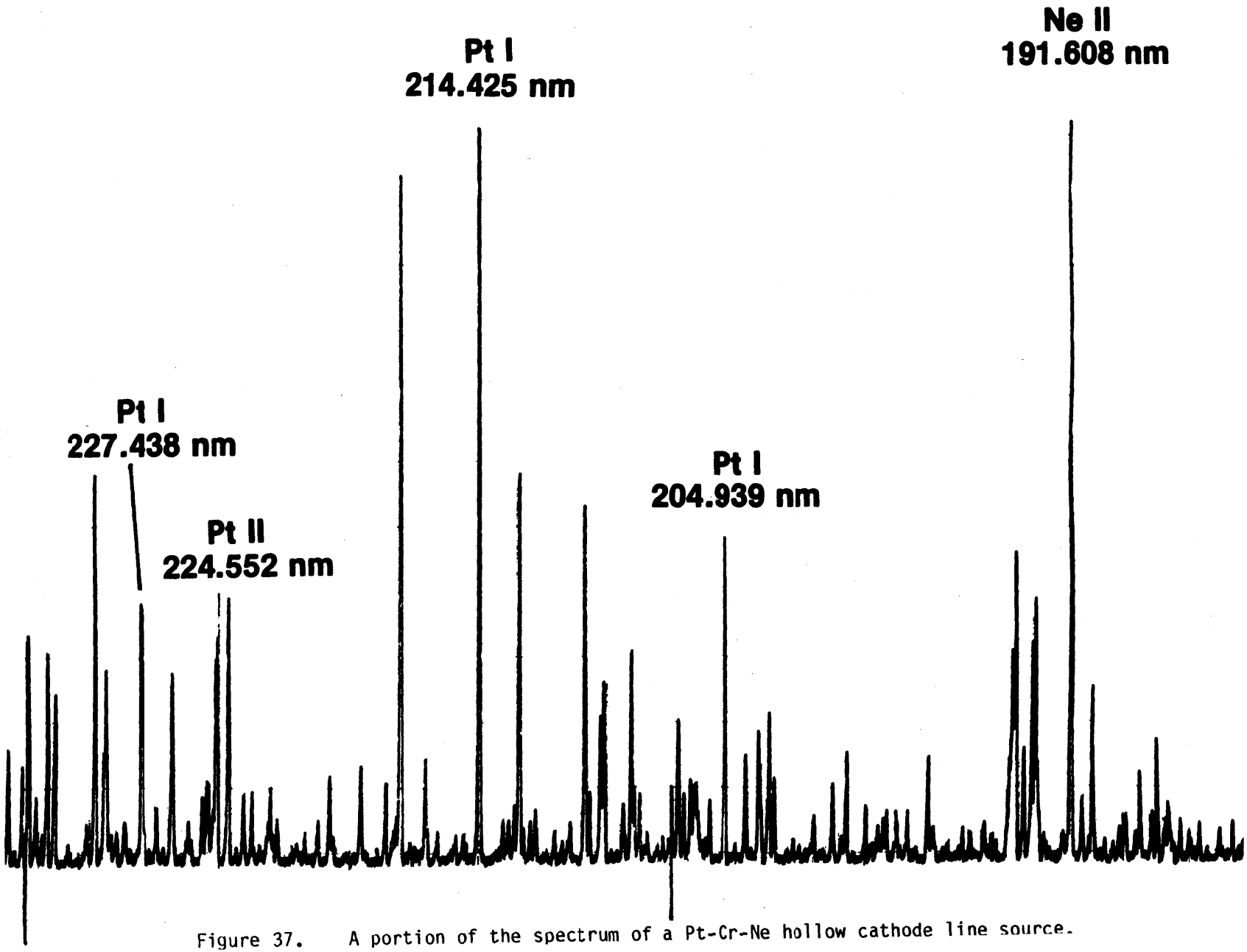

Figure 37. A portion of the spectrum of a Pt-Cr-Ne hollow cathode line source.

C. Rare Gas Dimer Lamps

Another type of lamp which has received considerable attention as a calibration source in the VUV for space experiments is the rf-excited rare gas dimer lamp.[40] These lamps emit significant radiation in the VUV but only over limited wavelength ranges of about 60 nm or less. Nevertheless, the lamps, which separately contain argon, krypton, and xenon, can provide between them a calibrated continuum from 115 nm to 200 nm.

The dimer lamps consist of pyrex cylinders with MgF_2 end-windows. In the original design each lamp is excited by a thin wire antenna which extends into a central channel in the barrel of the lamp. This design produced a non-uniform shell of radiation concentric with the channel, which resulted in annular emission through the window. With emission in this form the lamps could be calibrated in irradiance, but not conveniently in radiance. However, a new design, suggested by the NBS VUV Radiometry Group, was utilized to produce a lamp in which the radiation was emitted from the end of a capillary tube with a concentric coil antenna. The emission through the end-window then appeared as a circular spot, suitable for radiance calibration. This model lamp, calibrated in spectral irradiance, was used in the preflight calibration of the Faint Object Spectrograph, an instrument on the Space Telescope.[39]

These lamps are conveniently mounted in cylindrical exciters, 20 cm or less in length and 7.6 cm in diameter. The unit is compact, light, and low powered (15 W), making it a good candidate for use on experiments in space. The lamps and exciter are readily available commercially at reasonable prices. The usable wavelength ranges of the lamps are: argon, 115-155 nm; krypton, 125-180 nm; and xenon, 148-200 nm. Figure 19 shows the spectral irradiance of a xenon dimer lamp in comparison with other UV sources, and Fig. 38 shows the spectral radiance of a krypton dimer lamp.

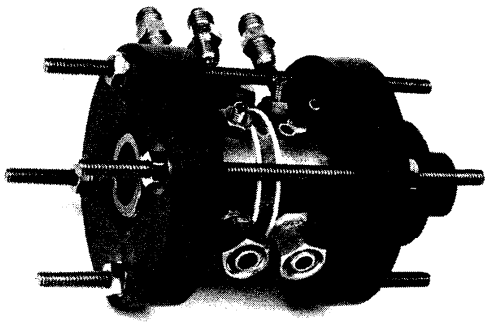

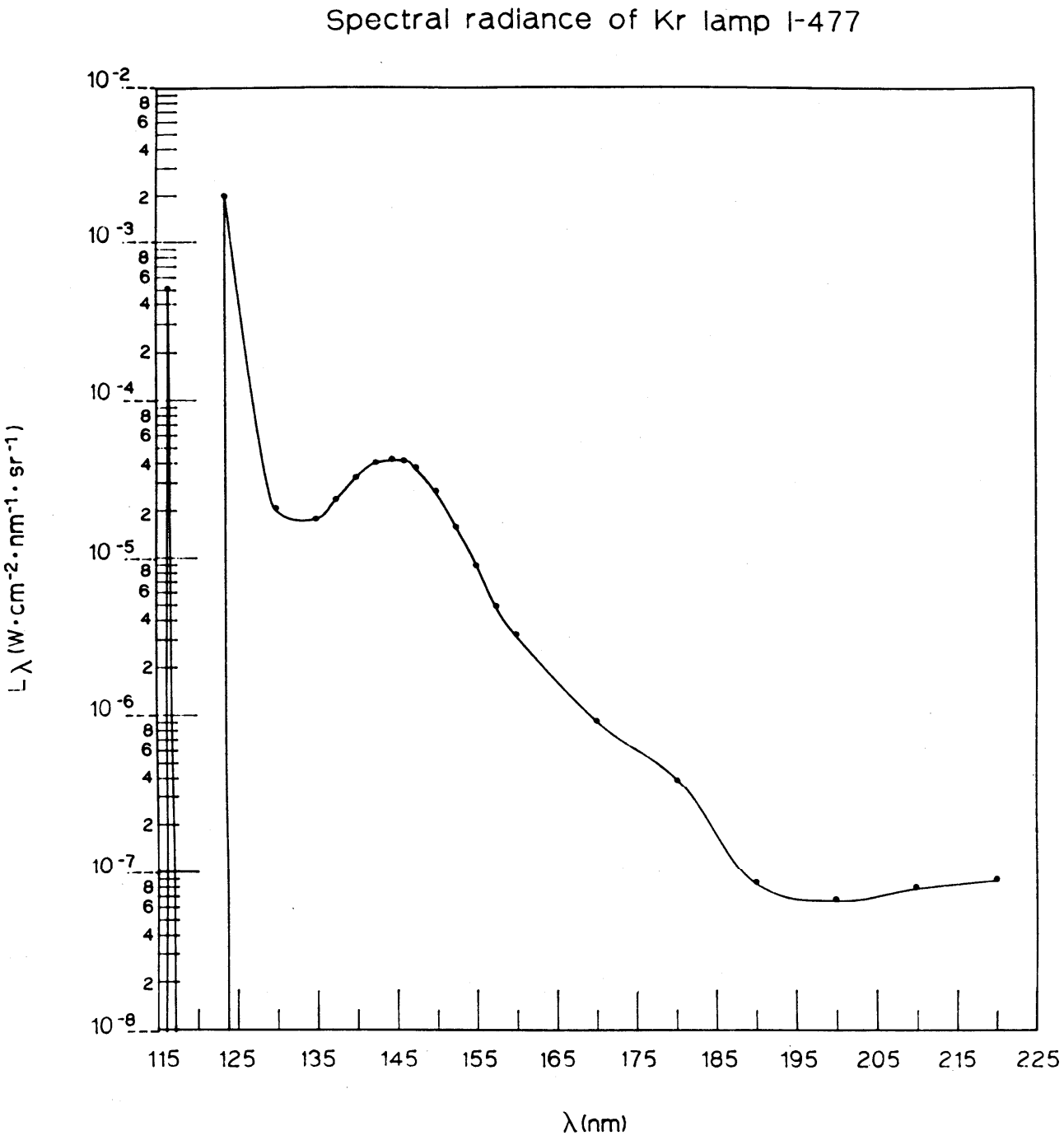

Figure 38. The spectral radiance of an rf-excited krypton dimer lamp.

D. Monochromatic Source of Lyman-α Radiation

For some time the VUV Radiometry Group at NBS has been concerned with development of a calibrated source emitting the radiation of an individual atomic transition.[41] Such a source would be of value since it could be used to calibrate detectors at its wavelength without the need of a monochromator. Furthermore, several such sources at different wavelengths could be used to calibrate spectrometers over the range of wavelengths of the sources. The Lyman-α radiation from the hydrogen atom at 121.6 nm was chosen for the initial development of a monochromatic source because of its high-intensity, its ready availability from hydrogen lamps, and the possibility of isolating it using a molecular oxygen filter.[41-43] The oxygen filter is needed since interference filters with reasonable peak transmissions at 121.6 nm (15-20%) have bandwidths (FWHM) of 15 nm or greater. Watanabe et al.[44] give the absorption coefficient of oxygen as a function of wavelength. They show a sharp minimum in the absorption coefficient at the wavelength of Lyman-α, providing a window for the transmission of Lyman-α radiation through an atmosphere of oxygen. Above the low-wavelength cutoff of MgF_2 at ≈115 nm, the behavior of the absorption coefficient indicates that most other emissions could be eliminated up to ≈170 nm. However, these authors show a decreasing absorption coefficient with further increasing wavelength indicating that a Lyman-α transmitting oxygen filter probably will not cut out lamp emission above ≈170 nm. Our work at NBS verifies the above inferences in that the oxygen filter transmits Lyman-α radiation and absorbs most other emissions up to 170 nm.[45] A Lyman-α transmitting interference filter had to be inserted to eliminate emissions above the upper wavelength cutoff of the oxygen filter.

As our emitter of Lyman-α radiation, we chose a commercially available 15-W rf-excited hydrogen-helium lamp with the helium at low pressure to enhance the Lyman-α emission and reduce visible radiation. This lamp has a MgF_2 window 1 cm in diameter, is equipped with a sidearm containing uranium hydride and metallic uranium, and is filled with helium at a pressure of 4 Torr. The uranium hydride (UH_3) is decomposed by heating to add hydrogen to the fill gas, and the metallic uranium acts as a getter to remove atmospheric contaminants. The commercial exciter used to operate the lamp has the capability of maintaining the UH_3 at preselected temperatures in the range of 100-200°C, enabling the hydrogen to be supplied reproducibly.

When a small flow of oxygen was added to the argon flow (0.3% O_2) purging the volume between the lamp window and the MgF_2 entrance window of the scanning monochromator, the Lyman-α peak at 121.6 nm was virtually unchanged, but the many-line spectrum of the Lyman bands of hydrogen out to ≈170 nm was almost completely eliminated. Only structure around 126.9 nm remained. Furthermore, increasing the flow of O_2 decreased the intensity of Lyman-α but at a slower rate than the decrease of the integrated intensity in the vicinity of 126.9 nm. This is shown in Fig. 39 and Table VIII, where the "impurity radiation" refers to the structure around 126.9 nm. Thus, in the region below ≈170 nm the purity of the Lyman-α radiation shows a positive gradient with oxygen flow. Finally, to obtain the pure Lyman-α source, the hydrogen con-

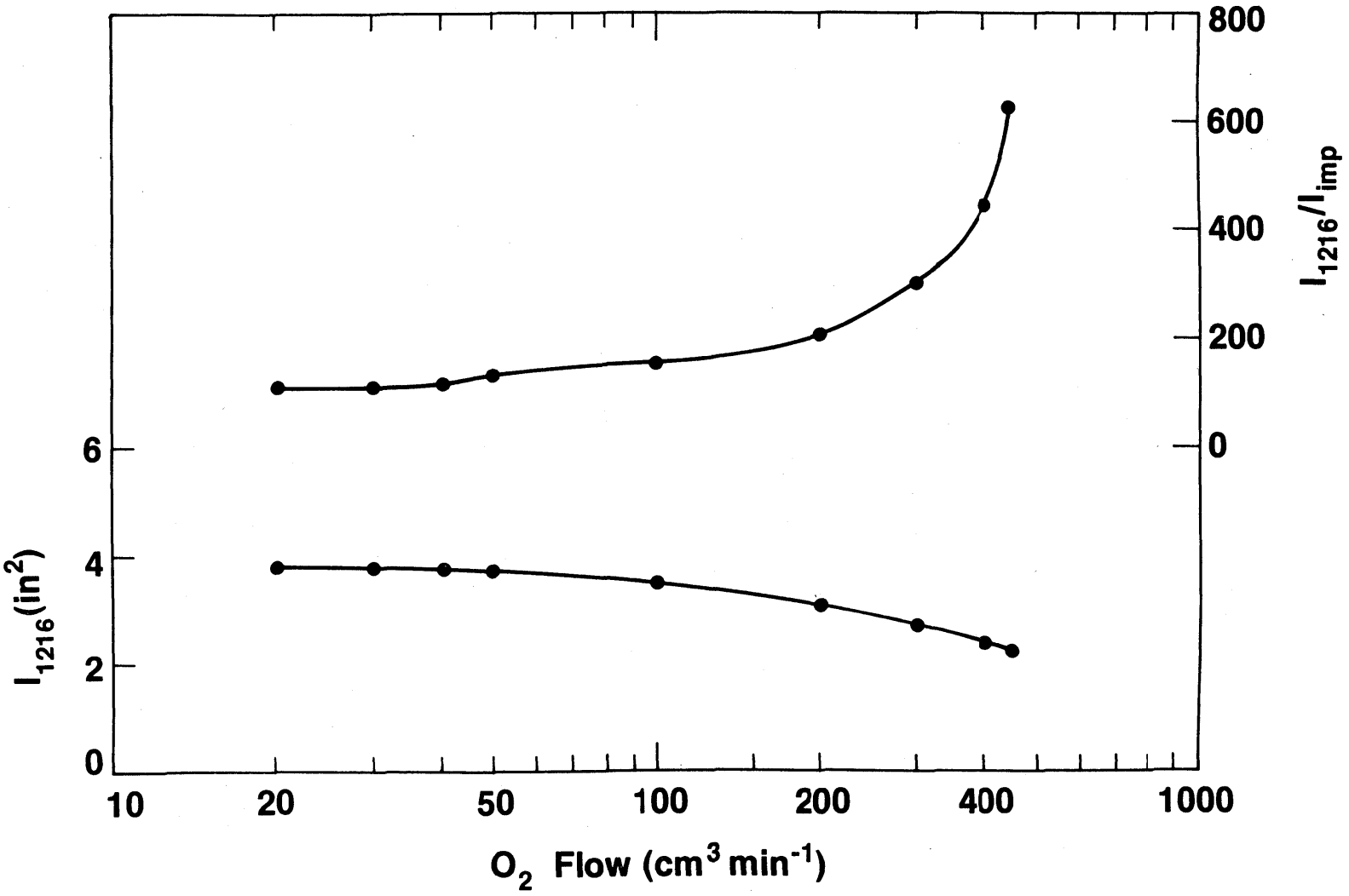

Figure 39. Intensity of Lyman-α emission and the ratio of the intensity of Lyman-α to that of the impurity radiation around 1269 Å as a function of oxygen flow. The intensities were determined by measuring the areas under the spectral distributions of both Lyman-α and the impurity radiation using a planimeter and adjusting the values according to the system efficiencies.

Table VIII. Lyman-α Source Line Irradiances at 50 cm

O_2 flow ($cm^3\ min^{-1}$)	E_{1216} ($\mu W\ cm^{-2}$)	Impurity radiation (%)	Reproducibility (%)
0	0.0461	—	4.4
20	0.0435	0.93	1.2
30	0.0430	0.92	1.2
40	0.0426	0.87	0.8
50	0.0418	0.78	0.8
100	0.0389	0.64	0.4
200	0.0342	0.48	0.9
300	0.0304	0.33	1.0
400	0.0272	0.23	1.3
450	0.0251	0.16	2.1

tinuum above ≈170 nm was eliminated through the addition of a standard interference filter with the specifications given above.

The irradiances of the source were obtained by applying the radiance-to-irradiance transfer method described above in Sec. IV-B,1 along with the previously described procedure for the determination of line irradiance.[45] In this determination the relative system efficiencies and the irradiance of the continuum were obtained by irradiating the spectroradiometer with an argon mini-arc calibrated for spectral radiance. Table VIII gives the irradiances of the source for different oxygen flows at a UH_3 temperature of 100°C and a source-to-defining-aperture distance of 50 cm.

In summary, we have found that by regulating the flow of oxygen through the filter cell, we can almost completely eliminate the Lyman bands (115-167.5 nm) from our hydrogen lamp spectrum. By next adding an interference filter with a transmission peak at 121.6 nm, we removed the hydrogen continuum (above 167.5 nm), giving a highly pure spectrum of Lyman-α (121.6 nm) radiation. We have also noted that the intensity of Lyman-α decreased with increasing oxygen flow but at a lower rate than the decrease in the intensity of the impurity radiation around 126.9 nm. Finally, we determined the line irradiances of our source along with the fractions of impurity radiation, the reproducibilities of the Lyman-α signals, and the accuracy of the irradiances. The out-of-band radiation around 126.9 nm ranges from ≈1% down to 0.2%, the reproducibility with oxygen flow is within 2%, and the overall 2σ uncertainty is 11%.[45] Thus, we have a useful source in that the line irradiance is not strongly dependent on oxygen flow, the spectral purity is high, and a region exists in which both the irradiance and spectral purity are relatively insensitive to oxygen flow. These properties make this source a good candidate for further development as a radiometric standard.

E. Safety Considerations

1. Extreme caution should be exercised when dealing with high voltages and currents.

2. Before an arc operation is begun, a check to ensure the electrical isolation of the anode and cathode should be made.

3. Before an arc operation is begun, a check to ensure electrical isolation of the arc plates should be made.

4. Insulating gloves are to be worn when adjusting the hydrogen arc electrodes.

5. Smoking is not allowed in the laboratory while the hydrogen arc is being operated, and the room ventilation must be sufficient to prevent an explosive mixture from building up.

6. Deuterium lamps in air are to be operated in the open with normal room air circulation only. Any UV-produced ozone will be dispersed by normal room convection currents.

7. Tungsten-quartz-halogen lamps are to be operated in the open clear of any flammable materials.

8. Precautions should be taken at all times to prevent the exposure of the eye to UV and high-intensity visible radiation.

FORM NBS-359
(3-69)

U.S. DEPARTMENT OF COMMERCE
NATIONAL BUREAU OF STANDARDS
WASHINGTON, D.C. 20234

Appendix F-1

REPORT OF TEST

October 22, 1985

VUV Spectral Radiance of Argon Mini-Arc

An argon mini-arc light source was calibrated in the wavelength range 118-335 nm. The lamp was calibrated according to procedures described in the accompanying report, "Argon Mini-Arc Calibration". The results of the calibration are given in Table 1. Uncertainties are given in Table 3.

For the Director,

W. L. Wiese

Wolfgang L. Wiese, Chief
Atomic and Plasma Radiation Division
Center for Radiation Research

J. M. Bridges

J. M. Bridges, Physicist
Atomic and Plasma Radiation Division
Center for Radiation Research

Test # 531/226179

Argon Mini-Arc Calibration

Argon mini-arc light sources are calibrated in the wavelength range 118 nm to 335 nm with the NBS argon mini-arc. The latter is a secondary standard and had been calibrated previously with three primary radiometric standards, the NBS wall-stabilized hydrogen arc[1] from 140 nm to 335 nm, a plasma blackbody-line radiator[2] from 118 nm to 165.6 nm, and a tungsten strip lamp[3] from 250 nm to 335 nm. The overlap of the wavelength bands of applicability of these three standards ensured consistency of the calibration base. The spectral radiance of the customer's mini-arc, in units of W cm^{-2} nm^{-1} sr^{-1}, is listed in Table 1 for an arc current of 38.00 A.

The values of spectral radiance listed in Table 1 apply to the radiation emitted by the mini-arc light source through a sealing window. Also listed in Table 1 is the transmission of the MgF_2 ultraviolet window attached to the light source and that of an additional MgF_2 window. The spectral radiance of the arc plasma itself is obtained by dividing the values given in Table 1, L_λ, by the transmission of the appropriate window. The spectral radiance of the light source using another window, for example window #2, is then obtained by multiplying the quotient by its transmission, for example

$$L_\lambda(\#2) = \frac{L_\lambda(\#1)}{T(\#1)} \times T(\#2).$$ (Where, for example, the arc was calibrated with window #1).

In this way damage to the arc window does not result in the loss of a calibrated light source. Also, it is possible through such substitution of a calibrated window, to periodically check for deterioration of the window due to, for example, condensation on the window of uv-photodissociated hydrocarbons in the vacuum system.

1. Calibration Conditions. A continuous flow of technical grade argon, (99.996% pure), was used to purge the arc source. The total flow rate was set to give a reading of 80 units on the flowmeter accompanying the arc. This argon flow was divided equally in a gas manifold and directed to the three input gas ports. The flowmeter, manifold, and gas connections used were those supplied by the customer. The output ports vented directly into the laboratory.

The arc was ignited by shorting out the anode (+) and cathode (-) with a tungsten striking rod inserted into the arc channel. Some tungsten "smoke" may be generated in this process, but the relatively high gas flow protects the window and purges the arc chamber within seconds.

The current was measured using a calibrated shunt and digital voltmeter.

The optical conditions for which the calibration is appropriate are as follows:

a) The radiation from the center arc plate of the mini-arc was focused on the spectrometer entrance aperture.

b) The calibrated area of the mini-arc was determined by the optical magnification (M =1) and by the entrance aperture (0.30 mm diameter).

c) The f number of the optical system was defined by a field stop located in front of the focusing mirror (f/100).

d) The spectrometer resolution was 0.1 nm.

e) A short gas cell is located between the mini-arc and the vacuum system. It is normally purged with argon at atmospheric pressure. Thus, the mini-arc uv window is not exposed to vacuum system contaminants during a calibration.

The light source was calibrated with its axis of symmetry coincident with the axis of the optical measuring system. Course adjustment was made using a telescope. Fine adjustment of the arc position was obtained photoelectrically by gently scanning the mini-arc image across the spectrometer entrance aperture until maximum signal was obtained.

2. Mini-Arc Characteristics. The radiance of the mini-arc is a function of pressure. The values in Table 1 apply to an ambient pressure of 1 atm. The radiance at other pressures is given by

$$L(p) = (1.57\ p - 0.57)\ L(o)$$

where p is the pressure in atmospheres and L(o) is the radiance at 1 atm. This relation holds for all wavelengths.

Although the mini-arc was calibrated for an optical aperture f/100, tests on the NBS mini-arc indicate that the spectral radiance is constant to within 1% for apertures as large as f/9. The spectral radiance decreased by about 2% for f/7 and by about 8% for f/6.

The horizontal and vertical alignment are critical for absolute calibrations. Figure 1, taken from reference 1, illustrates the dependence of the signal on arc position for four representative wavelengths. If the alignment is off by about 0.75 mm, the radiance is decreased to about 70% of the calibration value. The area calibrated is the central 0.3 mm diameter region where the discharge is nearly homogeneous. It should be clear that a correction must be made if an area larger than the 0.3 mm diameter calibration region is observed. The area of observation should be limited, however, to approximately a 2 mm diameter since the relative spectrum changes significantly for larger diameters.

Tests have shown that the MgF_2 window is the component most likely to cause a systematic change in the arc radiance. Measurements on the NBS arc indicated a negligible change in the radiance of the arc plasma itself after 24 hrs continuous operation. Window deterioration may arise from radiation damage, from vacuum system hydrocarbons, or from dust deposited on the arc side of the window. Windows have generally shown a wavelength dependent change in transmission of a few percent after several hours use. Therefore, periodic checking of the window transmission is recommended, as described on page 1.

The ultraviolet continuum spectrum is interrupted by several atomic and ionic emission lines, mainly in the wavelength region from 114 nm to 135 nm. These lines arise from air and water vapor impurities in the argon gas cylinder, the gas handling system, and the outgassing arc chamber. Table 2 lists the wavelengths of the lines emitted from an arc similar to the one calibrated, and

indicates the approximate relative intensity of the lines relative to the argon continuum for a bandpass of 0.25 nm. Figure 2 is a strip chart recording of a photoelectric scan of the spectrum under these conditions. The width of the lines is instrument-limited in this case. High resolution measurements indicate that all the lines have a halfwidth of about 0.01 nm. The line intensities will generally show large variations, since they arise from small impurities of the elements involved; other lines also may possibly appear at larger impurity levels.

3. Uncertainties. The uncertainties are a function of wavelength since three different primary standards were used in the calibration procedure and since the signal-to-noise ratio is a function of wavelength. In addition, the transmission of the vacuum sealing window (not the arc window) in our measurement system decreases slightly at the shorter wavelengths during the entire calibration process. This has been taken into account, but results in a loss of precision and contributes to the increased uncertainty below 140 nm. The uncertainties are summarized in Table 3.

References

1. J. M. Bridges and W. R. Ott, Appl. Opt. 16, 367 (1977).

2. W. R. Ott, K. Behringer, and G. Gieres, Appl. Opt. 14, 2121 (1975).

3. G. Boldt, Space Sci. Rev. 11, 728 (1970).

4. H. J. Kostkowski, D. E. Erminy, and A. T. Hattenburg, in Advances in Geophysics, Vol. 14, p. 111 (Academic Press, New York, 1970).

Table 1. Calibrated spectral radiance in units of W cm^{-2} nm^{-1} sr^{-1}. The area of the light source which is calibrated is the central 0.3 mm diameter region. Values of the spectral radiance are given for an arc current of 38.00 A.

λ(nm)	Spectral radiance, using window #79 W cm^{-2} nm^{-1} sr^{-1}	Transmission Window #79	Window #80
335.0	4.66 E-2	0.920	0.922
320.0	4.57 E-2	0.916	0.920
310.0	4.35 E-2	0.910	0.920
300.0	4.16 E-2	0.902	0.910
290.0	3.89 E-2	0.891	0.902
280.0	3.60 E-2	0.875	0.880
270.0	3.31 E-2	0.851	0.855
260.0	3.02 E-2	0.835	0.835
250.0	2.79 E-2	0.835	0.835
240.0	2.56 E-2	0.850	0.854
230.0	2.32 E-2	0.872	0.874
220.0	2.06 E-2	0.877	0.884
210.0	1.81 E-2	0.878	0.888
200.0	1.49 E-2	0.878	0.888
191.0	1.25 E-2	0.876	0.887
186.0	1.18 E-2	0.874	0.885
176.0	8.91 E-3	0.866	0.875
170.0	7.52 E-3	0.855	0.861
164.0	6.51 E-3	0.850	0.856
159.0	5.42 E-3	0.847	0.848
154.5	4.84 E-3	0.839	0.840
151.5	4.27 E-3	0.832	0.834
145.0	3.20 E-3	0.810	0.814
140.0	2.67 E-3	0.791	0.790
137.0	2.39 E-3	0.765	0.771
134.5	1.95 E-3	0.737	0.753
129.0	1.32 E-3	0.632	0.675
126.8	1.05 E-3	0.581	0.633
125.4	0.95 E-3	0.548	0.593
118.4	0.96 E-3	0.361	0.355

Table 2. Survey of emission lines present in the 38 A argon mini-arc spectrum. The spectrometer bandpass is 0.25 nm.

λ(nm)	Element	Radiance of line peak relative to continuum
115.22	O I	1
116.79	N I	1
117.69	N I	0.3
118.94	C I	0.3
119.38	C I	1
119.99	N I	30
121.57	H I	100
124.33	N I	5
126.13	C I	2
127.75	C I	5
128.98	C I	1
130.22	O I	15
130.55	O I	10
131.07	N I	1
131.95	N I	0.5
132.93	C I	4
133.53	C II	8
135.58	C I	0.2
141.19	N I	0.7
143.19	C I	0.1
145.91	C I	0.1
146.33	C I	1
146.75	C I	0.1
148.18	C I	0.2
149.26	N I	4
149.47	N I	6
156.10	C I	4
157.50	Ar II	0.2
160.04	Ar II	0.2
160.35	Ar II	0.1
160.65	Ar II	0.05
165.72	C I	2
174.27	N I	1
174.53	N I	0.5
175.19	C I	0.1
187.31	Ar II	0.05
188.90	Ar II	0.1
193.09	C I	2
247.86	C I	0.05
328.0-334.0		0.1
336.5-342.5		0.15
334.5-347.0	Ar II and Ar I	0.1
348.5-350.5	(broadened lines)	0.05
353 and above		

Table 3. Uncertainties in the mini-arc spectral radiance calibration.

λ(nm)	uncertainty (2σ)
250-335	4%
140-250	9%
118-140	20%

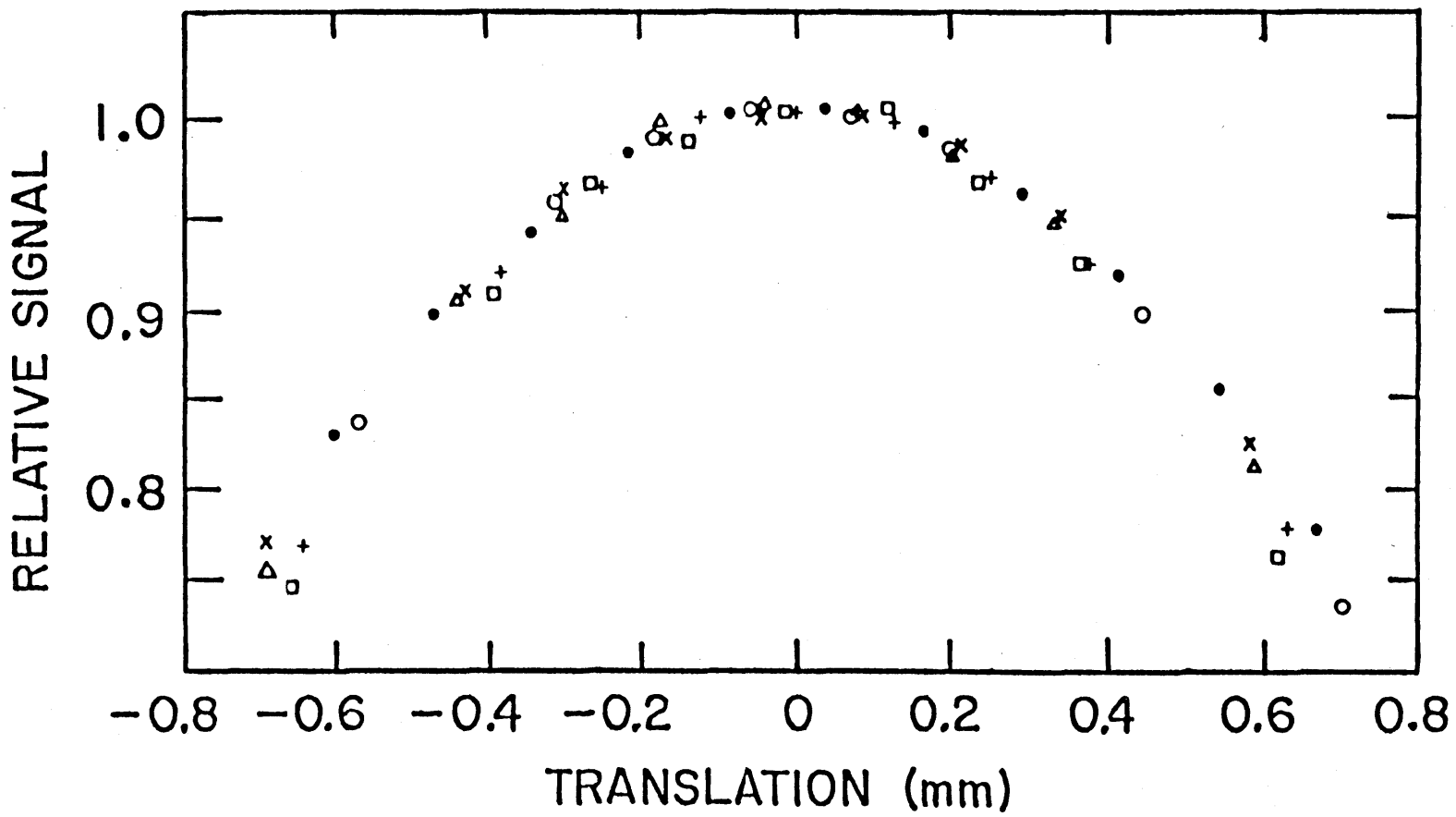

Figure 1. The dependence of the mini-arc spectral radiance on translational alignment for several field stops, arc currents, and wavelengths. The zero indication on the translation scale corresponds to the case where the arc axis is exactly aligned with the optical axis.

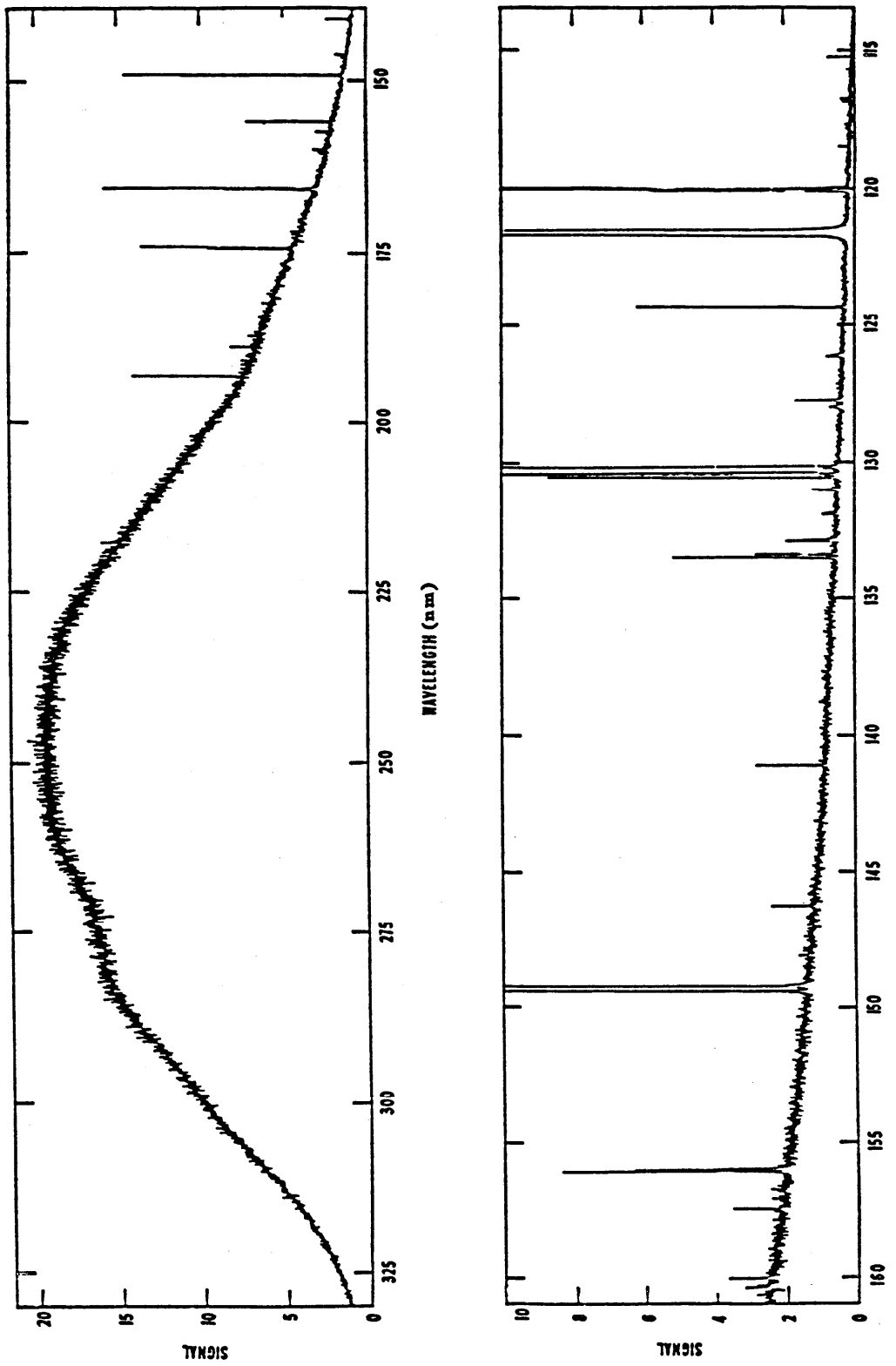

Figure 2 High resolution scan of the 38.00 Å argon mini-arc spectrum. The decreasing signal above 250 nm is due to the use of a solar blind photomultiplier in the measurement system.

FORM NBS-443
(REV. 12-65)

Appendix F-2

U.S. DEPARTMENT OF COMMERCE
NATIONAL BUREAU OF STANDARDS
WASHINGTON, D.C. 20234

April 16, 1984

REPORT OF CALIBRATION

VUV Spectral Irradiance of Argon Mini-Arc

An Argon mini-Arc light source was calibrated for spectral irradiance in the wavelength range 138mm to 335mm based upon the NBS argon mini-arc[1]. The latter is a secondary standard of spectral radiance and had been calibrated previously at 40.00A with three primary radiometric radiance standards, the NBS wall-stabilized hydrogen arc[2] from 140mm to 335mm, a plasma blackbody-line radiator[3] from 114.5mm to 165.6mm, and a tungsten strip lamp[4] from 250mm to 335mm. The overlap of the wavelength bands of applicability of these three standards ensured consistency of the calibration base.

The method used to transfer from a spectral radiance source (The NBS mini-arc) to a spectral irradiance source is outlined in Reference 5. The short-wavelength limit is set at 138mm due to low signal from the stopped-down radiance standard at shorter wavelengths. The long wavelength limit of 335mm is due to the increased density of argon spectral lines at longer wavelengths.

The spectral irradiance of the mini-arc, in units of $W\ cm^{-2}\ mm^{-1}$, is listed in Table 1 for an arc current of 40.00A.

The values of spectral irradiance listed in Table 1 apply to the radiation emitted by the mini-arc light source through a sealing window. Also listed in Table 1 is the transmission of the MgF_2 ultraviolet window attached to the light source and that of an additional MgF_2, window. The spectral irradiance of the arc plasma itself is obtained by dividing the values given in Table 1 by the transmission of the appropriate window. The spectral irradiance of the light source using another window, for example window 2, is then obtained by multiplying the quotient by its transmission, for example

$$E_\lambda(\#2) = \frac{E_\lambda(\#1)}{T(\#1)} \times T(\#2)$$ (where, for example, the arc was calibrated with window#1)

In this way damage to the arc window does not result in the loss of a calibrated light source. Also, it is possible through such substitution of a calibrated window, to periodically check for deterioration of the window due to, for example, condensation on the window of uv-photodissociated hydrocarbons in the vacuum system.

1. Calibration Conditions. A continuous flow of high purity (research grade) argon, with total gas cylinder impurities quoted to be less than 10 ppm (99.999% pure), was used to purge the arc source. The total flow was 5000 cc min^{-1} and was divided equally in a gas manifold and directed to the three input gas ports. The output ports vented directly into the laboratory. The pressure in the arc chamber was equal to the ambient pressure, measured to be 1.00 atm, or 760 mm Hg, $\pm$ 1%.

The tungsten cathode was positioned in its holder using the adjustment fixture supplied.

The arc was ignited by shorting out the anode (+) and cathode (-) with a tungsten striking rod inserted into the arc channel. After ignition, the cathode was withdrawn from the arc axis by unscrewing the cathode holder exactly five rotations from its inwardmost position.

The current was measured using the calibrated shunt, leads, and digital voltmeter supplied with the arc.

The optical conditions for which the calibration is appropriate are as follows:

a) The arc was aligned with its axis of symmetry along the optical path. The center arc plate of the arc was 50 cm from the entrance aperture, which was .5 mm x 1 mm. (See fig. 1)

b) The spectrometer resolution was 0.4 nm.

c) A short gas cell is located between the mini-arc and the vacuum system. It is normally purged with high purity argon at atmospheric pressure. Thus, the mini-arc uv window is not exposed to vacuum system contaminants during a calibration.

2. Mini-Arc Characteristics. Some properties of the mini-arc, determined from measurements on models similiar to the one calibrated, are described below.

The irradiance from the mini-arc is approximately uniform over a much larger solid angle than that used for the calibration. By observing the signal as the arc is rotated about its center, the variation of irradiance with angle from the arc axis was measured. This was done with signals at both 220 & 320 nm. The result is shown in Fig. 2; no change with wavelength was observed. The irradiance is seen to be essentially uniform over an angle of 8 degrees, corresponding to a solid angle of .015 rad (f/7).

The irradiance of the mini-arc is a function of pressure. The values in Table 1 apply to an ambient pressure of 1 atm. The irradiance at other pressures is given by

$$E(p) = (1.57p - 0.57)\, E(0)$$

where p is the pressure in atmosphere and $E(0)$ is the irradiance at 1 atm. This relation holds for all wavelengths.

Tests have shown that the MgF_2 window is the component most likely to cause a systematic change in the arc irradiance. Measurements on the NBS arc indicated a negligible change in the irradiance of the arc plasma itself after 24 hrs continuous operation. Window deterioration may arise from radiation damage or from vacuum system hydrocarbons. Some windows have shown a wavelength dependent change in transmission of a few percent after several hours use. Therefore, periodic checking of the window transmission is recommended, as described on page 1.

The ultraviolet continuum spectrum is interrupted by several atomic and ionic emission lines. These lines arise from air and water vapor impurities in the argon gas cylinder, the gas handling system, and the outgassing arc chamber. Table 2 lists the wavelengths where these lines occur for an arc current of 40 A and indicates the approximate relative intensity of the lines relative to the argon continuum for a bandpass of 0.25 nm. These line intensities will show large variations however, since they arise from small impurities of the elements involved.

Figure 3 is a strip chart recording of a photoelectric scan of the spectrum under these conditions. The width of the lines is instrument-limited in this case. High resolution measurements indicate that all the lines have a halfwidth of about 0.01 nm.

References

1. J.M. Bridges and W.R. Ott, Appl. Opt. 16, 367 (1977).

2. W.R. Ott, K. Behringer, and G. Gieres, Appl. Opt. 14, 2121 (1975).

3. G. Boldt, Space Sci. Rev. 11, 728 (1970).

4. H.J. Kostkowski, D.E. Erminy, and A.T. Hattenburg, in Advances in Geophysics, Vol. 14, p. 111 (Academic Press, New York, (1970).

5. W.R. Ott, J.M. Bridges and J.Z. Klose, Optics Letters 5, 225 (1980).

For the Director,

W. L. Wiese

Wolfgang L. Wiese, Chief
Atomic and Plasma Radiation
Division
Center for Radiation Research

J. M. Bridges

John M. Bridges, Physicist
Atomic and Plasma Radiation
Division
Center for Radiation Research

Attachments.

Table 1. Calibrated spectral irradiance of Arc in units of W cm^{-2} nm^{-1}. Values of the spectral irradiance are given for an arc current of 40.00 A, and at a distance of 50.0 cm from the center of the arc.

Estimated uncertainty is $\pm$ 6% for $\lambda \geq 200$ nm and $\pm$ 10% for $\lambda < 200$ nm.

The uncertainties are 2 standard deviations (2σ).

Wavelength (nm)	Spectral Irradiance with window #71 (W cm^{-2} nm^{-1})	Transmission Window #71	Window #72
335	8.46×10^{-7}	.931	.941
320	8.45×10^{-7}	.929	.938
310	8.01×10^{-7}	.929	.937
300	7.55×10^{-7}	.925	.934
290	7.03×10^{-7}	.917	.920
280	6.46×10^{-7}	.905	.894
270	5.88×10^{-7}	.893	.871
260	5.40×10^{-7}	.890	.866
250	4.95×10^{-7}	.892	.881
240	4.52×10^{-7}	.900	.901
230	4.05×10^{-7}	.905	.915
220	3.55×10^{-7}	.904	.921
210	3.04×10^{-7}	.904	.924
200	2.53×10^{-7}	.903	.924
195	2.29×10^{-7}	.902	.923
190	2.06×10^{-7}	.899	.923
185	1.82×10^{-7}	.895	.920
180	1.61×10^{-7}	.891	.916
176	1.45×10^{-7}	.887	.913
170	1.21×10^{-7}	.879	.907
163	$.995 \times 10^{-7}$	.868	.895
159	$.891 \times 10^{-7}$	.861	.886
152	$.734 \times 10^{-7}$	.847	.864
144.5	$.614 \times 10^{-7}$	.830	.837
138	$.559 \times 10^{-7}$	.810	.808

Table 2. Survey of emission lines present in the 40 A argon mini-arc spectrum. The spectrometer bandpass is 0.25 nm.

λ(nm)	Element	Radiance of line peak relative to continuum
115.22	O I	1
116.79	N I	1
117.69	N I	0.3
118.94	C I	0.3
119.38	C I	1
119.99	N I	30
121.57	H I	100
124.33	N I	5
126.13	C I	2
127.75	C I	5
128.98	C I	1
130.22	O I	15
130.55	O I	10
131.07	N I	1
131.95	N I	0.5
132.93	C I	4
133.53	C II	8
135.58	C I	0.2
141.19	N I	0.7
143.19	C I	0.1
145.91	C I	0.1
146.33	C I	1
146.75	C I	0.1
148.18	C I	0.2
149.26	N I	4
149.47	N I	6
156.10	C I	4
157.50	Ar II	0.2
160.04	Ar II	0.2
160.35	Ar II	0.1
160.65	Ar II	0.05
165.72	C I	2
174.27	N I	1
174.53	N I	0.5
175.19	C I	0.1
187.31	Ar II	0.05
188.90	Ar II	0.1
193.09	C I	2
247.86	C I	0.05
328.0-334.0		0.1
336.5-342.5		0.15
334.5-347.0	Ar II and Ar I	0.1
348.5-350.5	(broadened lines)	0.05
353 and above		

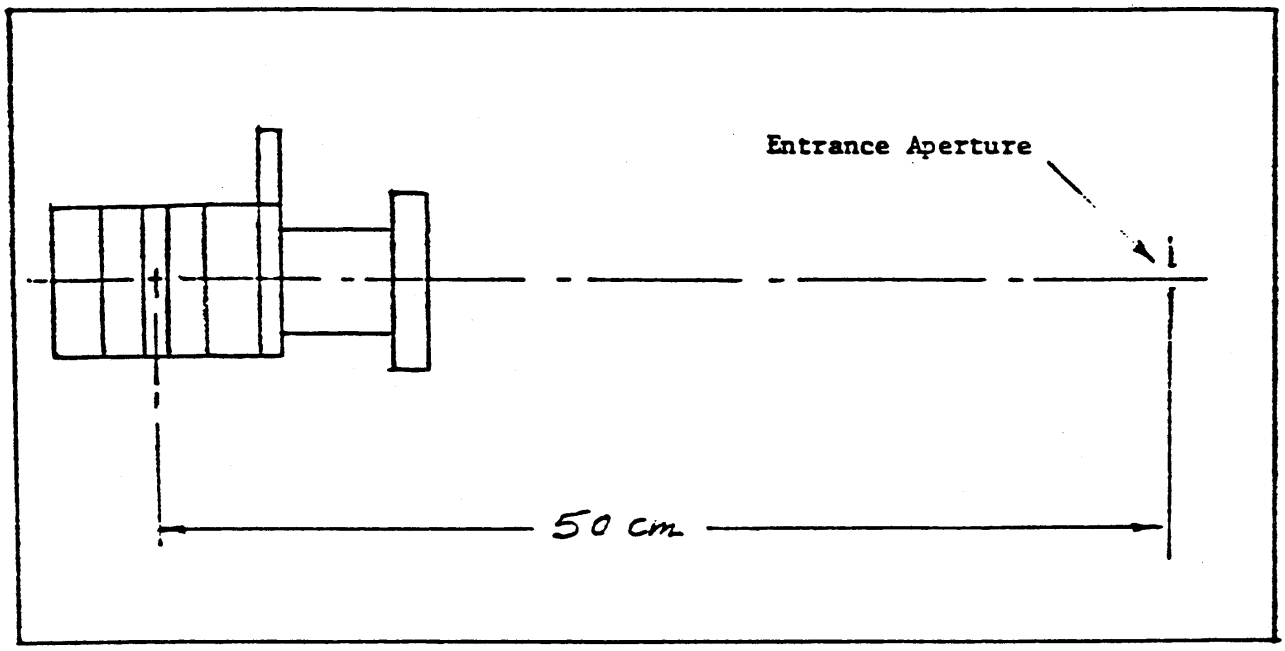

Figure 1. Position of arc relative to entrance aperture

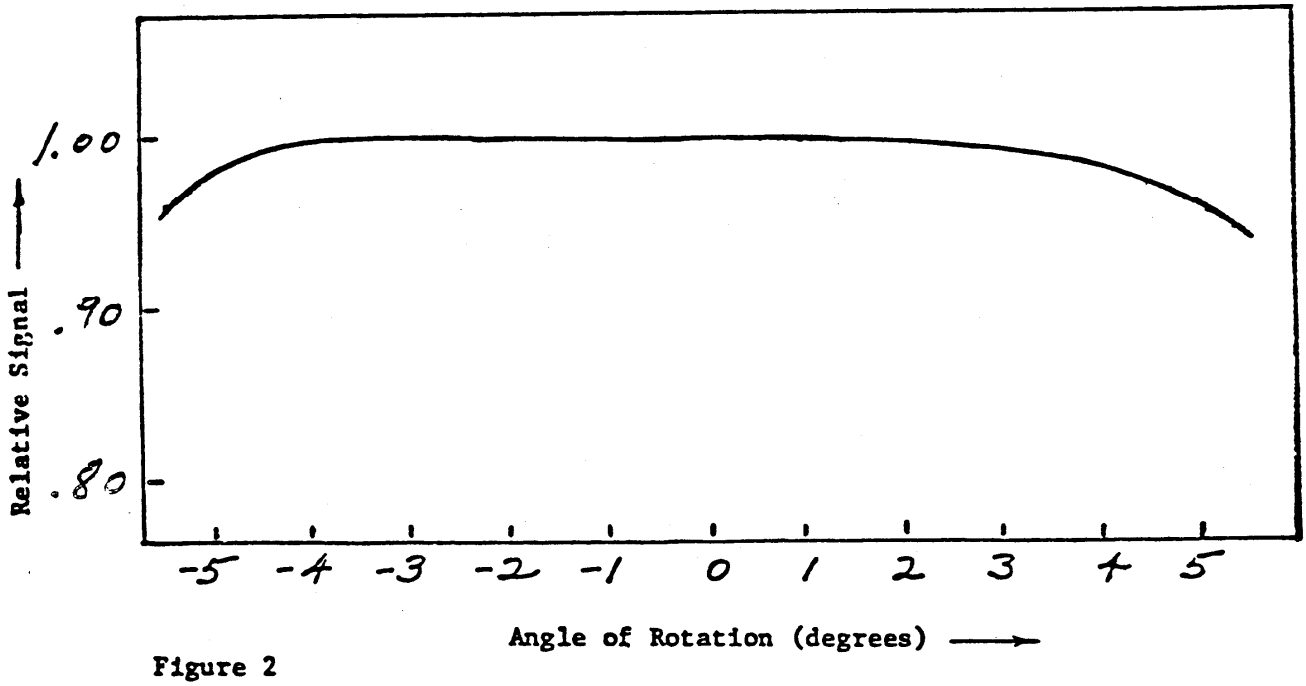

Figure 2

Relative signal vs angle of rotation of arc about its center.

(F-2)

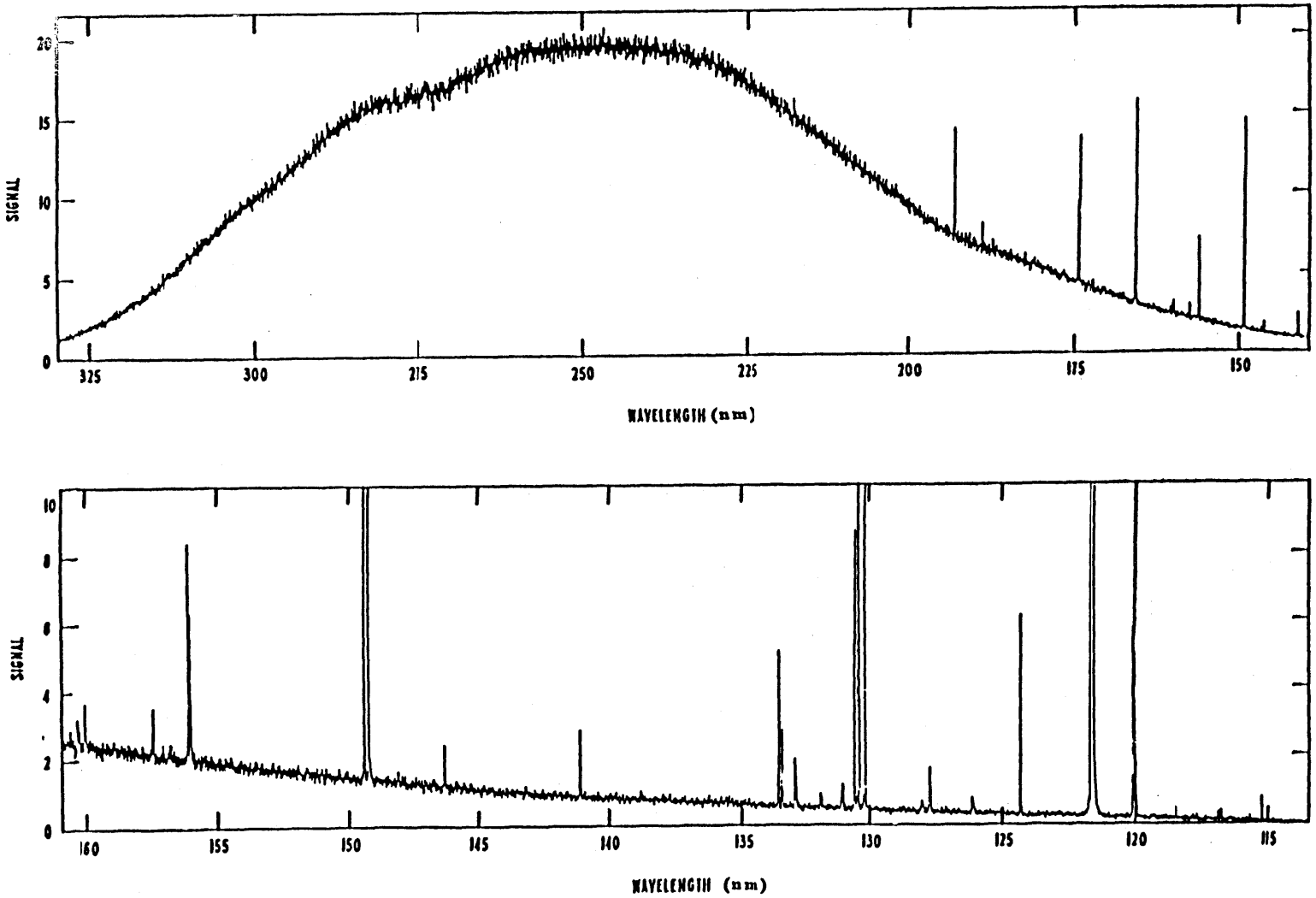

F-2-8

Figure 3 High resolution scan of the 40.00 A argon mini-arc spectrum. The decreasing signal above 250 nm is due to the use of a solar blind photomultiplier in the measurement system.

FORM NBS-259
(REV. 12-76)

U.S. DEPARTMENT OF COMMERCE
NATIONAL BUREAU OF STANDARDS
WASHINGTON, D.C. 20234

Appendix F-3

REPORT OF TEST

VUV Spectral Irradiance of Deuterium Lamp

The Spectral Irradiance of Deuterium Lamp EF132 was calibrated for the wavelength range 166-260 nm. An argon mini-arc radiance source was used to calibrate the relative spectral irradiance as a function of wavelength over this spectral range. An absolute scale was determined by calibrating the irradiance at 260 nm with a tungsten lamp irradiance standard furnished by the Radiometric Physics Division, CRR, NBS.

1. Method. A brief description of the method used to transfer from spectral radiance standard (the NBS mini-arc) to a spectral irradiance standard follows.

The calibrated area of the NBS mini-arc is the central 0.3 nm diameter region where the discharge is approximately homogeneous. In order to use this radiance source to calibrate the irradiance of another source, the radiation of the NBS arc from outside the central 0.3 mm region must be blocked. This was done by the use of a set of two collimating apertures located between the arc and the spectrometer. (One aperture also served as the entrance aperture to the spectrometer). The response of the spectroradiometer to the radiation from the region of the arc axis is then a relative measure of the sensitivity as a function of wavelength. For measuring the irradiance of the source to be calibrated, the aperture closest to the source was removed, so that the complete area of the unknown source was seen by the spectrometer. To account for slightly different solid angles of radiation entering the spectrometer from the two different sources, a diffuser was placed behind the spectrometer entrance aperture for both measurements.

2. Calibration Conditions. The D_2 lamp was operated at a current of 300 ma. The lamp was at a distance of 50 cm from the entrance aperture of the spectrometer, which was 2 mm x 1.0 mm. The spectrometer entrance and exit slits were of equal widths, giving a triangular slit function (wavelength bandpass) with width at half maximum of 0.84 nm. The lamp was

operated inside an enclosure which was purged with argon to prevent absorption. An argon flow rate of 20ℓ min^{-1} was chosen, since an increase in this rate produced no change in the signal at 170 nm.

The spectral irradiance of D_2 lamp EF132 is given in Table 1 for a current of 300 ma, at a distance of 50 cm.

3. Uncertainty. The estimated uncertainty of the spectral irradiance values is ± 7% at 190 nm, and ± 10% for $\lambda < 170$ nm. Uncertainties are 2σ.

For the Director,

W. L. Wiese, Chief
Atomic and Plasma Radiation Division
Center for Radiation Research, NML

John M. Bridges
Atomic and Plasma Radiation Division
Center for Radiation Research

Attachment

References

1. R. D. Saunders, W. R. Ott, and J. M. Bridges, Appl. Opt. 17, 593 (1978).

2. W. R. Ott, J. M. Bridges, and J. Z. Klose, Opt. Lett. 5, 225 (1980).

Lamp EF132

Table 1. Spectral Irradiance of Lamp at 50 cm for current of 300 ma.

Wavelength λ(nm)	Spectral Irradiance (W/cm^3)
260	0.261
200	0.496
195	0.486
190	0.456
187	0.431
184	0.402
182	0.377
180	0.352
178	0.323
176	0.284
174	0.260
173	0.248
172	0.244
171	0.243
170	0.250
168	0.273
167	0.303
166	0.384